

**HIGH THROUGHPUT SCREENING FOR ENZYME MODULATORS USING  
SEGMENTED FLOW COUPLED TO ELECTROSPRAY IONIZATION-MASS  
SPECTROMETRY**

**by**

**Shuwen Sun**

**A dissertation submitted in partial fulfillment  
of the requirements for the degree of  
Doctor of Philosophy  
(Chemistry)  
in the University of Michigan  
2015**

**Doctoral Committee:**

**Professor Robert T. Kennedy, Chair  
Professor Christin Carter-Su  
Professor Kristina I. Håkansson  
Assistant Professor Brandon T. Ruotolo**

© Shuwen Sun

---

All Rights Reserved

2015

**To my family and friends**

## **ACKNOWLEDGEMENT**

I would like to express my deepest gratitude to my advisor, Professor Robert Kennedy, for his support, guidance, and patience throughout my 5-year Ph.D. study. He introduced me into a world of miniaturization, trained me into an analytical chemist specializing in mass spectrometry, and showed me a perfect example of a serious scientist. I would not have been able to complete my projects without his valuable advice and constant encouragement. I also thank all members in the Kennedy lab. I have been so fortunate to work with such fantastic colleagues. I will never forget their help, ideas and friendship.

I thank Professor Kristina Håkansson, for being willing to serve on my committee, exposing me to the charm of mass spectrometry, and guiding me in my first rotation project. I thank Professor Brandon Ruotolo for always challenging me with a good deal of questions in committee meetings, which have helped me to gain better understanding of mass spectrometry and droplet microfluidics, as well as driven me to think out of my comfort zone. I am very thankful to Professor Christin Carter-Su. From a perspective of a biologist, she has offered fresh opinions to my research. My vision has been greatly broadened by our discussion. I also would like to thank Dr. Gary Valaskovic from New

Objective. Without his generous instrumental support, one of my projects would have been much harder or even impossible.

My special thanks go to my family. The education from my parents makes me an independent person. The unconditional love from my husband helps me trudge through the toughest times and brings in countless precious moments. I especially thank my little miracle Melody. Not only has she made the spring of 2014 exceptionally beautiful, but she also opens the door of a brand new world to me.

## TABLE OF CONTENTS

DEDICATION .....	ii
ACKNOWLEDGEMENT .....	iii
LIST OF FIGURES .....	ix
LIST OF TABLES .....	xvii
LIST OF APPENDICES.....	xviii
LIST OF ABBREVIATIONS.....	xix
ABSTRACT.....	xx
CHAPTER 1 INTRODUCTION .....	1
High Throughput Screening.....	1
Mass Spectrometry for High Throughput Screening .....	3
Segmented Flow for High Throughput Screening .....	9

Cathepsin B .....	17
Sirtuins .....	18
Dissertation Overview .....	26
CHAPTER 229 LABEL FREE SCREENING OF ENZYME INHIBITORS AT FEMTOMOLE SCALE USING ALL-DROPLET-ELECTROSPRAY IONIZATION- MASS SPECTROMETRY SYSTEM .....	29
Introduction.....	29
Experimental Section .....	32
Results and Discussion .....	41
Conclusion .....	50
CHAPTER 3 DROPLET-ELECTROSPRAY IONIZATION-MASS SPECTROMETRY FOR LABEL FREE HIGH THROUGHPUT SCREENING FOR ENZYME INHIBITORS .....	52
Introduction.....	52
Experimental Section .....	55
Results and Discussion .....	62

Conclusion .....	74
CHAPTER 4 DEVELOPMENT OF LABEL-FREE SIRTUIN 1 ASSAY FOR HIGH THROUGHPUT MODULATOR SCREENING USING SEGMENTED FLOW-ELECTROSPRAY IONIZATION MASS SPECTROMETRY.....	
	76
Introduction.....	76
Experimental Section .....	79
Results and Discussion .....	82
Conclusion .....	90
CHAPTER 5 DEVELOPMENT OF MASS SPECTROMETRY-BASED ASSAYS FOR HIGH THROUGHPUT SIRTUIN 6 MODULATOR SCREENING.....	
	92
Introduction.....	92
Experimental Section .....	94
Results and Discussion .....	98
Conclusion .....	108
CHAPTER 6 FUTURE DIRECTIONS .....	
	110
Carryover Reduction of Reagent Addition Chip .....	110



Large-scale All-droplet Enzyme Modulator Screening .....	112
Automation of Mass Spectrometry Plate Reader .....	114
Sample Cleanup .....	115
Tracking a Screening .....	118
Custom Data Analysis Program .....	119
APPENDICES .....	121
APPENDIX A .....	121
APPENDIX B .....	122
APPENDIX C .....	123
REFERENCES .....	127

## LIST OF FIGURES

### Figure

- 1-1** Scheme of electrospray ionization. ....4
- 1-2** A) Instrument setup of a 4-way parallel LC-MS/MS for high throughput analysis. B) Affinity-based MS binding screening (e.g., SpeedScreen). Ligands, target protein, and tracer/target ligand in a 96-well plate (1) are aspirated (2) and subsequently dispensed onto a 96-well filtration plate (3). After washing of the filtration plate (4) to remove nonbinders, methanol is added (5) to allow disruption and elution of binders (6) to another 96-well plate (7) for measurement by LC-MS (8). Quantification of the tracer/target ligand by triple-quadrupole MS allows determination of the percentage of tracer/target ligand displacement by unknown ligand binders. C) On-line solid phase extraction using Rapidfire<sup>®</sup> (chem.agilent.com): the in-line automated cartridge switching can switch up to 12 reusable SPE cartridges (> 2000 injections/cartridge). The system can automate 63 plate handling and 60 hours unattended operation with 20000+ injections. D) High-throughput flow injection mass spectrometry system. System configuration includes the following: HP 1100 series HPLC system, Gilson 215 multiprobe liquid-handling system modified to include a Valco Cheminert model C5 eight-position column selection valve, and a Micromass LCT electrospray ionization time-of-flight mass spectrometer. ....9
- 1-3** Segmented flow (droplets) and a modular approach of droplet-based screening system. 1) Droplets are pinched off by injecting oil from both sides of a cross fitting into the sample stream; 2) droplet library is stored on a spool; 3) the reagent is injected into individual droplet through a T-junction to initiate reactions; 4) Fiber optic detectors monitor the components of droplets in-line. ..10
- 1-4** A) Droplet splitting to different ratios by constructing outlet channels with different inner diameters; B) Scheme of reagent addition into droplets; C) Serial dilution using microfluidic dilutor: a buffer droplet approaches (0 ms), contacts the mother droplet (10 ms), coalesces and activates the soft valve (20 ms), and finally generates an output droplet (35 ms). After a series of buffer droplets

passing by, the output droplets contain gradually decreased concentration of the sample in the mother droplet; D) Droplet sorting: the drops flow as a solid plug to a junction where oil is added to separate the drops. The light drops contain 1 mM fluorescein, and the dark contain 1% bromophenol blue. Fluorescence levels are detected as the drops pass a laser focused on the channel at the gap between two electrodes. When sorting is on, the light drops, which are brighter than the threshold level, are sorted by dielectrophoresis into the bottom channel. ....12

- 1-5** Diagram of reformatting acetylcholinesterase assays into air-segmented plugs. The array of sample plugs were prepared by dipping the tip of a 75  $\mu\text{m}$  i.d. Teflon tubing prefilled with Fluorinert FC-40 into sample solution stored in a multiwell plate, aspirating a desired volume, retrieving the tube, aspirating a desired volume of air, and moving to the next well until all samples were loaded. Movement of the tubing was controlled with an automated micropositioner and sample flow was controlled with a syringe pump connected to the opposite end of the tubing. ....14
- 1-6** Screening of AchE inhibitors (in triplicates). The top droplet trace is the assay product choline, and the bottom one is the internal standard. Inset shows one mildly inhibited and one strongly inhibited reaction. ....15
- 1-7** Flow charts for in-droplet screening (left) and high density MWP-based screening (right). ....16
- 1-8** The sirtuin family's role in aging and age-associated pathologies. The sirtuin isoforms with substantial data indicating either a protective or aggravative role for specific age-related diseases are indicated. ....20
- 1-9** SIRT1 mediates metabolic benefits in various tissues, such as liver, heart, white adipose tissues (WAT), and skeletal muscle. In general, SIRT1 supports gluconeogenesis, inhibits glycolysis, promotes fatty acid oxidation, regulates cholesterol homeostasis, and protects against cardiac hypertrophy. Targets that directly activated by SIRT1 are shown in green, and those inhibited are in pink. ....21
- 1-10** Fluor de Lys<sup>®</sup> fluorescent assay: the Fluor de Lys<sup>®</sup> SIRT1 Substrate, which contains a peptide comprising amino acids 379-382 of human p53 (Arg-His-Lys-Lys(Ac)) is deacetylated by SIRT1 at present of  $\text{NAD}^+$ . Treating with the Fluor de Lys<sup>®</sup> Developer II, the deacetylated peptide produces a fluorophore. ....23
- 1-11** SIRT6's substrates and physiological impact. ....24
- 1-12** Sirtuin activity in the presence of free fatty acids. Fold change in SIRT1 and SIRT6 deacetylase activity was monitored in the presence of various fatty acids and compared to a reaction without fatty acid. SIRT1 (dark gray) and SIRT6 (light gray) were incubated with 70  $\mu\text{M}$  H3K9Ac peptide and 0.5 mM  $\text{NAD}^+$  in the presence of 100  $\mu\text{M}$  fatty acid and analyzed by HPLC. ....26
- 2-1** A) Diagram of oil-segmented droplet generation from a MWP. The XYZ-positioner causes the Teflon tube to dwell in sample or oil for predetermined

	time, and then move to another well. The syringe pump operates in refill mode at a constant flow rate. B) Diagram of ESI-MS analysis of sample droplets. The syringe drives droplets into the ESI source through a Pt-coated emitter. +1.7 kV is applied on the emitter. ....	33
<b>2-2</b>	Calibration curve for ZRR-OH. 10 solutions of ZRR-OH with concentration as 10, 20, 40, 60, 80, 100, 120, 140, 160, 180 $\mu$ M were formatted as sample plugs and driven into ESI-MS for analysis. The ESI conditions were same with all other experiments. Using the relative abundance of each peak, the calibration curve had slope of 0.56, y-intercept of -3.6443, $R^2$ of 0.9912. ....	35
<b>2-3</b>	Dose response curves of three known inhibitors determined by droplet-MS. Different concentrations of E-64 ( $10^{-7}$ , $10^{-4}$ , $10^{-3}$ , $10^{-2}$ , 0.1, 0.3, 1, 2, 3, 10, 100, 1000 $\mu$ M), Leupeptin ( $10^{-7}$ , $10^{-4}$ , $10^{-3}$ , 0.1, 0.3, 1, 2, 3, 10, 100, 1000 $\mu$ M), Antipain ( $5 \times 10^{-7}$ , $5 \times 10^{-5}$ , $5 \times 10^{-4}$ , $5 \times 10^{-3}$ , $5 \times 10^{-2}$ , 0.5, 1.5, 3, 5, 10, 15, 50, 500, 5000 $\mu$ M) were incubated with ZRR-AMC and the enzyme. Relative abundance of ZRR-OH peaks were used for construct the sigmoidal curves.....	36
<b>2-4</b>	Illustration of fused silica surface derivatized by trichloro(1H,1H,2H,2H-perfluorooctyl) silane. ....	39
<b>2-5</b>	A) Carry-over of the all-droplet system. <1 % of carry-over was observed in the emitter (upper left). 9% of carry-over was generated by the tee for one addition (upper right) and 16% for two additions (lower left). The carry-over of three addition is 25-30% (lower right). B) Carry-over of the Teflon tee for one addition. ....	40
<b>2-6</b>	A) Cathepsin B catalyzed proteolysis of ZRR-AMC and ESI mass spectrum of resulting reaction mixture. B) Cathepsin B catalyzed proteolysis of Ac-GFGFVGG-NH <sub>2</sub> and ESI mass spectrum of reaction mixture. ....	42
<b>2-7</b>	A) Result of in-well screening of Cathepsin B inhibitors using ZRR-AMC as the substrate. XICs show signal for ZRR-OH and the known inhibitors E-64, leupeptin, and antipain. Each of 24 reaction mixtures was formatted in quadruplicate. Droplets with low product signal are inhibitor sets. B) Result of screening using Ac-GFGFVGG-NH <sub>2</sub> as the substrate. XICs are product FVGG-NH <sub>2</sub> and the substrate. 12 reaction solutions were formatted in quintuplicate. ...	43
<b>2-8</b>	A) Diagram of all-droplet screening system coupled to ESI-MS analysis. Test compounds arrayed as droplets were pumped into a series of PDMS tees where enzyme, substrate, and quenchant were added in. (For the actual experiment, the third Teflon tube was sealed on both ends and incubated in a water bath prior to pumping droplets through the quenchant addition tee.) The inset is a photomicrograph of the PDMS tee. The droplet inlet is silanized 50 $\mu$ m i.d. $\times$ 150 $\mu$ m o.d. capillary, the outlet is 150 $\mu$ m i.d. $\times$ 360 $\mu$ m o.d. Teflon tube, and the reagent channel is non-derivatized 20 $\mu$ m i.d. $\times$ 150 $\mu$ m o.d. capillary. B) Results of all-droplet screening using ZRR-AMC as the substrate. XICs are ZRR-OH, antipain, E-64, and leupeptin. Each test compounds has 4 replicates. ....	46

- 2-9** A) Photomicrograph of Teflon tee. The droplet channel is 150  $\mu\text{m}$  i.d.  $\times$  360  $\mu\text{m}$  o.d. Teflon tube. The reagent channel is 40  $\mu\text{m}$  i.d.  $\times$  190  $\mu\text{m}$  o.d. non-derivatized capillary. B) Trace resulting from all-droplet screening with the Teflon tee using the non-fluorescent substrate. XIC is the product FVGG-NH<sub>2</sub>. Samples were run in quintuplicate. ....49
- 3-1** A) Left: Scheme of parallel oil-segmented droplet generation from MWP. FEP tubes are programmed to dwell in sample or oil for predetermined time, and then move to another well. The syringe pump operates in refill mode at a constant flow rate. Right: Picture of parallel droplets generation with different color food dye as samples. B) Diagram of ESI-MS analysis by direct infusion of segmented flow. Droplets are pumped into the ESI source through a treated ESI needle. ESI voltage is applied on the needle. In the gas phase, charged sample droplets (green) enter the MS and nebulized oil (yellow) does not. ....55
- 3-2** Droplets of food dye solution generated in 8 FEP tubes at 4.5 Hz. The RSD of droplets within each tube is <5% and across tubes <10%. Photos show close-up view of 8 tubes at different lengths along the tube. ....57
- 3-3** A) Assay reaction is cleavage of heptapeptide substrate GFGFVGG by cathepsin B; B) Full scan mass spectrum of direct infusion of the reaction mixture; C) Linear calibration of FVGG from 0 to 500  $\mu\text{M}$ ; D) Reaction progression in 60 min with 100  $\mu\text{M}$  GFGFVGG and 50 nM cathepsin B; E) Michaelis-Menten data of the reaction ( $K_m > 200 \mu\text{M}$ ). ....59
- 3-4** Data from validation of assay conditions. A) 20 test compounds (No. 5-24) and 4 negative controls (No. 1-4) were used. Compound 5, 6, 7, 8 are known cathepsin B inhibitors: chymostatin, antipain, leupeptin and E-64, respectively. The rest are non-inhibitors. B) Dose response curves of the 4 known inhibitors. Fitted IC<sub>50</sub> values are  $8.3 \pm 0.5$  nM for E-64,  $24 \pm 8$  nM for leupeptin,  $41 \pm 6$  nM for antipain and  $0.40 \pm 0.04 \mu\text{M}$  ( $n = 3$ ) for chymostatin, which generally agree with the published values: E-64 = 55 nM, leupeptin = 21.5 nM, antipain = 0.48  $\mu\text{M}$  and chymostatin = 1.8  $\mu\text{M}$ . ....60
- 3-5** Demonstration that oil does not affect the analysis of target molecules: A) left: averaged mass spectra of direct infusing FVGG ( $m/z$  379) and FVG\*G ( $m/z$  382) in continuous flow (top) and in segmented flow (bottom); right: oil segments in 107 y-axis scale (top) and same oil segments in 105 y-axis scale (bottom); B) averaged mass spectra of perfluorodecalin at different periods of time. The signal intensity of the oil is low. The absence of consistent peaks indicates that the oil is not ionized in the source and does not interfere with the analysis of any other compound. ....63
- 3-6** Top: Traces of 384 droplets containing 5  $\mu\text{M}$  adenosine (solvent: 20% methanol, 0.1% formic acid) analyzed in 1.3 min (5 Hz). Droplets are 50 nL each and the infusion rate is 30  $\mu\text{L}/\text{min}$ . Bottom: the zoom-in view of 0.2-0.4 min. The RSD of droplet signal is ~5%. Droplets are segmented by oil plugs which are not charged thus do not yield signal. MS method: single reaction monitoring (SRM),  $m/z$

	268→136. Each droplet-oil pair consists of 10 to 12 data points. ....	64
<b>3-7</b>	Carry-over evaluation at different analysis rate. 5 $\mu$ M adenosine and solvent (20% methanol, 0.1% formic acid) alternating droplets (5 each) were infused into the ESI source for analysis. At 0.9 Hz, the carry-over is almost zero; at 1.8 Hz, it increases to 10%; at 3.6 Hz, it becomes as high as 20~30%. Red arrows indicate blank droplet that contains signal due to carry-over. ....	66
<b>3-8</b>	A) Top: droplet traces of partial cathepsin B inhibitor screening (Plate #4, 320 test compounds, 16 negative controls (-), and 16 positive controls (+)). Each reaction is analyzed in triplicate. The analysis rate is 1.6 Hz (1056 droplets detected in 670 s. Bottom: The enlarged view of 550-670 s. Inhibitors (blue arrows) are identified by the low intensity ratio of FVGG/FVG*G. B) Top: the analysis result of Plate #4. Each bar is the averaged FVGG/FVG*G of an assay. The negative control is normalized to 100% activity. Bottom: the last 135 reactions and controls (green). Inhibitors (red) are identified by the low % of activity (n = 3). ....	68
<b>3-9</b>	. A) Sample droplet traces for portion of cathepsin B inhibitor screening (Plate #3, 320 test drugs, 16 negative controls (-), and 16 positive controls (+)). The analysis rate is 1.6 droplets/s; B) Zoom-in view shows the transition from negative control to positive control. The carry-over (red arrow) is only 12.5% for the first positive control. For the first 3 positive controls, the carry-over only affects the signal by 4.8%. ....	69
<b>3-10</b>	Dose response curves of the identified inhibitors. A) inhibitor hits that found to be related to cathepsins (chlorexidn, luteolin, triclabendazole, ethacrynic acid, disulfiram, hexachlorophene (also strong inhibitor), anthralin, raloxifene, triclosan, and diacerein (strong inhibitor)); B) drug molecules that reduced the yield by more than 50% in the primary screen but had no prior link to cathepsins (cefmetazole, zafirlukast, thioguanosine, didanosine, alexidine, avobenzone, and tegaserod); and C) those reduced the yield by ~40% in the primary screen but had no previous link to cathepsins (cefaclor, colistin, pinaverium, metergolin, diethylstilbestrol, butenafine and pimozide). Error bars are for 3 replicates. ....	71
<b>3-11</b>	Comparison of dose response curves of 6 hits from fluorescent assay with MS assay. Fitted IC <sub>50</sub> values generally agree with each other. ....	73
<b>3-12</b>	Timing diagram for batch mode operation using mass spectrometry plate reader. Reformatting samples from MWP into 3,072 droplets takes 12 min (4.5 Hz); MS analysis takes 30 min (2 Hz, plus the tubing switching time). By overlapping the reformatting and analysis of continuous batches, 147,456 droplets could be analyzed in a day. ....	74
<b>4-1</b>	Diagram of SIRT1 assay: SIRT1 was dialyzed from Tris buffer into formate buffer using a centrifugal dialysis unit; then the deacetylation reactions were conducted in formate buffer in a multi-well plate; reaction mixtures were afterwards reformatted into oil-segmented droplets in a piece of FEP (fluorinated ethylene propylene) tube; finally, droplets were infused into an orthogonal ESI	

source through a modified ESI needle. The FEP tube and the needle were connected by a ZDV (zero dead volume) union. The signal intensity of the reaction product and its isotopic internal standard are monitored. Oil segment did not generate any ESI signal thus showed as spacing between sample droplets. ....79

- 4-2** Deacetylation of H3K9(Ac) by SIRT1. The reaction is shown on the top. The lower mass spectra show a reaction without any modulator (negative control) and a reaction with an inhibitor. Triply charged and quadruply charged H3K9 (red arrow), H3K9\* (black arrow) and H3K9(Ac) (blue arrow) are monitored. Intensity ratio of H3K9/ H3K9\* is calculated for quantification. ....83
- 4-3** Left: reaction conducted in the Tris buffer. Observed from TIC (total ion current), nearly 100% yield was achieved. Right: reaction conducted in the formate buffer. A little substrate was not converted. But the yield was still high enough which indicates good enzyme activity. (Column: made-in-house 8 cm fused- silica capillary column (75  $\mu\text{m}$  i.d./360  $\mu\text{m}$  o.d.) packed with 5  $\mu\text{m}$  C18 particle. Mobile phase A: 0.15% formic acid aqueous solution. Mobile phase B: methanol. Linear gradient: initial, 0% B; 10 min, 50% B; 15 min, 50% B; 18 min, 95% B; 20 min, 100% B). ....85
- 4-4** A) Michaelis-Menten model of H3K9(Ac) with 0.5  $\mu\text{M}$  SIRT1. The fitted  $K_m$  value is 22  $\mu\text{M}$ . B) Linear reaction within 2 h. C) Linear calibration curve of 0 to 25  $\mu\text{M}$  H3K9. Intensity ratio of H3K9 to H3K9\* was measured ( $n = 3$ ). ....87
- 4-5** Epigenetic library screening: A) Raw droplet traces of the screening. The upper trace is the reaction product H3K9, the lower one is the isotope-labeled internal standard H3K9\*. The first 3 sets are negative controls at the beginning, in the middle, and at the end of the assay plate, respectively. B) Enlarged view of the control, reaction containing suramin, and some other test reactions droplets. C) The final analysis of the screening. Each bar is the averaged H3K9/H3K9\* of an assay. The negative control (green) is normalized to 100% enzyme activity. 4 reactions showed that the enzyme activity was lowered by more than 50% ( $n = 3$ ). ....89
- 4-6** Dose response curves of 4 inhibitor hits. Negative control of each experiments were normalized to 100% activity ( $n = 2$ ). ....90
- 5-1** Deacetylation of H3K9(Ac) by SIRT6. LC-MS chromatogram showed a 24 h incubated reaction (3  $\mu\text{M}$  SIRT6, 60  $\mu\text{M}$  H3K9(Ac) and 500  $\mu\text{M}$   $\text{NAD}^+$ ). ....99
- 5-2** A) The linear part of Michaelis-Menten model. The velocity linearly increased for at least 0-150  $\mu\text{M}$  H3K9(Ac), thus the  $K_m$  should be higher than 75  $\mu\text{M}$ . B) Reaction progress of SIRT6 deacetylating H3K9(Ac). ....99
- 5-3** Direct MS analysis of 20-fold diluted reaction mixture (4.5 h incubation). Despite of the presence of noises, peaks of H3K9, H3K9\*, and H3K9(Ac) can be observed. ....101

<b>5-4</b>	Linear calibration of reaction product H3K9. 0, 0.1, 0.3, 0.5, 0.7 and 1 $\mu\text{M}$ of H3K9 was calibrated against 0.5 $\mu\text{M}$ isotopic internal standard H3K9*. Each solution also contained 3, 2.9, 2.7, 2.5, 2.3 and 2 $\mu\text{M}$ H3K9(Ac) and 20-fold-diluted $\text{NAD}^+$ -Tris buffer. The $R^2$ of linearity is 0.998. ....101	101
<b>5-5</b>	Direct MS analysis of 100 $\mu\text{M}$ oleic acid activated SIRT6 reaction (4.5 h incubation). Compared with the negative control (see <b>Figure 5-3</b> ), the yield was twice high. ....102	102
<b>5-6</b>	Droplet trace of DMSO evaluation assay (3 droplets/reaction, reactions were duplicated). The top trace is product H3K9, the middle is internal standard H3K9*, and the bottom is substrate H3K9(Ac). 100 $\mu\text{M}$ oleic acid reactions show higher yield than 1% DMSO, which means the reactions were activated. 5% and 10% DMSO reactions show low yield and low peptide intensity. ....103	103
<b>5-7</b>	Droplet traces of 25-compound test screening. Top to bottom: product H3K9, internal standard H3K9*, and substrate H3K9(Ac). Left: triplicate detection in which each reaction was made into 3 droplets. Right: single detection for 1 droplet/reaction. (-): inhibitor controls in which no $\text{NAD}^+$ were in the buffer. (+): activator controls in which 100 $\mu\text{M}$ oleic acid was in the reactions. (0): negative controls in which 1% DMSO was in the reactions. Red arrows: reactions with 25 $\mu\text{M}$ EX-527. ....105	105
<b>5-8</b>	The analysis of the screening. The y-axis is the intensity ratio of H3K9 over H3K9*. The x-axis is compounds ID. The red line is the activator criteria, and the black line is the inhibitor criteria. C11 is EX-527 reaction. Triplicate detection means each reaction was made into 3 droplets. Single detection means each reaction was made into 1 droplet. ....106	106
<b>5-9</b>	Direct infusion the MS-compatible SIRT6 deacylation assay using formate buffer. P: product H3K9(10-mer), P*: isotope-labeled internal standard H3K9(10-mer)*, S: substrate H3K9(decanyl). ....107	107
<b>5-10</b>	SIRT6 kinetics with 10-mer H3K9(decanyl) as the substrate. A) Michaelis-Menten model. The fitted $K_m$ of H3K9(decanyl) is 27 $\mu\text{M}$ . B) Reaction progress of SIRT6 de-decanoylation. Reaction rate decreased after 2 h. ....108	108
<b>6-1</b>	A) Single-channel reagent addition device that reported to have low carryover; B) Multi-channel reagent addition chip. ....111	111
<b>6-2</b>	Solid phase extraction plates. A) Filter-based SPE plate (3M Empore <sup>TM</sup> : each well of the plate contains a standard density Empore <sup>TM</sup> polypropylene membrane for efficient sample extraction). B) Particle-based SPE plate (Glysci Slit Plate <sup>TM</sup> : separation media is filter-less chromatographic particles. A 1-2 $\mu\text{m}$ slit at the bottom of each well in Slit Plate permits liquid to pass through). C) Magnetic beads-based SPE (Xiril AG Magnetic Plate-X: separation particles are coated on magnetic beads residing in each well. Separation is realized by attracting beads to	



	the corner of each well of the assay plate by the magnets array inserted under the assay plate). .....	116
<b>6-3</b>	Comparison of mass spectra of the desalted reaction (left, desalted by C-18 spin column, undiluted) and the intact reaction mixture (right, diluted by 20 folds in order to observe peptides). The noise level of treated reaction is significantly lower. Despite the low yield, product peaks are observed in the desalted reaction mass spectrum. ....	117
<b>6-4</b>	Top: scheme of droplet-based SPE. Bottom: total ion current of sequentially injected 4 samples. Reproduced with permission from Qiang Li and University of Michigan. ....	118

## LIST OF TABLES

### Table

<b>1-1</b>	Comparison between traditional HTS and droplet-microfluidic based HTS. ...	11
<b>6-1</b>	Comparison between MWP-based SIRT6 modulator screening and all-droplet-system-based screening. ....	113

## LIST OF APPENDICES

### Appendix

<b>A</b>	SEQUENCE OF TEST COMPOUNDS IN CATHEPSIN B ASSAY.....	121
<b>B</b>	GOODNESS OF FIT OF INHIBITOR HITS IN CATHEPSIN B INHIBITOR SCREENING .....	122
<b>C</b>	STRUCTURES OF INHIBITOR HITS IN CATHEPSIN B INHIBITOR SCREENING.....	123

## LIST OF ABBREVIATIONS

ADP	Adenosine Diphosphate
AVE	Average
DTE	Dithioerythritol
DTT	Dithiothreitol
ESI	Electrospray Ionization
FEP	Fluorinated Ethylene Propylene
FIA	flow injection analysis
FS	Fused Silica
H3K9	Histone H3 Lysine 9 (1-21 residue)
H3K9(10-mer)	Histone H3 Lysine 9 (4-13 residue)
H3K9*	+12 Da isotopic H3K9 (1-21 residue)
H3K9*(10-mer)	+8 Da isotopic H3K9 (4-13 residue)
HTS	High Throughput Screening
MALDI	Matrix Assisted Laser Desorption Ionization
MS	Mass Spectrometry
MSPR	Mass Spectrometry Plate Reader
MWP	Multi-well Plate
NAD <sup>+</sup>	Nicotinamide Adenine Dinucleotide
oAADPR	o-acetyl-ADP-ribose
o(decanoyl)ADPR	o-decanoyl-ADP-ribose
PFD	Perfluorodecalin
QqQ	Triple Quadrupole
RSD	Relative Standard Deviation
SD	Standard Deviation
SIRT1	Sirtuin 1
SIRT6	Sirtuin 6
SEC	Size Exclusion Chromatography
SPE	Solid Phase Extraction
SPR	Surface Plasmon Resonance
SSMD	Strictly Standardized Mean Difference
STACs	Sirtuin Activating Compounds
TOF	Time of Flight

## ABSTRACT

In drug discovery, it is important to use high throughput screening (HTS) technologies to rapidly identify active compounds for biological targets (usually enzymes) from large chemical libraries. The state of art strategy for HTS is coupling multiwell-plates (MWP) to optical readers. Higher throughput, less reagent use and minimal labeling are always pursued in HTS. Mass spectrometry (MS) is a powerful label-free analyzer due to its high speed and sensitivity. Segmented flow (droplets) can reliably manipulate nanoliter samples and miniaturize reactions with high precision and automation. Novel high throughput screening systems have been developed by interfacing oil-segmented droplets to electrospray ionization (ESI)-MS.

To miniaturize a screening, we designed an all-droplet system for conducting assays inside nanoliter droplets. A microfabricated reagent addition device was used for injecting multiple reagents into the droplet array of test compounds to initiate enzymatic reactions. The reaction droplets were directly analyzed by ESI-MS. This all-droplet system was demonstrated by a cathepsin B inhibitor screening with high reliability (Z-factor = 0.8), high analysis rate (0.8 Hz) and straightforward interpretation. Reagents

consumption was at picomoles to femtomole level, which is 1000-fold less than the traditional MWP-based assays.

Integrating droplet-ESI-MS with existing MWPs screening workflow can extend the application of both systems. With this concept, we developed a ‘MS plate reader’ (MSPR). It can reformat 3072 samples from eight 384-well plates into oil-segmented droplets in 13 min (4.5 Hz), and then analyze them in 30 min (up to 2 Hz). Using MSPR, a label-free screen for cathepsin B inhibitors against 1280 chemicals was completed in 45 min (triplicate assay, 1.6 Hz). 11 novel inhibitors were identified and validated.

We also developed MS assays for two health beneficial enzymes: SIRT1 and SIRT6. Both assays are applicable to large-scale screenings using MSPR. An 80-compound pilot screening for SIRT1 modulators identified 4 strong inhibitors (> 50% inhibition), all of which were confirmed by dose-dependent experiments. A 25-compound test screening of SIRT6 modulators demonstrated the reliability of this assay by identifying the known activator (> 200% activation). It also showed that the single assay is as robust (Z-factor=0.6) as the replicated assay.

## **CHAPTER 1**

### **INTRODUCTION**

#### **High Throughput Screening**

High throughput screening (HTS) has been widely used in drug discovery and many related fields of biology and chemistry. To identify biologically active molecules, high throughput assays rapidly measure the activity of a large quantity of test compounds against certain biological targets. The increasing size of chemical libraries provided by combinatorial synthesis, the expanding pool of the targets resulted from our knowledge in life science, and the growing demand on rapid determination of physiochemical and pharmacological properties of screening hits urge more efficient assay techniques to be developed. Common strategies for HTS involve automation, parallelization and miniaturization. Many fully automated HTS liquid handling instruments are available on the market. For example, the Multidrop Combi (Thermo) can dispense microliter level reagents into 384-well plates within 10 s by using 8 parallel reagent transportation tubes; the Caliper pin tool and Biomek workstation can transfer all test compounds from a 384-

well-format library into assay plates in less than 30 s; the Mosquito HTS utilizes tiny disposable pins to reliably manipulate down to 10 nL liquid. Generally, high throughput is defined as testing 10,000 to 100,000 chemicals per day.<sup>1,2</sup> In current days, HTS technologies are not only used in drug discovery. Searching for catalysts for chemical reactions, initiators for polymerization reactions, and mutant proteins for protein engineering can all be benefitted from HTS technologies.

In drug discovery, the most important biomolecule targets include enzymes, G protein coupled receptors (GPCRs), nuclear hormone receptors and ion channels. Enzymes play significant roles in metabolic processes in life. Over or under-expression, and malfunctioning of enzymes often lead to diseases. Molecules that influence the activity of enzymes are frequently of interest as drug candidates or chemical biology tools. Nearly half of small molecule drugs on the market are enzyme inhibitors.<sup>1,3</sup> With our growing knowledge in life sciences, even more enzymes have been identified as potential therapeutic targets.<sup>1</sup> Thanks to the rapid development in combinatorial chemistry, we are supplied with increasingly large-size chemical libraries.<sup>4</sup> Creating novel HTS techniques to screen for enzyme modulators from those libraries is in demand. The biochemical assays for finding enzyme modulators are typically performed in 384- and 1536-well plates, in which the responses are measured by optical plate readers.<sup>5</sup>

Fluorescence detection systems are among the most popular readout methods for HTS. They are fast, robust, sensitive, and compatible with homogeneous and small volume assays.<sup>2</sup> Despite their many advantages, fluorescence detectors are limited by the reliance on incorporating labels or coupling reactions.<sup>6</sup> Extra effort and expense are



typically invested in an assay for generating fluorescent signals; however the success is not always guaranteed. Also, false positive signals which are caused by, for example, test compounds affecting the label instead of the target reactions and false negative signals which are caused by, for example, the label affecting the target reaction, are not rare and would cost more money and time in the screening.

Because of the aforementioned reasons, label-free analysis has gained increasing attention in HTS. There are several advantages for screening without optical labels: 1) those methods require minimized manipulation on the chemistry being studied; 2) they usually do not have artifacts such as auto-fluorescence of certain test compounds; 3) they allow studying the primary cells instead of genetically modified ones; 4) and the assays are less difficult to develop.<sup>6</sup> Several label-free screening approaches have been established, such as impedance, surface plasmon resonance (SPR), waveguides, photonic biosensor, and mass spectrometry.<sup>6,7</sup>

### **Mass Spectrometry for High Throughput Screening**

Mass spectrometry (MS) is a powerful label-free analyzer. The analysis is entirely based on the mass-to-charge ratio of the molecules of interest, and thus avoids the interference from artificial labels. MS has been revolutionized in the last two decades since the invention of electrospray ionization (ESI) (**Figure 1-1**) and matrix assisted laser desorption ionization (MALDI). Both methods are soft ionization methods, which

preserve the integrity of thermo-labile molecules. And due to their wide applicability in ionizing a variety of compounds, they have become dominant in MS.

With the improvement in the sensitivity, selectivity and speed of mass analyzers in recent years, both ESI-MS and MALDI-MS have been explored for HTS applications. For example, inhibitors of 3 enzymes were screened using MALDI-MS for less than 10 s/sample;<sup>8</sup> the commercial FlashQuant™ workstation (MDS Sciex) combining a patented MALDI source with a triple quadrupole MS can analyze 96 samples in 5 min (~3 s/sample); Rapidfire® (Agilent Technologies) which couples automated solid phase extraction (SPE) to ESI-MS/MS can analyze complex samples as fast as 6-10 s/sample.

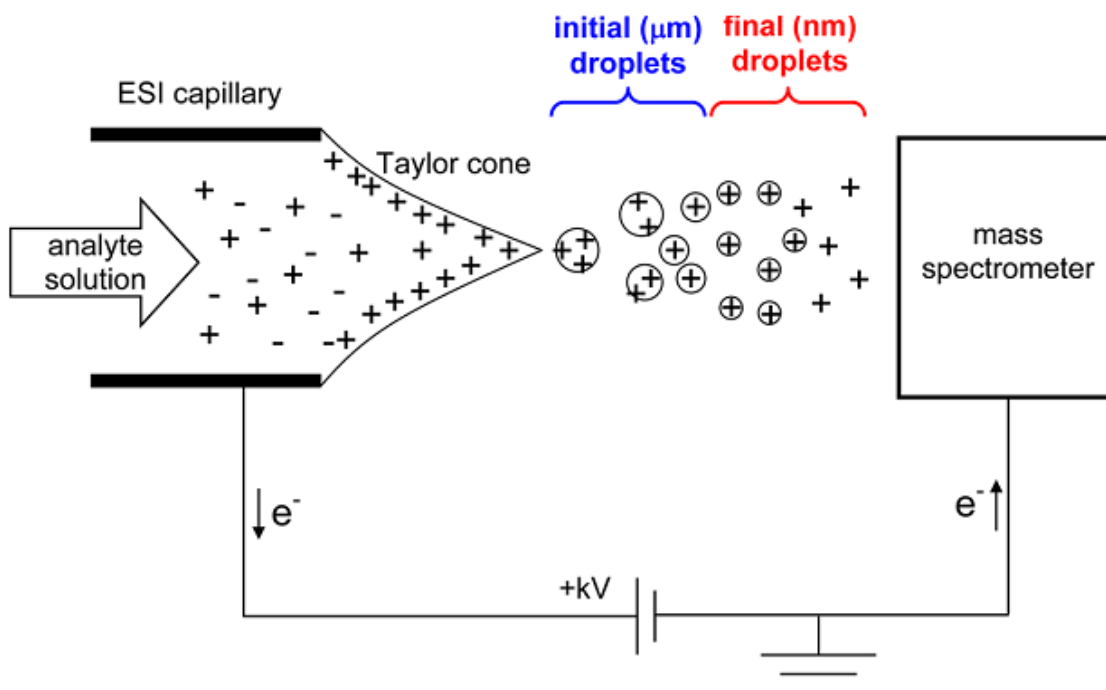


**Figure 1-1.** Scheme of electrospray ionization.<sup>9</sup> Reproduced with permission from ACS Publications.

Further improving the throughput of ESI-MS-based HTS is limited by the slow sample introduction approaches. Because of the ion suppression effect on the target analytes from non-volatile salts, matrix, surfactants, and co-existing molecules, sample preparation is often mandatory prior to the analysis. Also, if too many compounds are present in the sample, the dynamic range of MS will be limited because of the saturation of both ESI process and the detector. In that case, high performance liquid chromatography (HPLC) is required to disperse the molecules. Sample cleanup and chromatography improve MS performance, but they decrease the overall throughput.

To understand ion suppression, one should first understand the basics of ESI. Researchers have strived to unveil the true mechanism of ESI for many years. So far, three models: ion evaporation model (IEM), charge residue model (CRM) and chain ejection model (CEM) best explain how gas-phase ions are formed.<sup>9</sup> The ESI process is generally agreed to be: 1) a high voltage is applied onto the analyte solution inside a metal capillary (ESI needle). The solution at the tip of the needle is distorted into a Taylor cone. When the repulsion among charges overcomes the surface tension, a jet of liquid is emitted, containing many micrometer level droplets.<sup>10</sup> 2) Rapid solvent evaporation increases the charge density on shrinking droplets. When Rayleigh limit is reached, smaller offspring droplets are formed by fission. After cycles of solvent evaporation and fission, nanometer level, highly charged droplets are produced (**Figure 1-1**). 3) Gas-phase ions are formed following the aforementioned three mechanisms.

Low molecular weight molecules are often considered released to gas phase via IEM: The electric field on the nanometer droplet is sufficiently high to eject small

solvated ions from the surface. The solvation shell will be lost by collisions with background gas and finally the ion enters gas phase. Large globular species are transferred to gas phase by CRM: The highly charged nanometer droplet containing one analyte keeps evaporating until all solvent shells dry. Polymers and unfolded proteins undergo ESI by CEM: The hydrophobic chain migrates to the surface of the nanometer droplet. When one terminus is expelled into gas phase (like IEM), the rest of the chain is sequentially ejected out of the droplet carrying charges on it.<sup>9</sup>

Based on the ESI mechanisms, solvent evaporation, droplet shrinkage and analytes acquiring charges from the droplet surface are key factors affecting ESI efficiency. Ion suppression is caused by: 1) matrix components or any other compounds competing with target analytes for the access to the droplet surface; 2) interference competing with the analytes for surface charges; 3) interference co-precipitating the analytes; 4) high concentration non-volatile components increasing the viscosity and surface tension of the sample solution, which reduces the efficiency of desolvation; 5) salts forming adducts with the analyte, as a result spreading out the charge state, as well as the intensity.<sup>11-13</sup> Ion suppression increases the limit of detection of the target analyte, jeopardizes quantification, and compromises the reproducibility. To resolve this issue, sample cleanup, extended sample separation, introducing internal standard, and dilution are the main strategies.

Chromatography hyphenated to MS has become the standard scheme for MS analysis as they alleviate ion suppression from matrix and other sample components. The potential of chromatography-MS-based HTS has been explored for many years.<sup>14,15</sup>

Multiplex-liquid chromatography (LC)-MS system arranges several LC columns in parallel to improve the throughput<sup>16</sup>. Multiplexed affinity selection assesses protein-ligand interaction by coupling parallel size exclusion chromatography (SEC) to ESI-MS.<sup>17,18</sup> Rapidfire<sup>®</sup> system (SPE-ESI-MS/MS) analyzes each sample in ~8 s, and a multiplex assay has been shown to increase the throughput by 4 folds.<sup>19</sup> Parallel SPE has also been coupled to MS analysis, the throughput of which can be as high as 6 s/sample (0.18 Hz).<sup>16,20</sup> **(Figure 1-2 A-C)**

However, the long duty cycle of separation does not match the high scan speed of MS. If ion suppression is not severe and sufficient resolution can be achieved by the MS, chromatography or sample preparation can be bypassed. Some researchers have attempted to bypass the chromatography or sample preparation by using flow injection analysis (FIA). In FIA, a series of sample plugs are sequentially injected into a stream of aqueous buffer which flows into ESI-MS for continuous analysis. This approach has been successfully applied to monitor active ingredients in tablets<sup>21</sup> and metabolites in cell extract.<sup>22</sup> Utilizing an 8-probe liquid handling system, samples in a 96-well plate can be analyzed in 5 min (~3s/sample).<sup>23</sup> **(Figure 1-2 D)**

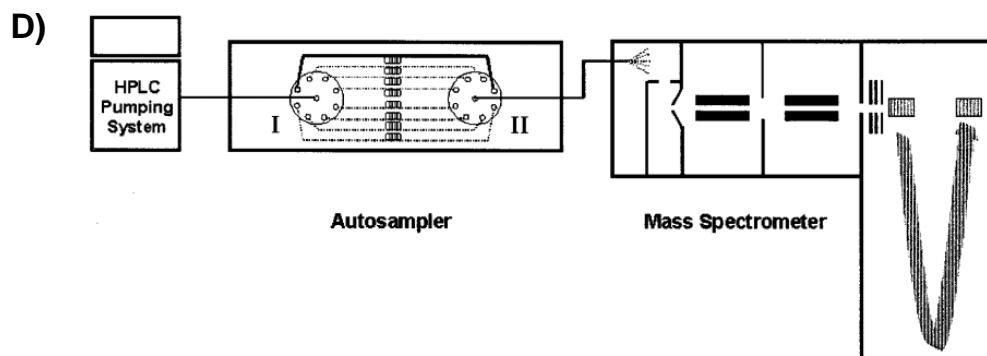
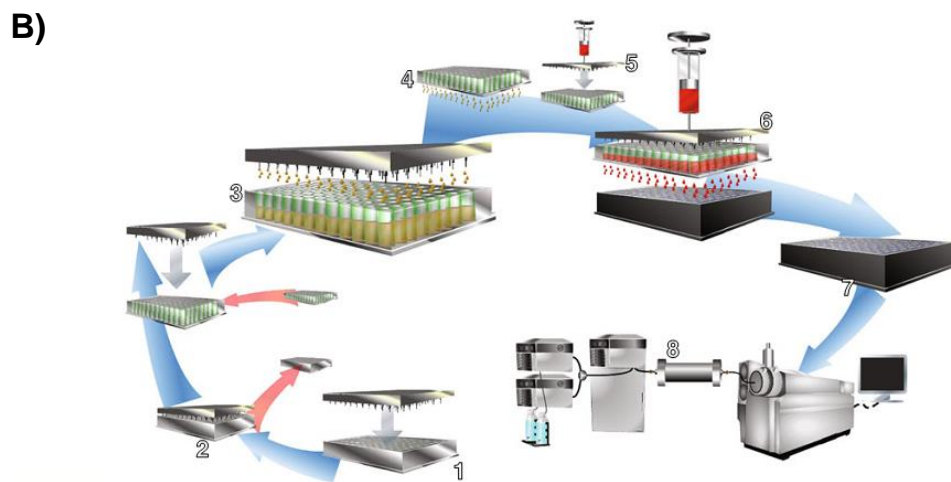
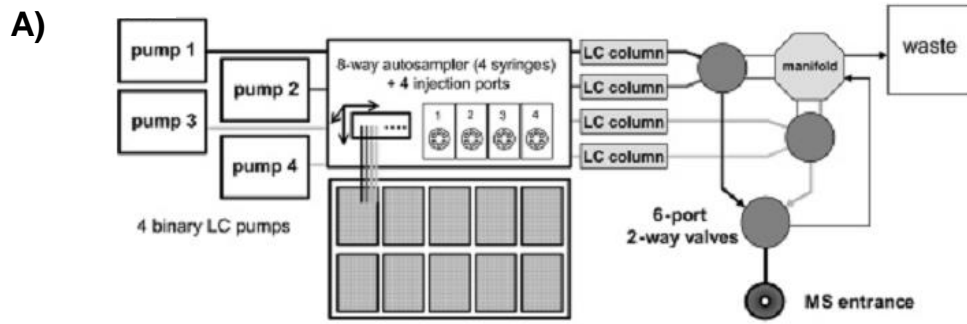


**Figure 1-2.** A) Instrument setup of a 4-way parallel LC-MS/MS for high throughput analysis.<sup>24</sup> B) Affinity-based MS binding screening (e.g., SpeedScreen). Ligands, target protein, and tracer/target ligand in a 96-well plate (1) are aspirated (2) and subsequently dispensed onto a 96-well filtration plate (3). After washing of the filtration plate (4) to remove nonbinders, methanol is added (5) to allow disruption and elution of binders (6) to another 96-well plate (7) for measurement by LC-MS (8). Quantification of the tracer/target ligand by triple-quadrupole MS allows determination of the percentage of tracer/target ligand displacement by unknown ligand binders<sup>25</sup>. C) On-line solid phase extraction using Rapidfire<sup>®</sup> (chem.agilent.com): the in-line automated cartridge switching can switch up to 12 reusable SPE cartridges (> 2000 injections/cartridge). The system can automate 63 plate handling and 60 hours unattended operation with 20000+ injections. D) High-throughput flow injection mass spectrometry system. System configuration includes the following: HP 1100 series HPLC system, Gilson 215 multiprobe liquid-handling system modified to include a Valco Cheminert model C5 eight-position column selection valve, and a Micromass LCT electrospray ionization time-of-flight mass spectrometer.<sup>23</sup> Reproduced with permission from the publishers.

Although FIA is promising in improving the MS analysis rate, it is limited by the nature of single phase continuous flow. Taylor dispersion is a phenomenon associated with laminar flow, because of which cross-contamination and band broadening are expected. Sample adsorption is also likely to happen because samples are in direct contact with the sample channel.<sup>26</sup> Those issues can be addressed by segmented flow system.

### **Segmented Flow for High Throughput Screening**

Segmented flow is a subcategory of droplet microfluidics. It is a flow system that compartmentalizes reagents in nanoliter to picoliter small droplets by the 2<sup>nd</sup> immiscible continuous phases, such as air and oil (**Figure 1-3**).<sup>27</sup> The use of perfluorinated oil has

gained increasing popularity because it is much less compressible than air. Also, most compounds are unlikely to partition into the fluorocarbons.<sup>28</sup> Protected by the immiscible carrier fluid, cross-contamination and adsorption-caused sample loss can be largely reduced. Compared with continuous flow, the size of each droplet is significantly lower. This feature is especially valuable for HTS as the bottleneck of a screening is often the reagent procurement.<sup>29</sup> **Table 1-1** shows the comparison of time and costs for a screening using traditional methods and droplet microfluidics.<sup>30</sup> The advances of microfluidic technology allow rapid and flexible control over the droplets. Droplet split,<sup>31</sup> reagent addition,<sup>32</sup> series dilution,<sup>33</sup> and sorting<sup>30</sup> have been realized (**Figure 1-4**).

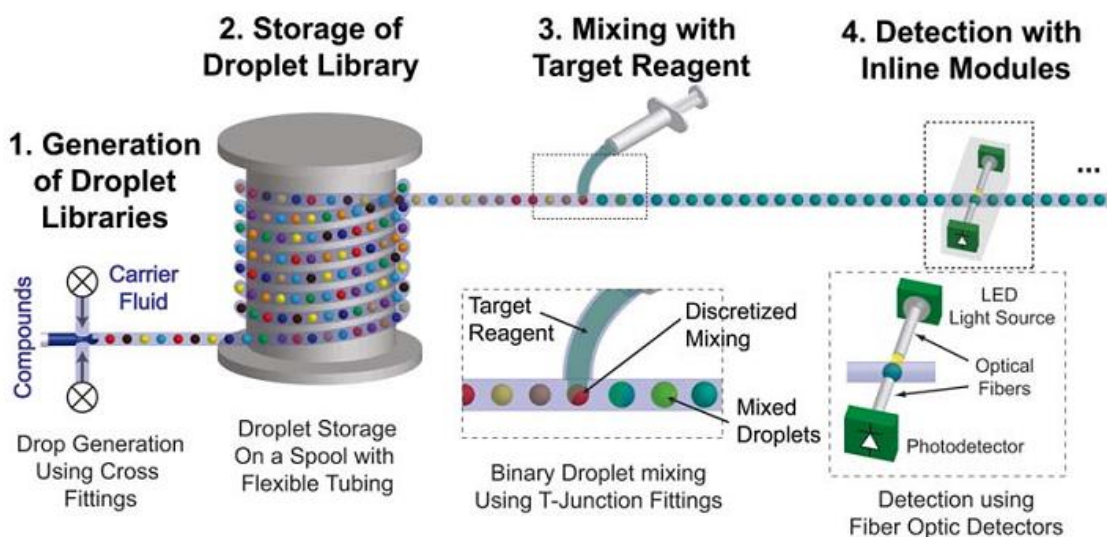


**Figure 1-3.** Segmented flow (droplets) and a modular approach of droplet-based screening system.<sup>27</sup> 1) Droplets are pinched off by injecting oil from both sides of a cross fitting into the sample stream; 2) droplet library is stored on a spool; 3) the reagent is injected into individual droplet through a T-junction to initiate reactions; 4) Fiber optic detectors monitor the components of droplets in-line. Reproduced with permission from RSC Publishing.



**Table 1-1.** Comparison between traditional HTS and droplet-microfluidic HTS.<sup>30</sup>

Reproduced with permission from National Academy of Sciences.

	<b>Robot</b>	<b>Microfluidic drops</b>
<b>Total reactions</b>	$5 \times 10^7$	$5 \times 10^7$
<b>Reaction volume</b>	100 $\mu$ L	6 pL
<b>Total volume</b>	5000 L	150 $\mu$ L
<b>Reaction/day</b>	73000	$1 \times 10^8$
<b>Total time</b>	2 years	7 h
<b>Number of plates/devices</b>	260000	2
<b>Cost of plates/devices</b>	\$520000	\$1
<b>Cost of tips</b>	\$10 million	\$0.3
<b>Amortized cost of instruments</b>	\$280000	\$1.7
<b>Substrate</b>	\$4.75 million	\$0.25
<b>Total cost</b>	\$15.81 million	\$2.5

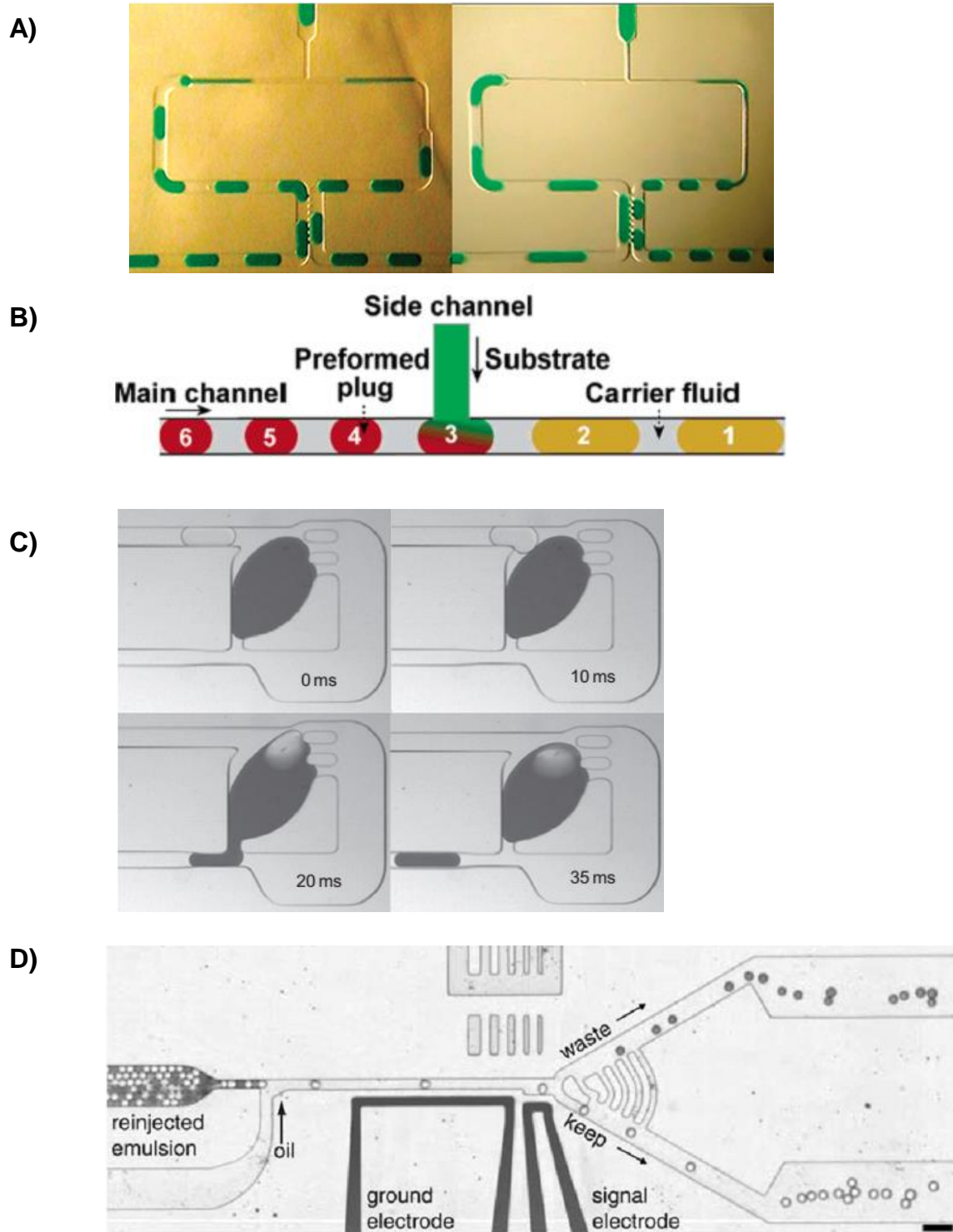


**Figure 1-4.** A) Droplet splitting to different ratios by constructing outlet channels with different inner diameters;<sup>31</sup> B) Scheme of reagent addition into droplets;<sup>32</sup> C) Serial dilution using microfluidic dilutor: a buffer droplet approaches (0 ms), contacts the

mother droplet (10 ms), coalesces and activates the soft valve (20 ms), and finally generates an output droplet (35 ms). After a series of buffer droplets passing by, the output droplets contain gradually decreased concentration of the sample in the mother droplet;<sup>33</sup> D) Droplet sorting: the drops flow as a solid plug to a junction where oil is added to separate the drops. The light drops contain 1 mM fluorescein, and the dark contain 1% bromophenol blue. Fluorescence levels are detected as the drops pass a laser focused on the channel at the gap between two electrodes. When sorting is on, the light drops, which are brighter than the threshold level, are sorted by dielectrophoresis into the bottom channel.<sup>30</sup> Reproduced with permission from publishers.

In recent years, sophisticated droplet microfluidic devices have been built. A variety of high throughput assays were tried with them. For example, new mutant proteins were screened at kilohertz from directed evolution,<sup>30</sup> deacetylation reaction conditions were optimized with only 20  $\mu\text{g}$  reagent consumption,<sup>34</sup> a screening for photosensitizer activity were carried out with multi-parameter detection,<sup>35</sup> protein crystallization conditions were screened with nanoliter level protein solution use,<sup>36</sup> high throughput dose dependent experiment was performed based on confining concentration gradient into droplets, arranged in a serial fashion within a channel.<sup>37</sup>

Interfacing segmented flow with ESI-MS has been explored for several years. Some groups extract the aqueous sample out of droplet system before analysis.<sup>38,39</sup> Our group is pursuing a similar path but we instead directly infuse droplets into a ESI source.<sup>40</sup> An inhibitor screening for acetylcholinesterase (AChE) was performed in droplet fashion.<sup>41</sup> In the study, reaction mixtures were deposited into a 96-well plate and then covered by a thin layer of fluorinated oil: FC-40. Samples were aspirated as air-segmented plugs into a piece of Teflon tubing by the force of a pulling syringe. The inner surface of the tubing was wet by FC-40. The tubing movement was controlled by an

XYZ-positioner (**Figure 1-5**). A linear ion trap was used for monitoring the intensity of the reaction product: choline. The inhibited reactions showed low intensity of choline while non-inhibited reactions showed similar intensity with the negative control (**Figure 1-6**). This small screening proved that ESI-MS is amenable for HTS by employing segmented flow as sample introduction method. However, some improvement needs to be made: 1) air-segmented droplets are prone to coalescence when being pushed in the tubing due to the compressibility of the air; 2) the reagent consumption was high because reactions were conducted in a standard 96-well plate; 3) the salt-free buffer used in this AchE assay cannot be generalized because many proteins are only active in the buffers which may have ion suppression effect on ESI-MS.

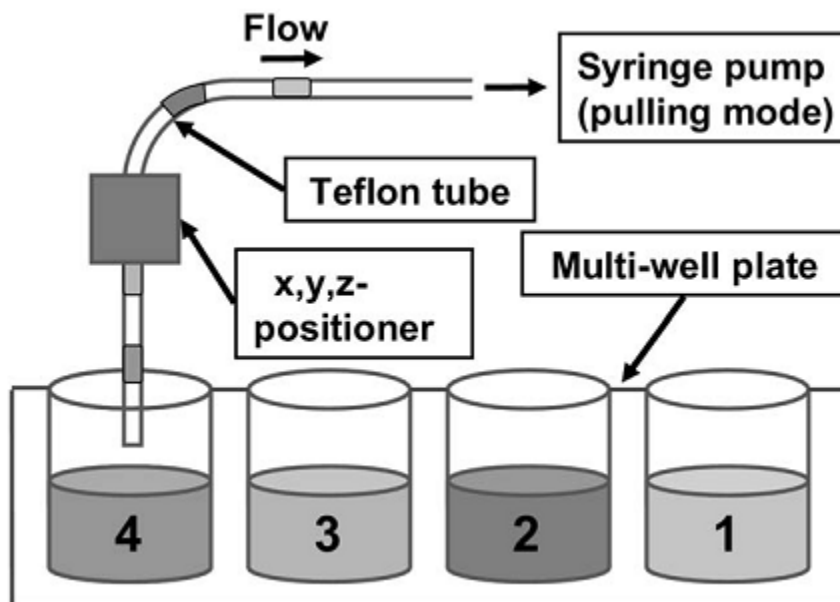


**Figure 1-5.** Diagram of reformatting acetylcholinesterase assays into air-segmented plugs. The array of sample plugs were prepared by dipping the tip of a 75  $\mu\text{m}$  i.d. Teflon tubing prefilled with Fluorinert FC-40 into sample solution stored in a multiwell plate, aspirating a desired volume, retrieving the tube, aspirating a desired volume of air, and moving to the next well until all samples were loaded. Movement of the tubing was controlled with

an automated micropositioner and sample flow was controlled with a syringe pump connected to the opposite end of the tubing.<sup>41</sup> Reproduced with permission from Elsevier Inc..

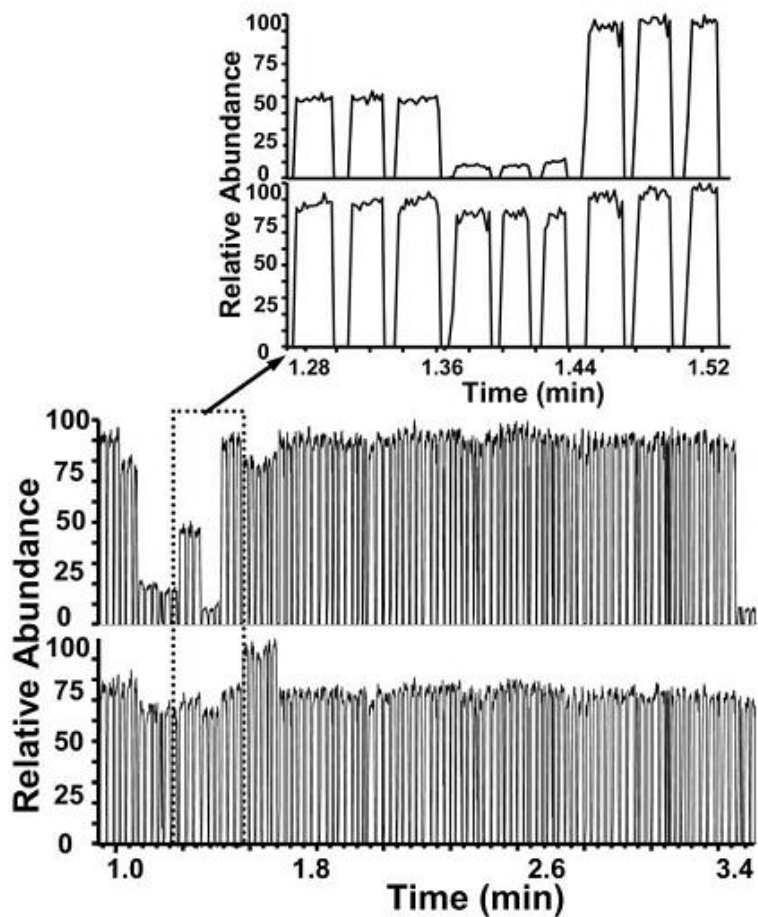


**Figure 1-6.** Screening of AchE inhibitors (in triplicates). The top droplet trace is the assay product choline, and the bottom one is the internal standard. Inset shows one mildly inhibited and one strongly inhibited reaction.<sup>41</sup> Reproduced with permission from Elsevier Inc..

Replacing air with oil can address the coalescence issue. Perfluorinated oils are preferred in segmented flow because they are not compressible, and most compounds are insoluble in them.<sup>28</sup> Our group has evaluated the compatibility of different perfluorinated oils with ESI-MS. The result showed that FC-40 and perfluorodecalin (PFD) do not generate signal at up to 1.5 kV in nanospray mode, and up to 3 kV in regular ESI mode.<sup>42</sup> PFD or FC-40 segmented droplets can be directly infused into ESI-MS without having interfering oil signals. In all experiments described in this dissertation, sample droplets were segmented by PFD. To reduce sample consumption, one can miniaturize the whole screening by conducting reactions inside droplets, or utilize high density MWPs. In this dissertation, both approaches are described (see screening workflow in **Figure 1-7**). A larger scale screening was performed with the second approach. To facilitate direct analysis of assays consisting of components that may disrupt ESI process, sample cleanup or sample dilution is required. Chapter 5 and 6 discuss the operation in details.

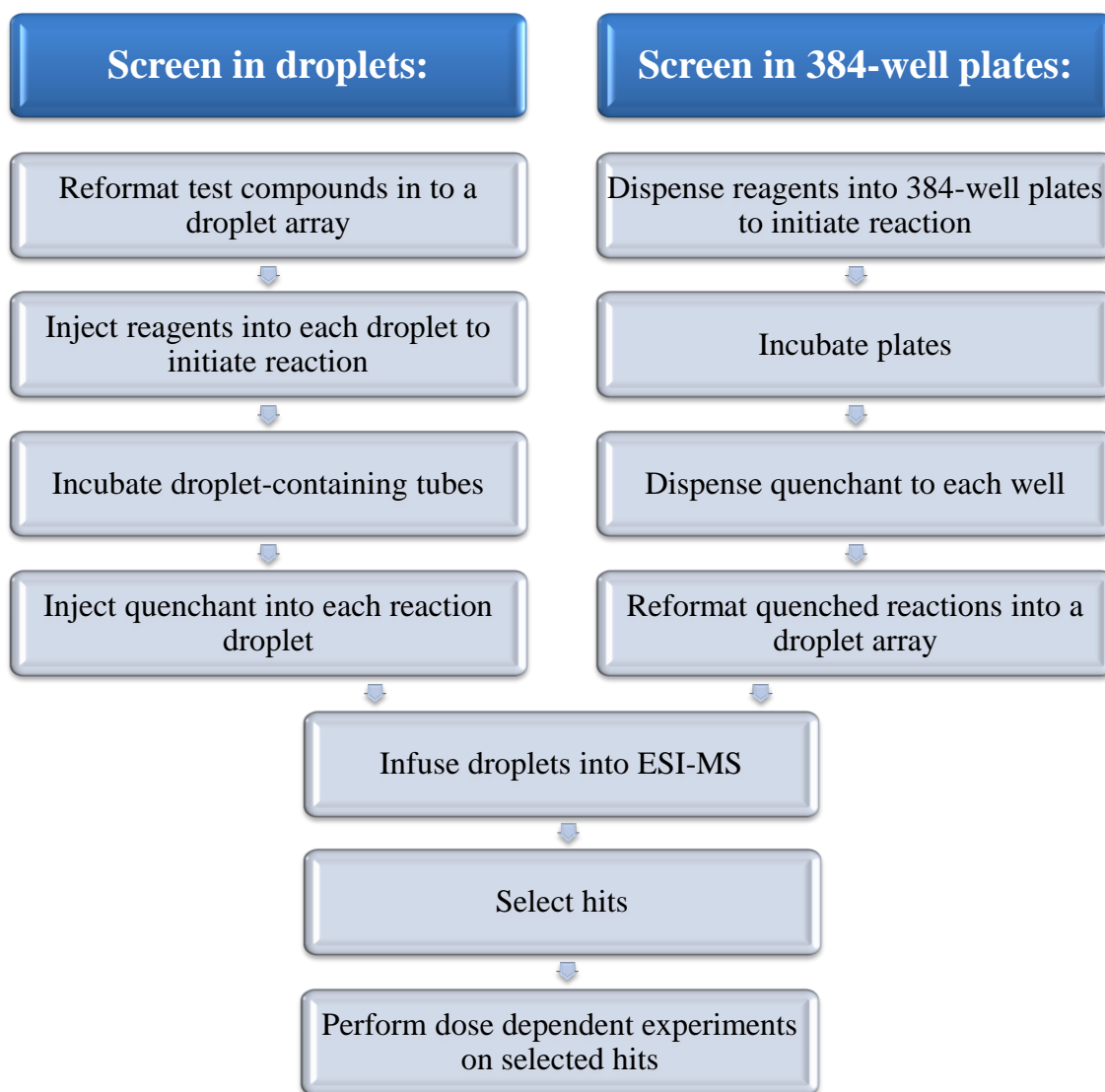


**Figure 1-7.** Flow charts for in-droplet screening (left) and high density MWP-based screening (right).

### Cathepsin B

Cathepsin B belongs to the cathepsin family, which is a group of cysteine proteases of the papain family. They are predominantly endopeptidases which localize in

lysosomes of cells.<sup>43</sup> Cathepsin B is a 30 kD protein. It is constitutively expressed for protein turnover. Functioning as an endopeptidase, cathepsin B prefers substrates with large hydrophobic side chains and two N-terminal residues to the hydrolysis site. Cathepsin B can also act as an exopeptidase which removes dipeptides from the C-terminus of proteins and peptides.<sup>44</sup> Cathepsin B is considered a potential therapeutic target because its relationship with several diseases has been established.<sup>45</sup> The increase in expression of cathepsin B has been consistently found in human tumors, especially in epithelial cells of premalignant lesions.<sup>46</sup> To date, the tumor proliferation, angiogenesis and metastasis in brain, lung, prostate, breast, and colon have been linked to cathepsin B overproduction.<sup>47</sup> The expression of cathepsin B in such cancers are often positively correlated with a poor prognosis for patients.<sup>48</sup> Inhibiting cathepsin B along with other cathepsins is able to retard the growth of pancreatic islet tumors in mice.<sup>49</sup> Specifically inhibiting cathepsin B has been showed to reduce metastasis of murine breast cancer.<sup>50</sup> Aside from cancer, cathepsin B has been found to promote various viral infection diseases, including Ebola and SARS. It also plays a role in trematodes,<sup>51</sup> rheumatoid arthritis<sup>52</sup> and Alzheimer's disease<sup>53-55</sup>. With such broad implication with diseases, inhibition of cathepsin B is always considered to be holding great therapeutic potential.

## **Sirtuins**

Sirtuins are a class of evolutionarily conserved nicotinamide adenine dinucleotide (NAD<sup>+</sup>)-dependent deacetylases, the expression of which are responsive to diet and



environmental stress. Human sirtuins include 7 members: SIRT1 to SIRT7. They control a wide range of cellular processes including gene silencing, regulation of p53, fatty acid metabolism, cell cycle regulation and life span extension.<sup>56,57</sup> Last decade has witnessed growing attention towards sirtuins for their regulatory role in metabolism and aging. Numerous studies have been carried out to reveal the function of each individual sirtuin. The results are depicted in **Figure 1-8**.<sup>56</sup>

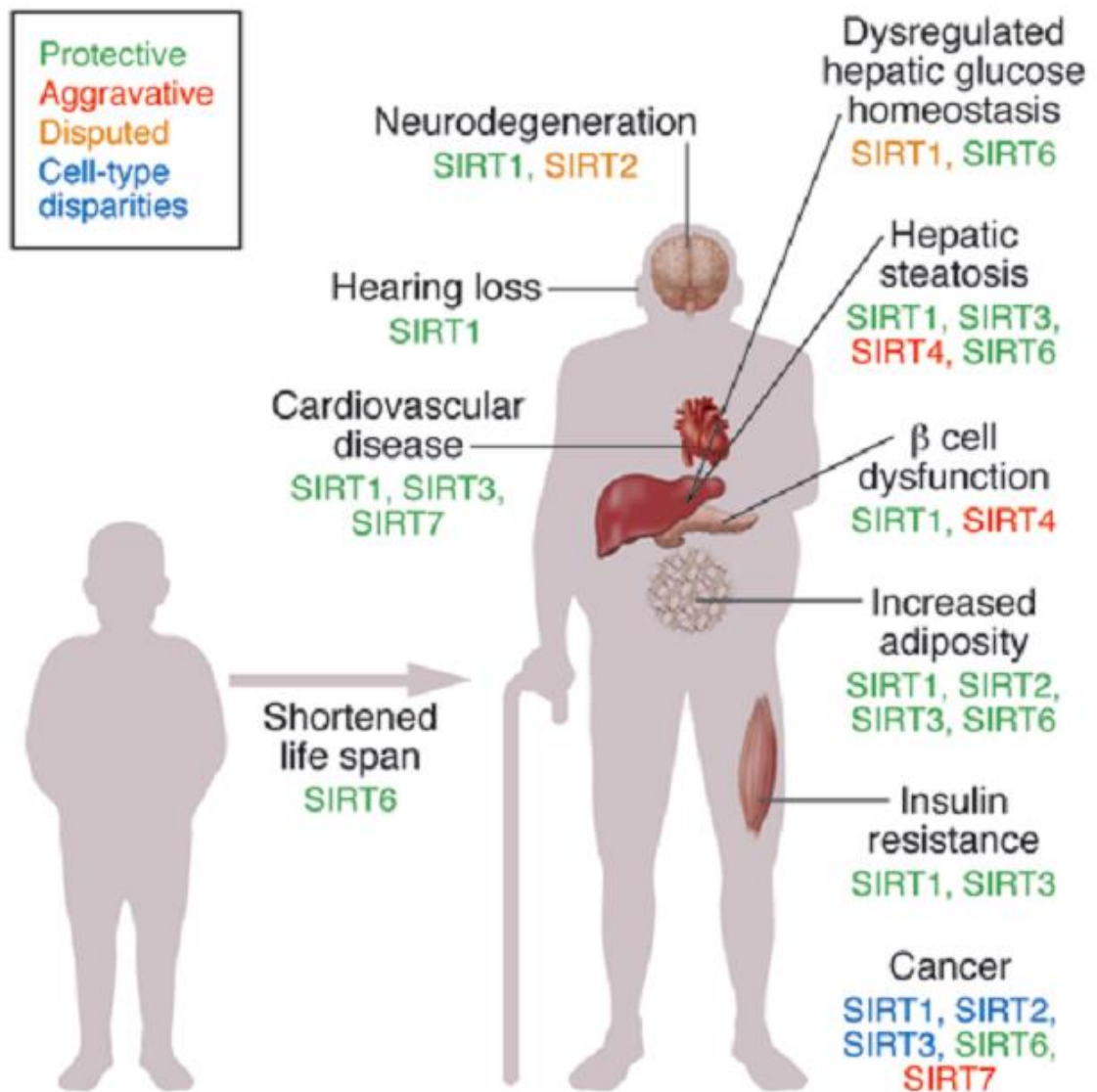


**Figure 1-8.** The sirtuin family’s role in aging and age-associated pathologies. The sirtuin isoforms with substantial data indicating either a protective or aggravative role for specific age-related diseases are indicated.<sup>56</sup> Reproduced with permission from The American Society for Clinical Investigation.

SIRT1 is the most extensively studied sirtuin. It deacetylates various transcription factors and enzymes, hence regulates chromatin structure, transcription, apoptosis,

tumorigenesis, energy expenditure, and oxidative stress. It relieves metabolic dysfunction in numerous tissues, including liver, muscle, heart, and fat tissue (**Figure 1-9**).<sup>56,57</sup> In vivo studies have proved that SIRT1 can prolong murine lifespan, suppress certain types of cancer, type 2 diabetes, neurodegenerative diseases, and many other aging-related diseases.<sup>56,58-60</sup>

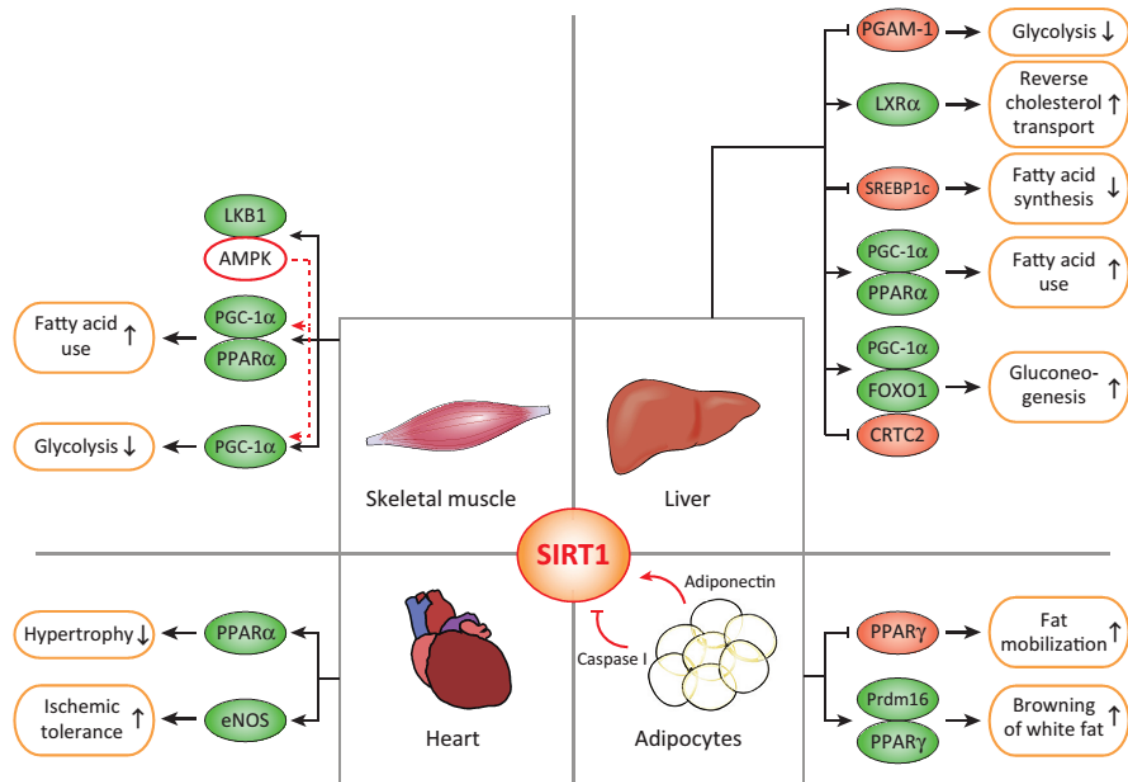


**Figure 1-9.** SIRT1 mediates metabolic benefits in various tissues, such as liver, heart, white adipose tissues (WAT), and skeletal muscle. In general, SIRT1 supports gluconeogenesis, inhibits glycolysis, promotes fatty acid oxidation, regulates cholesterol homeostasis, and protects against cardiac hypertrophy. Targets that directly activated by SIRT1 are shown in green, and those inhibited are in pink.<sup>57</sup> Reproduced with permission from Elsevier Inc..

Because of the promising therapeutic value of SIRT1 activation, people have passionately searched for SIRT1 modulators. A series of SIRT1 activating compounds (STACs) were discovered based on a fluorescent screening. The activation mechanism is promoting substrate-protein binding. Most of the STACs are plant-based polyphenols, including resveratrol, a molecule found in red wine. In the fluorescent assay, the synthetic fluorogenic peptide substrate is sensitized to fluorescence developer after being deacetylated by SIRT1 (**Figure 1-10**). The developed fluorophore indicates the level of deacetylation.<sup>59</sup> Corroborating the finding is considerable amount of studies that showing improved metabolic syndrome by STACs.<sup>60-66</sup> However, further investigation of the activation mechanism revealed that STACs indeed enhance the binding and deacetylation of the fluorogenic substrate, but exert no effect on native peptides.<sup>56,67-70</sup> Although later studies have argued that the bulky, hydrophobic fluorophore activates SIRT1 allosterically,<sup>71,72</sup> which might mimic hydrophobic moieties of certain natural substrates, the true relations between STACs and SIRT1, and their beneficial effect in aging-related diseases are still under debate.

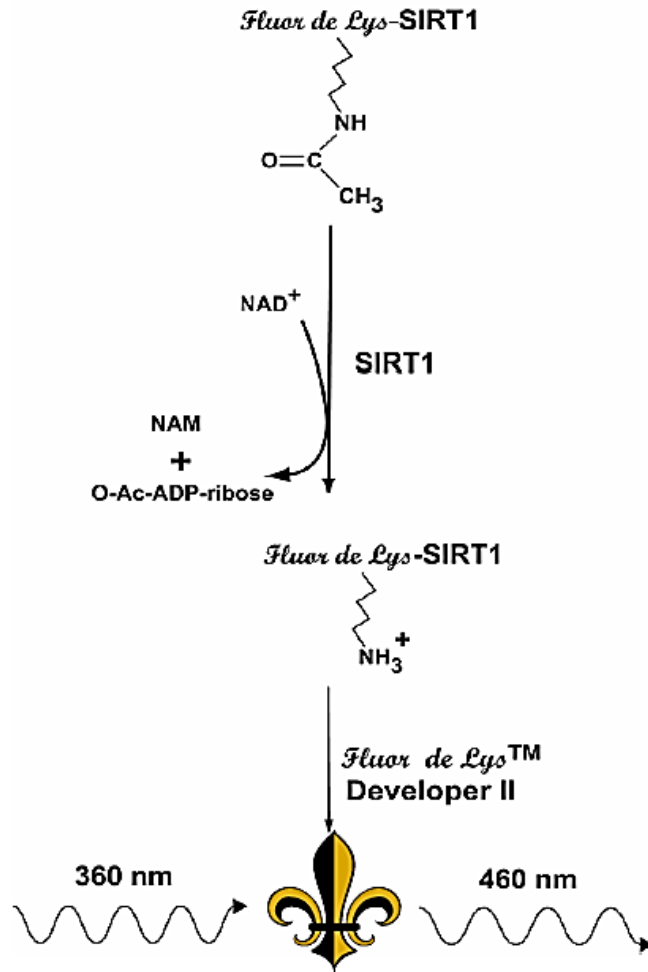


**Figure 1-10** Fluor de Lys<sup>®</sup> fluorescent assay: the Fluor de Lys<sup>®</sup> SIRT1 Substrate, which contains a peptide comprising amino acids 379-382 of human p53 (Arg-His-Lys-Lys(Ac)) is deacetylated by SIRT1 at present of NAD<sup>+</sup>. Treating with the Fluor de Lys<sup>®</sup> Developer II, the deacetylated peptide produces a fluorophore (<http://www.enzolifesciences.com>).

Sirtuin 6 (SIRT6) is predominantly localized inside the nucleus and associated with the chromatin. It was initially categorized as a mono adenosine diphosphate (ADP) ribosyl transferase.<sup>73</sup> In 2008, the deacetylation of histone H3 lysine 9 (H3K9(Ac)) by SIRT6 was discovered. This activity was proposed to contribute to the telomere protection capability of SIRT6.<sup>74</sup> Later, another substrate, histone H3 lysine 56

(H3K56(Ac)) was confirmed. Deacetylation of H3K56(Ac) is also linked to maintaining the stability of telomeric chromatin during cell cycle.<sup>73</sup> In 2012, researchers noticed that SIRT6 overexpression can extend the lifespan of male mice. It has been the first direct relationship between sirtuins and longevity.<sup>75</sup> The comprehensive interrogation of all possible functions of SIRT6 has been carried out ever since. Increasing evidence shows that SIRT6 participates in a variety of cellular pathways by deacetylating a broad spectrum of post translational modifications: it stabilizes DNA in most tissues, especially in liver, heart and muscle; it helps maintain normal glucose homeostasis; it reduces cell apoptosis and senescence by deacetylating NF- $\kappa$ B; it suppresses cancer initiation but on the other hand helps the survival of already-formed tumors;<sup>76</sup> it controls partitioning circadian transcription,<sup>77</sup> and so on (**Figure 1-11**).

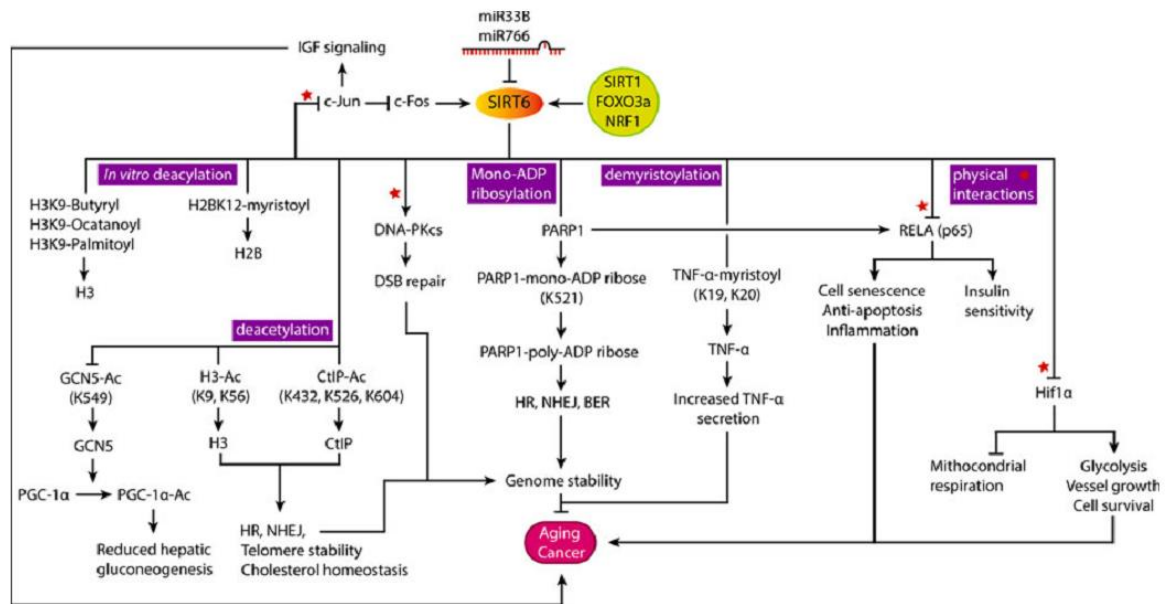


**Figure 1-11.** SIRT6's substrates and physiological impact.<sup>76</sup> Reproduced with permission from Springer Publishing.

Intrigued by the broad sphere of health benefits (though conflicting effects exist), the search for SIRT6 modulators have been attempted recently<sup>76</sup>. However, due to the low deacetylation activity, it is hard to develop a reliable SIRT6 assay, thus very few valid modulators have been established. In 2013, one research group reported that SIRT6 can hydrolyze an endogenous long-chain fatty acylated protein (lysine 19 and lysine 20 on TNF- $\alpha$ ) with high efficiency. Later, they found that this deacetylation activity is independent on the protein sequence.<sup>78</sup> Based on this breakthrough discovery, another research group found that the low deacetylation activity of SIRT6 can be elevated by fatty acids, which are the first type of SIRT6 activators being reported. And such activation effect is exclusively in SIRT6 (**Figure 1-12**).<sup>79</sup> Very recently, SIRT6 modulator screenings based on fluorogenic assays using H3K56 and myristoylated peptide as substrates have been published, a handful of common sirtuin inhibitors were proved to slightly inhibit SIRT6.<sup>80,81</sup>

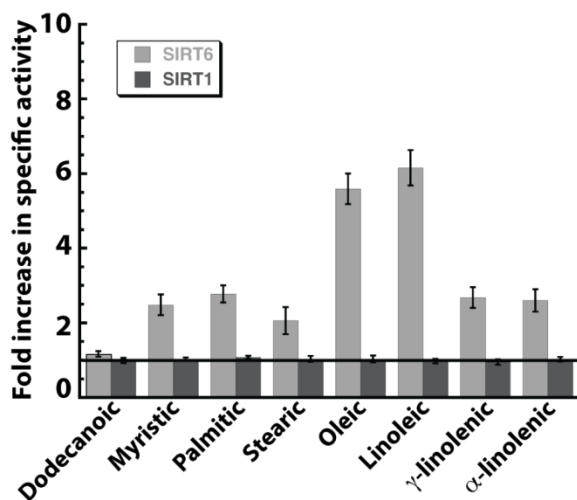


**Figure 1-12.** Sirtuin activity in the presence of free fatty acids. Fold change in SIRT1 and SIRT6 deacetylase activity was monitored in the presence of various fatty acids and compared to a reaction without fatty acid. SIRT1 (dark gray) and SIRT6 (light gray) were incubated with 70  $\mu\text{M}$  H3K9Ac peptide and 0.5 mM  $\text{NAD}^+$  in the presence of 100  $\mu\text{M}$  fatty acid and analyzed by HPLC.<sup>79</sup> Reproduced with permission from American Society for Biochemistry and Molecular Biology.

## Dissertation Overview

The research presented in this dissertation aims at elaborating the work previously accomplished by the Kennedy group. Droplet-ESI-MS system is a novel high throughput screening platform. Efforts have been made to miniaturize a screening by conducting reactions inside droplets through microfabricated reagent addition chips; hyphenate the system with well-established, commercially available, MWP-based high throughput screening workflow; develop three enzymatic assays which can be directly analyzed by ESI-MS with minimum sample preparation; apply the miniaturized all-droplet system and integrated MWP-to-droplet system to enzyme modulator screenings.

Chapter 2 discusses the potential to reduce reagent use by performing enzymatic assays inside nanoliter level droplets. In this work, we developed an all-droplet system coupling to ESI-MS which realized rapid label-free cathepsin B inhibitor screening with ultralow sample consumption and a superb Z-factor ( $\sim 0.8$ ). Multistep reactions were carried out inside 100 test compound droplets of 8 nL each and the result was analyzed by ESI-MS at up to 0.77 Hz. Microfabricated PDMS tees were used for adding the enzyme, substrate and quenchant into the droplets array for each step. Teflon tubes were used as storage and incubation vessels. By using this all-droplet system, 0.8 picomoles of



each test compound, 1.6 picomoles of substrate and 5 femtomoles of enzyme were consumed per reaction, which was ~10000-fold less than a MWP-based approach. This work was published on *Analytical Chemistry* in 2012.<sup>82</sup>

Chapter 3 presents a work integrating the droplet-ESI-MS scheme to MWP-based high throughput screening workflow. We developed a ‘MS Plate Reader’ which coupled standard MWP-based HTS workflow to droplet ESI-MS. The MS plate reader can reformat 3072 samples from eight 384-well plates into nanoliter droplets segmented by an immiscible oil at 4.5 samples/s and sequentially analyze them by MS at 2 samples/s. Using the system, a label-free screen for cathepsin B modulators against 1,280 chemicals was completed in 45 min with a high Z-factor ( $> 0.72$ ) without a false positive (24 of 24 hits confirmed). The assay revealed 11 structures not previously linked to cathepsin inhibition. For even larger-scale screening, reformatting and analysis could be conducted simultaneously, which would enable more than 145000 samples to be analyzed in one day. This work was published on *Analytical Chemistry* in 2014.<sup>83</sup>

Chapter 4 discusses the development of an ESI-MS-compatible SIRT1 assay. The assay is suitable for high throughput modulator screening. To enable direct ESI-MS analysis, SIRT1 was dialyzed into a buffer which does not affect the MS analysis of any molecules, and the deacetylation reaction was conducted in such buffer. The reaction yield was comparable to using the traditional Tris buffer. The assay conditions were optimized by enzyme kinetic studies, and validated by an 80-compound library screening. The high Z-factor (0.7) and high confirmation rate (all 4 inhibitor hits confirmed) indicate a reliable assay.

Chapter 5 shows that the droplet-ESI-MS system can be applied to another enzyme: SIRT6. Two SIRT6 assays were developed using two different substrates. Because for substrate H3K9(Ac), the activity of SIRT6 is low in most MS-compatible buffers, we ran the reaction in the original Tris buffer and then diluted the mixture to the extent that buffer components have little ion suppression effect on the reaction product, and the product is not too diluted for a quantifiable measurement. A test screen showed reliable quantification for this dilution approach. The standard deviation of negative control was low, and the known activator was identified. Aside from that, we confirmed that screening without replicates can yield similar results with a triplicated one. Though the analysis rate for each droplet decreased from 2 Hz (maximum rate) to 1 Hz for a more reliable readout, reducing the number of droplets for each reaction by 2/3 ended up with 33% improvement in the overall throughput. SIRT6 hydrolyzes another substrate H3K9(decanoyl) with high efficiency. For that, we elected to use similar MS-compatible condition described in Chapter 4. A SIRT6 deacylation assay was also developed for large-scale droplet-ESI-MS-based screening.

Chapter 6 discusses the possible improvement for current systems, including reducing the carryover of reagent addition chip, scaling up the screening using all-droplet system, fully automating MS plate reader, integrating sample cleanup in to droplet-ESI-MS, tracking a screen, and developing custom data analysis software.

## **CHAPTER 2**

# **LABEL FREE SCREENING OF ENZYME INHIBITORS AT FEMTOMOLE SCALE USING ALL-DROPLET-ELECTROSPRAY IONIZATION-MASS SPECTROMETRY SYSTEM**

### **Introduction**

Droplet-based microfluidics has emerged as a powerful tool for analysis of low volume samples.<sup>84,85</sup> In this approach, samples are compartmentalized within an immiscible fluid that is manipulated within a microfluidic channel or tube. This technology is descended from continuous flow analysis,<sup>86</sup> commonly used for automated analysis prior to multi-well plates (MWP) and flow injection analysis. When droplets are large enough to span the walls of the channel, they form plugs and the resulting system is referred to as segmented flow. Droplets can be moved through a microfluidic system by pressure-induced flow where operations such as reagent addition,<sup>32,87,88</sup> dilution,<sup>33</sup> splitting,<sup>31,89</sup> or sorting<sup>90,91</sup> may be performed. A variety of chemical measurements

including enzymatic activity,<sup>41,92,93</sup> enzyme kinetics,<sup>94-97</sup> and cell-based assays<sup>98-100</sup> have been developed for droplet format.

Salient features of droplet systems are their small sample volumes (picoliter to nanoliter volumes are typical) and high throughput (e.g., reagents can be added to segmented samples at rates as high as 10 Hz<sup>27</sup>). These properties make droplet microfluidics attractive for screening applications. The small scale can greatly reduce cost of reagents compared to screens performed at microliter volumes in MWP while the high speed enables the necessary throughput. Droplet microfluidics have been used for screening for engineered proteins,<sup>30</sup> protein crystallization,<sup>36</sup> and reaction catalysts.<sup>101</sup>

Most chemical measurements in droplets have relied on optical detection such as fluorescence or colorimetric changes. While such methods are powerful and rapid (allowing analysis at up to kilohertz rates<sup>30</sup>), they are restricted to single component detection unless wavelength resolution is used. More importantly, they require engineering an optical change into the reaction being screened by use of either labels or coupled reactions. Incorporation of optical properties can slow investigation of a new target and in some cases may not be feasible. Even when feasible, labels can affect the reaction being studied, generate false signals,<sup>102</sup> and add expense to the screen because of increased reagent cost. For these reasons, label-free screening is desirable.<sup>6,7,102</sup>

A potentially powerful method for label-free screening at droplet scale is mass spectrometry (MS). In one study, segmented samples were deposited onto a plate for matrix-assisted laser desorption ionization (MALDI)-MS analysis.<sup>34</sup> This approach

allowed optimization of a deacetylation reaction using just 20  $\mu\text{g}$  of substrate illustrating the feasibility of screening at reduced scale. Electrospray ionization (ESI) would be a valuable complement to MALDI methods. Several techniques for interfacing droplets to ESI-MS have been reported.<sup>38-40,103</sup> Methods involve either extraction of droplets into a stream that flows to the ESI source or directly passing the segmented stream into the ESI source. While either approach may be used, we favor the latter because it is simple and allows samples to remain encapsulated up to the point of detection to avoid dilution and reduce potential for carry-over. Segmented flow ESI-MS has been used to monitor chemical reactions<sup>103</sup> and for analysis of fractions collected from capillary LC columns.<sup>42</sup> It has also been used to screen an enzymatic reaction that did not involve a color change (acetylcholinesterase catalyzed hydrolysis of acetylcholine<sup>41</sup>). In that study however, the reaction was performed in MWP-scale and then reformatted for segmented flow, therefore miniaturization of the reaction was not realized.

In this work we seek to demonstrate the potential for label-free screening of reactions at nanoliter scale using segmented flow ESI-MS. The system is tested using Cathepsin B catalyzed proteolysis as a model reaction. Inhibitors of this protein are of interest for treatment of Alzheimer's disease,<sup>104</sup> various types of cancer,<sup>105</sup> arthritic disease,<sup>106</sup> and trematode infection.<sup>107</sup> This enzyme is presently screened using a fluorogenic substrate, nevertheless it provides a useful test case for segmented flow ESI-MS.

## Experimental Section

**Chemicals and Materials.** Unless otherwise specified, all solvents were purchased from Honeywell Burdick & Jackson (Muskegon, MI) and were certified ACS grade or better. All reagents were purchased from Sigma Aldrich (St. Louis, MO).

**Droplet Generation from MWP.** Oil-segmented sample droplets were generated by sampling from a MWP using a protocol described previously (**Figure 2-1**).<sup>40</sup> Samples were pulled into a 150  $\mu\text{m}$  i.d.  $\times$  360  $\mu\text{m}$  o.d. Teflon tube (IDEX Health and Science, Oak Harbor, WA) connected to a 100  $\mu\text{L}$  Hamilton syringe (Fisher Scientific, Pittsburgh, PA) mounted on a PHD 200 programmable syringe pump (Harvard Apparatus, Holliston, MA). The syringe and Teflon tube were pre-filled with perfluorodecalin (PFD, 95% purity, Acros Organics, NJ). To fill the tube with oil-segmented droplets, a computer-controlled XYZ-positioner (built in-house from XSlide assemblies, Velmex Inc., Bloomfield, NY) was used to move the inlet of the Teflon tube from sample to sample on the MWP while the syringe was withdrawing at 150-180 nL/min. The samples were covered with PFD to prevent aspiration of air as the tube moving from sample to sample. (The edges of the MWP were built-up to 3 mm height using epoxy to hold PFD over the wells.) Droplets with 5 to 15 nL volume separated by 10-20 nL oil were produced by controlling the time that the tube dwelled in sample or oil. The relative standard deviation (RSD) of droplet size was  $< 5\%$ .

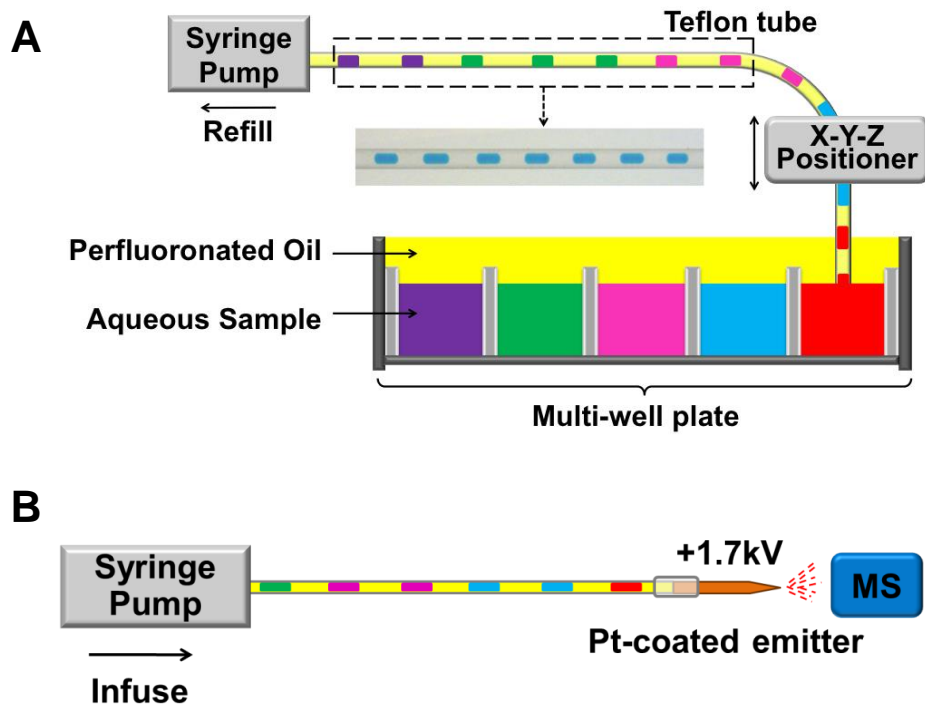


**Figure 2-1** A) Diagram of oil-segmented droplet generation from a MWP. The XYZ-positioner causes the Teflon tube to dwell in sample or oil for predetermined time, and then move to another well. The syringe pump operates in refill mode at a constant flow rate. B) Diagram of ESI-MS analysis of sample droplets. The syringe drives droplets into the ESI source through a Pt-coated emitter. +1.7 kV is applied on the emitter.

**MS Analysis.** Teflon tubes containing segmented samples were connected to a 75  $\mu\text{m}$  i.d. Pt-coated fused-silica electrospray emitter (FS-360-75-30-CE, New Objective, Woburn, MA) pulled to 30  $\mu\text{m}$  i.d. at the tip (**Figure 2-1B**). The emitter was mounted onto the nanospray source of the mass spectrometer. A syringe pump (Fusion 400, Chemyx, Stafford, TX) operated from 0.75 to 1.8  $\mu\text{L}/\text{min}$  drove sample droplets through the emitter. PFD emerging from the tip was siphoned away using a Teflon tube placed near the tip as described before.<sup>42</sup> ESI voltage of +1.7 kV was directly applied to the

emitter. MS analysis was performed with a LTQ XL linear ion trap MS (Thermo Fisher Scientific, Waltham, MA) operated in positive mode, scanning from 350-690 m/z in 0.1 s. Extracted ion currents (XICs) of assay components were used for analysis. Peak detection was performed using Qual Browser (Version 2.0, Thermo Electron Co.).

**In-well Cathepsin B Inhibitor Screening.** Cathepsin B assays were initially tested by performing the reactions in vials or wells and then formatting for segmented flow. These assays used carboxybenzyl-Arg-Arg-7-amido-4-methylcoumarin (ZRR-AMC) as substrate and were modified from previous reports.<sup>108</sup>

First, the calibration curve of the standard assay product (ZRR-OH, > 99%, custom synthesized by AnaSpec Inc., Fremont, CA) is obtained in the range from 10  $\mu$ M to 180  $\mu$ M. Solutions were prepared in 20% (v/v) methanol and 0.2% (v/v) acetic acid. Different solutions were made into plugs and directly infused into MS. The relative signal abundance (relative peak height) of each sample was used for analyzing how MS response is related to sample concentration. A linear relationship was obtained with  $R^2 = 0.991$ . In addition, no obvious ion suppression between analytes was observed in our experiment. The signal of the assay product was always reversely related to that of the substrate, and both of them were not affected by either samples or byproducts. All experiments were done in this calibration range (**Figure 2-2**).



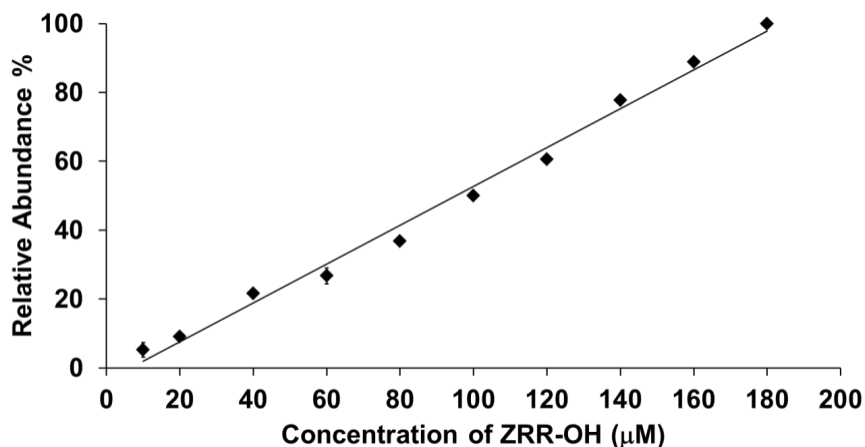


**Figure 2-2.** Calibration curve for ZRR-OH. 10 solutions of ZRR-OH with concentration as 10, 20, 40, 60, 80, 100, 120, 140, 160, 180  $\mu\text{M}$  were formatted as sample plugs and driven into ESI-MS for analysis. The ESI conditions were same with all other experiments. Using the relative abundance of each peak, the calibration curve had slope of 0.56, y-intercept of -3.6443,  $R^2$  of 0.9912.

Second, the assay conditions were tested by the dose response experiments of three known inhibitors of Cathepsin B: E-64 (L-trans-3-carboxyoxiran-2-carbonyl-L-leucylagmatine), Leupeptin (acetyl-Leu-Leu-Arg-al N-Acetyl-L-leucyl-L-leucyl-L-argininal), and Antipain ([*(S)*]-1-Carboxy-2-phenylethyl]carbamoyl-L-arginyl-L-valyl-argininal) were prepared in a series of aqueous solutions whose concentration ranged from  $10^{-7}$   $\mu\text{M}$  to  $10^3$   $\mu\text{M}$  to obtain the dose response relations with Cathepsin B. The final concentration of the substrate ZRR-AMC was 180  $\mu\text{M}$  and Cathepsin B 8.1  $\mu\text{g/mL}$ . The quenched reaction mixtures were analyzed using relative abundance of ZRR-OH in its XIC. The results showed sigmoidal relationship between the concentration of the inhibitor and the relative signal intensity of ZRR-OH produced. The  $\text{IC}_{50}$ s of three

inhibitors under our specific experiment conditions were generally agreed with reported values (E-64: 55 nM, leupeptin: 21.3 nM, antipain 0.98  $\mu$ M, **Figure 2-3**)

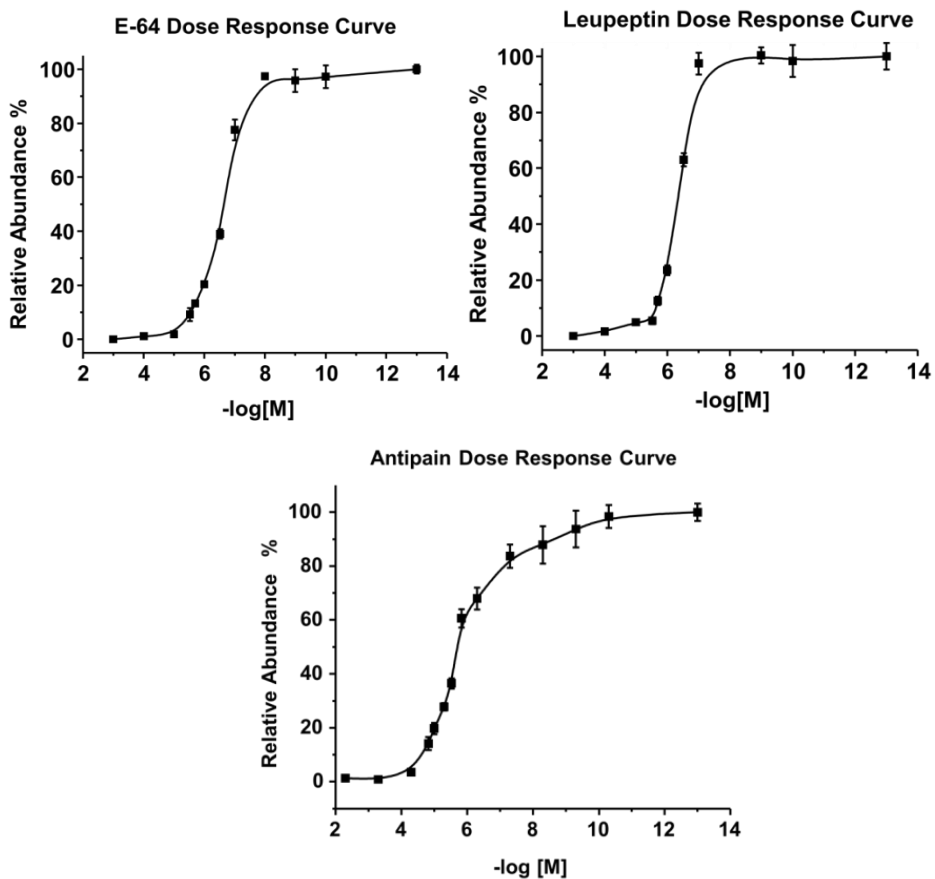


**Figure 2-3.** Dose response curves of three known inhibitors determined by droplet-MS. Different concentrations of E-64 ( $10^{-7}$ ,  $10^{-4}$ ,  $10^{-3}$ ,  $10^{-2}$ , 0.1, 0.3, 1, 2, 3, 10, 100, 1000  $\mu$ M), Leupeptin ( $10^{-7}$ ,  $10^{-4}$ ,  $10^{-3}$ , 0.1, 0.3, 1, 2, 3, 10, 100, 1000  $\mu$ M), Antipain ( $5 \times 10^{-7}$ ,  $5 \times 10^{-5}$ ,  $5 \times 10^{-4}$ ,  $5 \times 10^{-3}$ ,  $5 \times 10^{-2}$ , 0.5, 1.5, 3, 5, 10, 15, 50, 500, 5000  $\mu$ M) were incubated with ZRR-AMC and the enzyme. Relative abundance of ZRR-OH peaks were used for construct the sigmoidal curves.

24 test compounds, including three known Cathepsin B inhibitors: E-64, leupeptin and Antipain were dissolved in water at 200  $\mu$ M. (See **Appendix A** for other test

compounds.) 50  $\mu\text{L}$  of each test compound solution was mixed with 30  $\mu\text{L}$  of 27  $\mu\text{g}/\text{mL}$  bovine spleen Cathepsin B and 200  $\mu\text{M}$  1,3-dithioerythritol (DTE) in 20 mM ammonium formate buffer at pH 6.7 and incubated for 5 min at room temperature. 18  $\mu\text{L}$  of substrate 1 mM ZRR-AMC in water was then added to start turnover. After 10 min of incubation in a 40  $^{\circ}\text{C}$  water bath, 20  $\mu\text{L}$  of a quenchant consisting of 98% methanol and 2% acetic acid (v/v) was rapidly added. 80  $\mu\text{L}$  of each quenched reaction mixture was pipetted into a 384-well plate (Axygen Scientific, Union City, CA). 96 sample droplets (4 from each reaction mixture) of 11 nL each were generated using the procedure described above and pumped into MS at 0.75  $\mu\text{L}/\text{min}$  through a Pt-coated emitter. XICs of the product carboxybenzyl-Arg-Arg (ZRR-OH) were used for analysis.

In experiments using unlabeled peptide Ac-GFGFVGG-NH<sub>2</sub> (American Peptide Company Inc., Sunnyvale, CA) as substrate, the procedures were the same except that test compounds were prepared at 40  $\mu\text{M}$  and the enzyme 54  $\mu\text{g}/\text{mL}$ . Each reaction mixture was made into 14 nL of droplets, in quintuplicate. XICs of the product FVGG-NH<sub>2</sub> (m/z 378.5) were used for analysis.

**All-droplet Cathepsin B Inhibitor Screening.** To perform the assay reaction in droplets, test compounds were prepared as a 100-droplet array (8 nL each) consisting of 4 droplets for each of 25 test compounds at 100  $\mu\text{M}$ . Droplets were prepared with a 16 nL oil plug between them and loaded into a 150  $\mu\text{m}$  i.d. x 360  $\mu\text{m}$  o.d. Teflon tube. Cathepsin B (54  $\mu\text{g}/\text{mL}$ ), ZRR-AMC (600  $\mu\text{M}$ ), and quenchant were added to the test compound droplets in sequence using PDMS tees. (See **Appendix A** for test compounds.)

Droplets were pumped into the inlet channel of the tee at 2  $\mu\text{L}/\text{min}$  while solution to be added was pumped in an orthogonal channel at 200  $\text{nL}/\text{min}$ . The resulting droplets exited the outlet channel and were collected into a Teflon tube. Cathepsin B solution was injected into the droplets first and required 1 min for 100 sample droplets. Substrate was then added and the resulting tube of droplets was sealed with Sticky Wax (KerrLab, Orange, CA) and placed into a 40  $^{\circ}\text{C}$  water bath for 15 min. After incubation the ends of the tube were trimmed off and quenchant was added. The final droplets containing quenched reaction solutions were infused into the MS at 1.5  $\mu\text{L}/\text{min}$ .

In other experiments, native substrate was used with a Teflon tee.<sup>109</sup> 5  $\text{nL}$  of 80  $\mu\text{M}$  test compounds were loaded into the Teflon tube with 10  $\text{nL}$  plugs of oil between them. Enzyme (108  $\mu\text{g}/\text{mL}$ ), substrate (600  $\mu\text{M}$ ) and quenchant were added using the same flow rates. Resulting droplets were pumped into the MS at 0.75  $\mu\text{L}/\text{min}$ .

**PDMS Tee Fabrication.** Polydimethylsiloxane (PDMS) reagent addition tees were fabricated using soft lithography.<sup>110</sup> The droplet channel was rendered hydrophobic by silanization immediately after plasma bonding by pumping 1:100 (v/v) trichloro(1*H*,1*H*,2*H*,2*H*-perfluorooctyl) silane solution in anhydrous hexadecane through it (**Figure 2-4**). A 3 cm length of pre-silanized 50  $\mu\text{m}$  i.d. x 150  $\mu\text{m}$  o.d. fused silica capillary (Polymicro Technologies, Phoenix, AZ) was inserted from the side of the tee into the droplet inlet channel, and a 6 cm length of non-derivatized 20  $\mu\text{m}$  i.d. x 150  $\mu\text{m}$  o.d. capillary was inserted into the reagent channel. A 3 cm length of 150  $\mu\text{m}$  i.d. x 360

$\mu\text{m}$  o.d. Teflon tube was inserted into the outlet channel. Capillaries and the Teflon tube were glued over the ends with 5 minute Epoxy (Devcon, Danvers, MA).

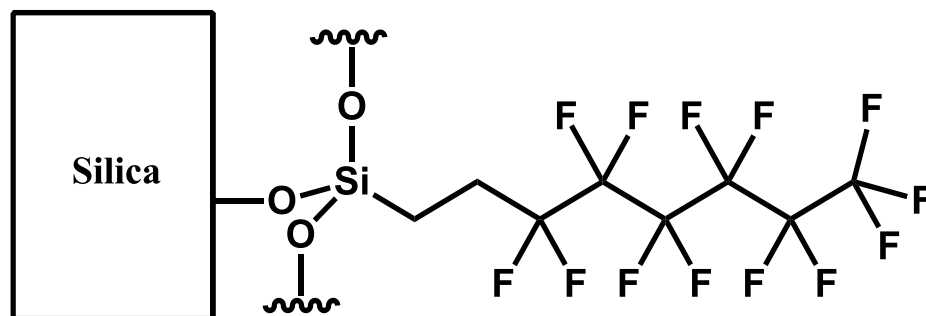


**Figure 2-4.** Illustration of fused silica surface derivatized by trichloro(1H,1H,2H,2H-perfluorooctyl) silane.

**Carry-over measurement.** Carry-over of the spray emitter was measured by pumping alternating sample/blank droplets (sample droplets contained 200  $\mu\text{M}$  ZRR-OH dissolved in 20% methanol and 0.2% acetic acid ESI buffer, blank droplets only contained the buffer) through the emitter tip to ESI-MS. The signal intensity of each droplet was used for analysis. < 1% carry-over occurred in the spray emitter, which was in agreement with previous results<sup>40</sup> (**Figure 2-5A**). Carry-over of the PDMS tee for one addition was measured by adding quenchant (98% methanol and 2% acetic acid) into 10 nL alternating sample/blank droplets (the sample was 200  $\mu\text{M}$  ZRR-OH water solution, and the blank is water), where we observed  $\sim$  9% of carry-over. 2 additions were conducted by adding water, and then adding quenchant into the same alternating droplets.

The carry-over increased to 16% with 2 additions. In results of the real screening, 3 additions led to more than 25% of carry-over (**Figure 2-8**).

We also measured the carry-over of the Teflon tee for one addition. Same quenchant was added into alternating droplets in which sample droplets contained 200  $\mu\text{M}$  Ac-GFGFVGG-NH<sub>2</sub> and blank droplets contained water. The carry-over could be as low as 2% (**Figure 2-4B**).

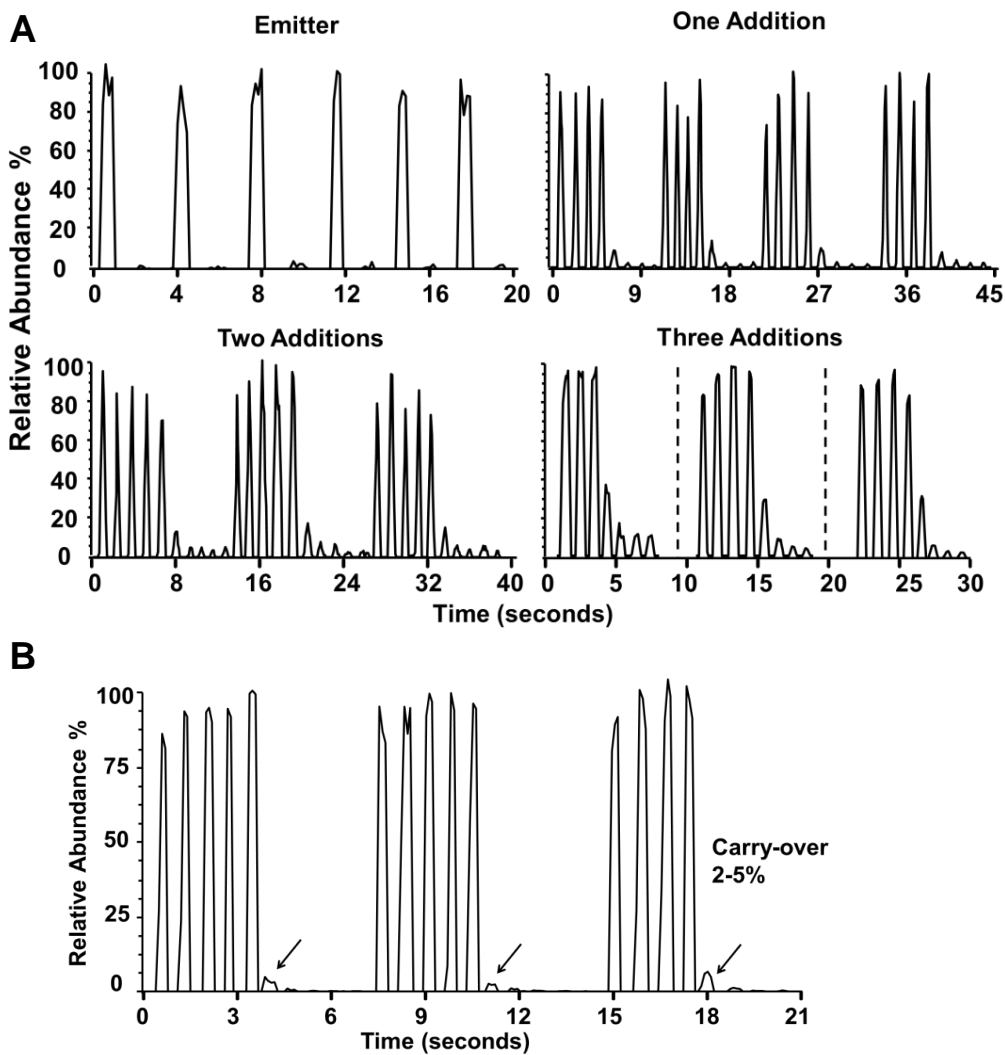


**Figure 2-5** A) Carry-over of the all-droplet system. <1 % of carry-over was observed in the emitter (upper left). 9% of carry-over was generated by the tee for one addition (upper right) and 16% for two additions (lower left). The carry-over of three addition is 25-30% (lower right). B) Carry-over of the Teflon tee for one addition.

## Results and Discussion

**In-well Cathepsin B Inhibitor Screening.** Cathepsin B is commonly screened using the fluorogenic substrate ZRR-AMC by the reaction shown in **Figure 2-6A**. By performing the reaction in a low concentration buffer (6 mM ammonium formate and 60 M DTE) and quenching the reaction with 98% methanol and 2% acetic acid, both the substrate and product can be readily detected by ESI-MS. These results suggest that the buffer conditions are both suitable for retaining enzymatic activity and are MS friendly. Although a fluorescent substrate for Cathepsin B has been devised, the MS can also detect native substrates. To demonstrate this we synthesized the non-fluorescent heptapeptide Ac-GFGFVGG-NH<sub>2</sub> that should serve as a good substrate according to previous studies on the selectivity of this enzyme.<sup>111,112</sup> The reaction and mass spectrum of the reaction mixture illustrating detection of substrate and product (FVGG-NH<sub>2</sub>) are shown in **Figure 2-6B**. These results illustrate the potential of ESI-MS for detecting different substrate-product pairs, reactions of unlabeled substrates, and for detecting substrate and product simultaneously as long as reaction conditions are enzyme and ESI-MS compatible.

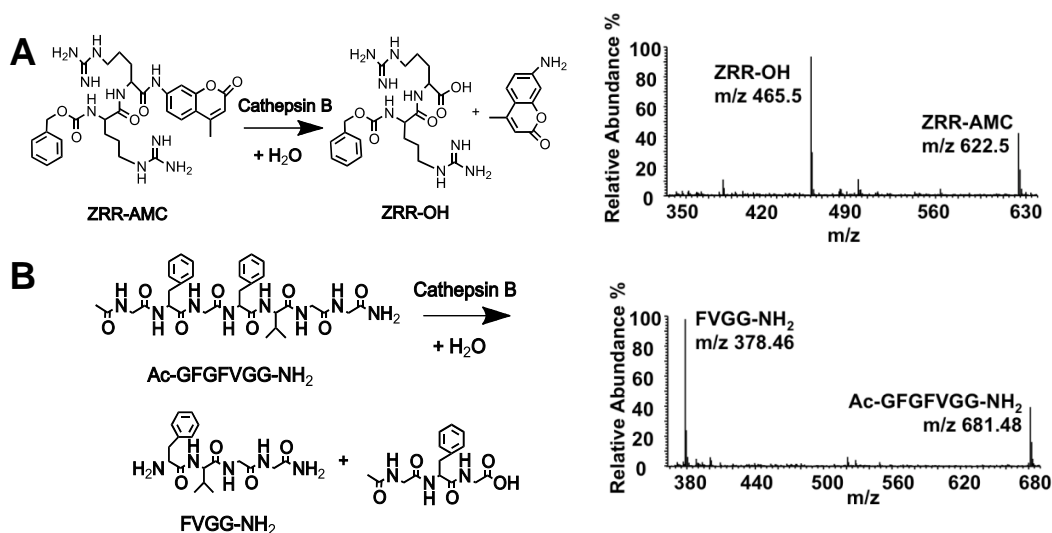


**Figure 2-6.** A) Cathepsin B catalyzed proteolysis of ZRR-AMC and ESI mass spectrum of resulting reaction mixture. B) Cathepsin B catalyzed proteolysis of Ac-GFGFVGG-NH<sub>2</sub> and ESI mass spectrum of reaction mixture.

We then tested both assays in a screening format. Reaction solutions were reformatted to segmented flow from a MWP, and then analyzed by ESI-MS. The result of screening 24 test compounds (one negative control, three positive controls and 20 randomly chosen small molecules as potential inhibitors) in quadruplicate using the substrate ZRR-AMC is illustrated in **Figure 2-7A**. The result of a similar experiment using 12 samples in quintuplicate using unlabeled peptide substrate is shown in **Figure 2-7B**. Each droplet is detected as a burst of current separated by low signal that corresponds to oil exiting the emitter nozzle. As shown previously, PFD does not spray or generate signal under these conditions.<sup>42</sup> Each sample current burst consists of a series of mass spectra (~10 spectra for each droplet) so that different m/z channels can be simultaneously monitored allowing detection of the substrate, product, and inhibitors.



The impact of inhibitors on the enzyme is evident in low signal intensity for product when inhibitors are present. The assay has good reproducibility with RSD < 3% in droplet peak height each test compound set. The MS detection is also rapid with the throughput of 0.66 Hz.

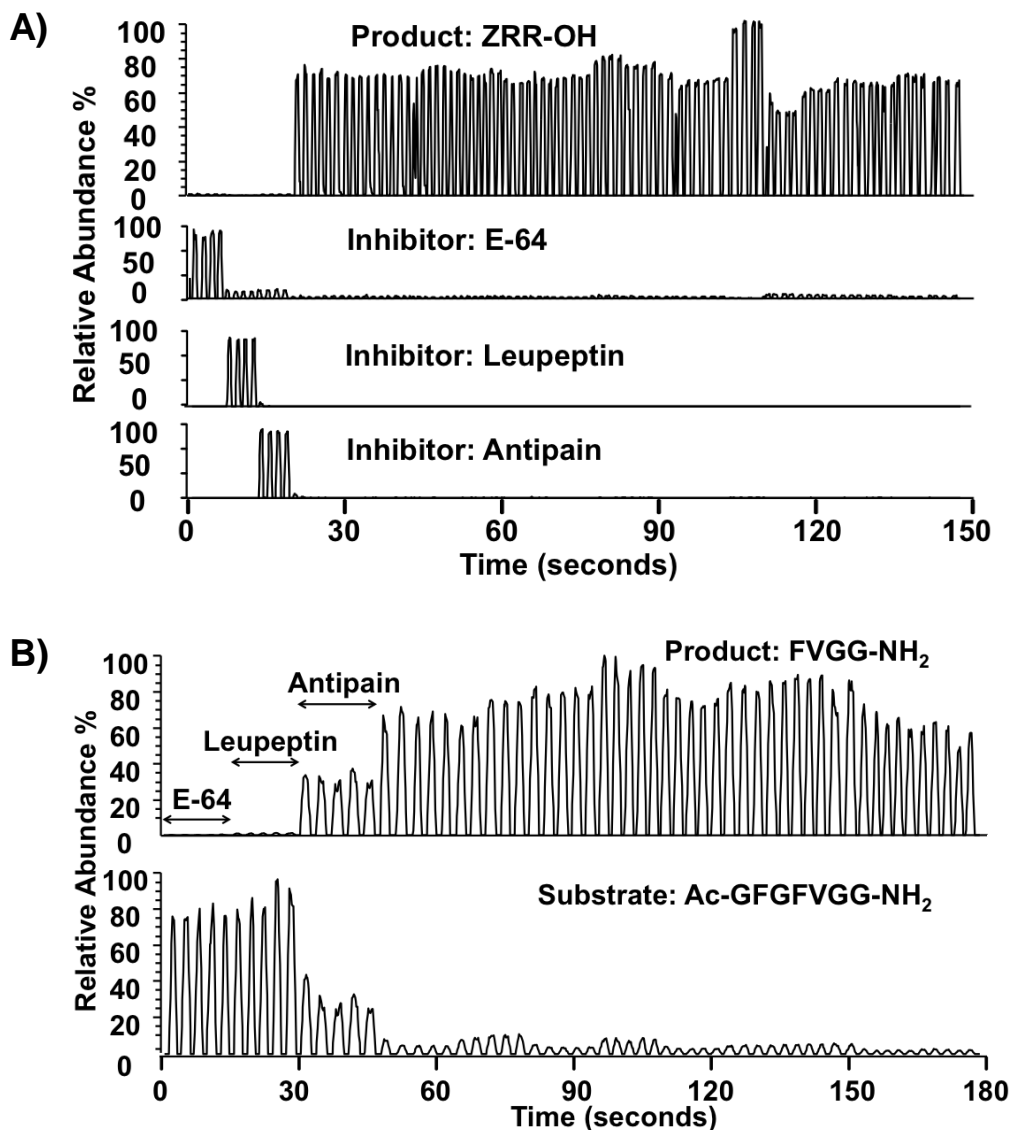


**Figure 2-7.** A) Result of in-well screening of Cathepsin B inhibitors using ZRR-AMC as the substrate. XICs show signal for ZRR-OH and the known inhibitors E-64, leupeptin, and antipain. Each of 24 reaction mixtures was formatted in quadruplicate. Droplets with

low product signal are inhibitor sets. B) Result of screening using Ac-GFGFVGG-NH<sub>2</sub> as the substrate. XICs are product FVGG-NH<sub>2</sub> and the substrate. 12 reaction solutions were formatted in quintuplicate.

The suitability of the assay for screening was evaluated using Z-factor.<sup>113</sup> Z-factor is a statistic defined as  $Z = 1 - 3 \times (\mu_{\text{pos}} + \mu_{\text{neg}}) / (\mu_{\text{pos}} - \mu_{\text{neg}})$ , where  $\mu_{\text{pos}}$  and  $\mu_{\text{neg}}$  represent the SD of the response in positive and negative control, and  $\mu_{\text{pos}}$  and  $\mu_{\text{neg}}$  are the mean response of each. Z-factor exceeding 0.5 is considered suitable for HTS. In our experiment, Z-factors were 0.92 (E-64), 0.91 (leupeptin), and 0.91 (antipain) for the fluorescent substrate, and 0.93 (E-64), 0.93 (leupeptin), and 0.70 (antipain) for the unlabeled substrate.

The assays can also provide quantitative characterization of the reaction. A linear relationship between sample concentration and relative signal intensity was obtainable from 10  $\mu\text{M}$  to 180  $\mu\text{M}$  ( $R^2 = 0.991$ ). IC<sub>50</sub>s of three inhibitors determined from dose response analysis under our experiment conditions generally agreed with reported values. These results illustrate that each reaction result can be rapidly analyzed at nanoliter scale by segmented flow ESI-MS and that the results are suitable for screening and quantitative assay of inhibitors.

**All-droplet Cathepsin B Inhibitor Screening.** With the assay established, we sought to miniaturize the system to take advantage of the small quantities used for actual detection of segmented flow ESI-MS. To do so, we performed the entire Cathepsin B inhibitor screen in an all droplet format (**Figure 2-8A**). In this approach, 25 test

compounds were first formatted as droplets (8 nL each, in quadruplicate) in a tube. The droplets were then pumped through a series of reagent addition tees where 2-3 nL of enzyme, substrate, and quenchant could be added for each step. The final droplet size was about 16 nL. Fixing the droplet flow rate at 2  $\mu\text{L}/\text{min}$ , one reagent addition was completed at 1.4 Hz. 100 droplets were analyzed in 2.2 min (0.8 Hz), as illustrated in **Figure 2-8B**.

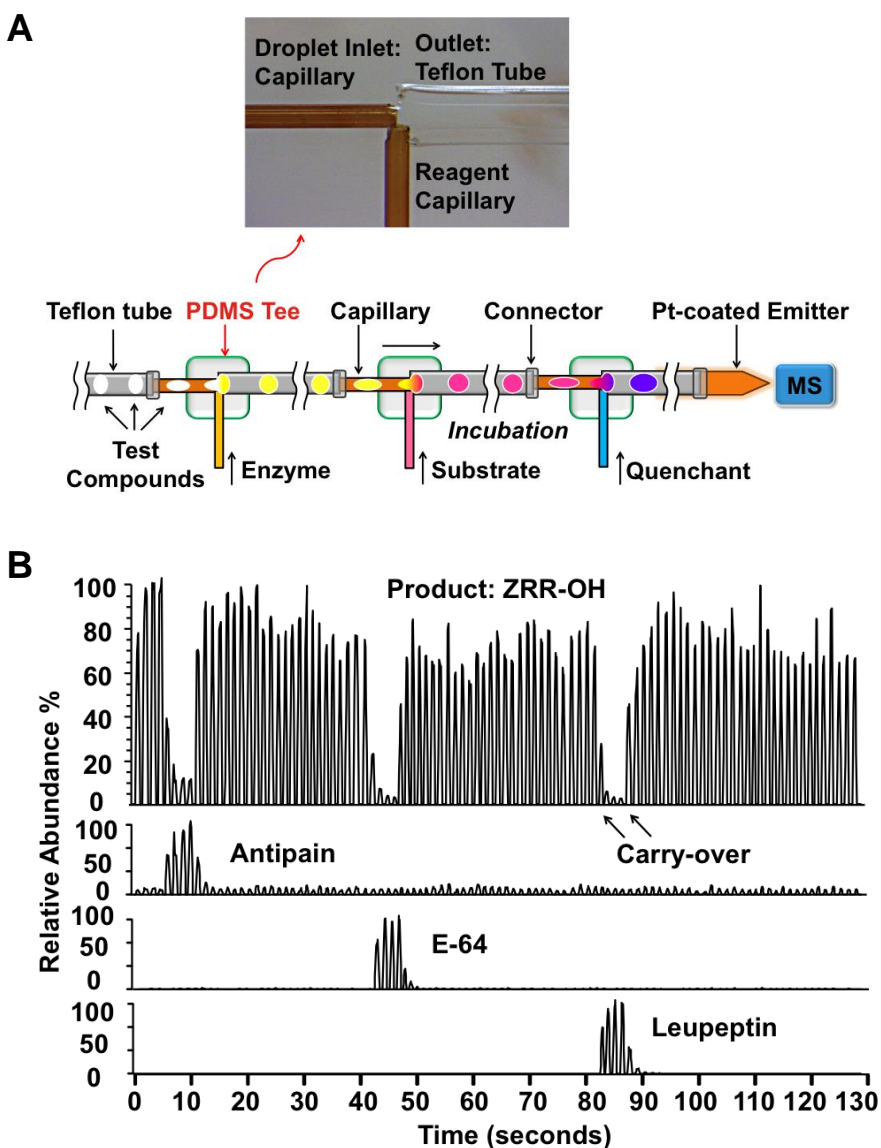


**Figure 2-8.** A) Diagram of all-droplet screening system coupled to ESI-MS analysis. Test compounds arrayed as droplets were pumped into a series of PDMS tees where enzyme, substrate, and quenchant were added in. (For the actual experiment, the third Teflon tube was sealed on both ends and incubated in a water bath prior to pumping droplets through the quenchant addition tee.) The inset is a photomicrograph of the PDMS tee. The droplet inlet is silanized 50  $\mu\text{m}$  i.d.  $\times$  150  $\mu\text{m}$  o.d. capillary, the outlet is 150  $\mu\text{m}$  i.d.  $\times$  360  $\mu\text{m}$  o.d. Teflon tube, and the reagent channel is non-derivatized 20  $\mu\text{m}$  i.d.  $\times$  150  $\mu\text{m}$  o.d. capillary. B) Results of all-droplet screening using ZRR-AMC as the substrate. XICs are ZRR-OH, antipain, E-64, and leupeptin. Each test compounds has 4 replicates.

XICs of the assay product ZRR-OH allowed easy detection of inhibitors and non-inhibitors. Some carry-over was observed in that signal of the first droplet of each inhibitor set was higher than the rest. Also, signal for the first droplet of non-inhibitor was lower than its replicates if following an inhibitor, as pointed out in **Figure 2-8B**. To avoid the impact of carry-over, RSD and Z-factors were calculated using the signal intensity of the 2<sup>nd</sup>-4<sup>th</sup> droplet of each set. The RSD was 11% on average, which was larger than in-well screening due to the higher throughput which compromised the number of data points for each droplet, and the accumulation of the slight variation in each reagent addition. The Z-factors were 0.82, 0.85, and 0.76 for E-64, leupeptin, and antipain, respectively. For each reaction, 1.6 picomoles of ZRR-AMC, 0.8 picomoles of test compound, and 5 femtomoles of Cathepsin B were consumed. This represents a 10,000-fold reduction compared to the in-well assay. Further, in droplet screening these amounts used can be achieved with no waste or requirements for larger reservoirs of compounds.

For these experiments, we used the reagent addition tee shown in **Figure 2-8A**. The geometry of the tee was designed to avoid formation of reagent-only droplets

between sample droplets. As reagent continuously flows out of the reagent capillary, the interfacial tension between water and PFD prevents it from being detached from the end of the channel. When an aqueous droplet arrives at the junction, it merges with the accumulated reagent and flows away from the tee. However, if oil gaps between droplets are too long, or the reagent flow rate is too high, reagent droplets may form and be swept off by the oil. The results of having reagent-only droplets include irreproducible addition ratio, non-uniform droplet train, and uneven pressure, all of which are detrimental to multistep reactions. As described elsewhere, a larger outlet prevents reagent-only droplet formation effectively.<sup>114</sup> Indeed, no unexpected signal was detected between droplets (**Figure 2-8B**) showing that this design effectively prevented reagent-only droplets.

**Carry-over and Alternative Reagent Addition Device.** Although the all-droplet system was effective in many ways, we further studied it to determine if improvements were possible. Our carry-over measurement showed that < 1% of carry-over was caused by the emitter, in agreement with previous results.<sup>41</sup> One reagent addition using the PDMS tee resulted in ~9% of carry-over, which increased to 16% with 2 additions and 25% with 3 additions. This carry-over appears to be related to the low Péclet number (ratio of advection rate to diffusion rate) developed in the tee. Advection facilitates merging while diffusion causes contamination during reagent addition.<sup>115</sup> The broad outlet of the tee slows down the reagent that prevents reagent-only droplets from forming, but it also slows down the passing droplet that leads to longer diffusive mixing of sample and reagent at the junction. Commonly carry-over is circumvented by inserting a “rinse” droplet between samples.<sup>34</sup> We achieved a similar effect here by running samples in

quadruplicate and discarding the first sample of each set. The carry-over of the 2<sup>nd</sup> blank droplets was < 6%, even after 3 additions, which did not affect the Z-factor.

Using replicate droplets is effective and easy to implement. It also adds little time to a small scale screen. However, for large screens it would be desirable to avoid the carry-over completely to minimize the time spent rinsing between samples. We therefore evaluated a Teflon tee.<sup>109</sup> This tee yielded approximately 2-5% carry-over per reagent addition (**Figure 2-5B.**) The raw trace for assay product FVGG-NH<sub>2</sub> from a small-scale screen with the non-fluorescent substrate is shown in **Figure 2-9**. The total carry-over in the 1<sup>st</sup> droplet was 10-14% and negligible in following droplets. The low carry-over of the Teflon tee can be attributed to (1) a narrow outlet that allowed relatively high velocity through tee; (2) partial coverage of the reagent outlet by Teflon that prevents droplets from sticking to the capillary. Both tees were demonstrated as good reagent addition devices for this application. Other tee designs have been reported to yield low carry-over and high addition ratio that may produce even better results.<sup>32</sup>

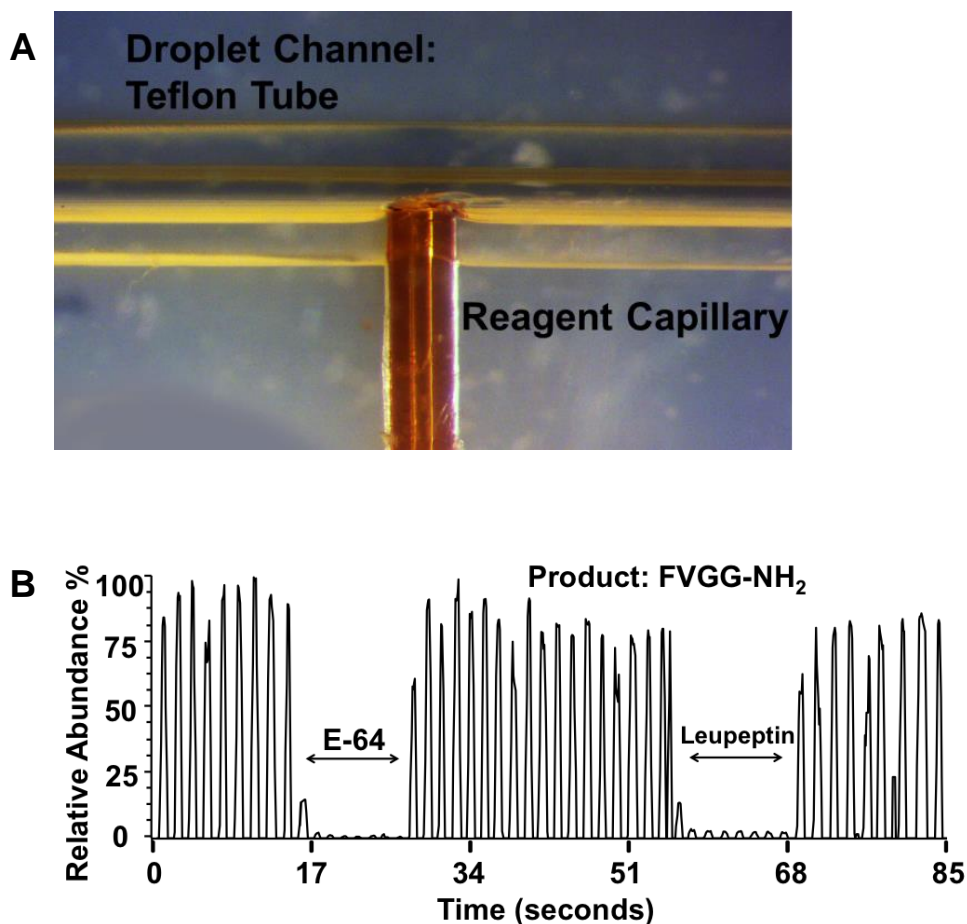


**Figure 2-9.** A) Photomicrograph of Teflon tee. The droplet channel is 150  $\mu\text{m}$  i.d.  $\times$  360  $\mu\text{m}$  o.d. Teflon tube. The reagent channel is 40  $\mu\text{m}$  i.d.  $\times$  190  $\mu\text{m}$  o.d. non-derivatized capillary. B) Trace resulting from all-droplet screening with the Teflon tee using the non-fluorescent substrate. XIC is the product FVGG-NH<sub>2</sub>. Samples were run in quintuplicate.

**Throughput.** The emphasis in this work is on miniaturizing label-free enzyme assays. This miniaturization should be valuable when protein target or reagents are difficult or expensive to obtain. Miniaturization is also beneficial in scale-up of a screen. The biggest expense of large scale screens is often reagents,<sup>34</sup> so reduction of volume can make screens more affordable. Droplet assays also have potential utility in high-

throughput screening. For the all droplet-assay, the steps to completing a screen are: (1) droplet generation, (2) all-droplet reactions, (3) MS analysis. In this experiment around 10 min is required to load 96 droplets using the XYZ-positioner; however, faster positioners and parallel operation can greatly reduce this time. Further, it may be feasible to reformat libraries to droplets before they are needed thus eliminating this time for a screen. Reagent addition was performed 1.4 samples/s, which was comparable with other studies; although rates up to 10 Hz have been reported.<sup>27</sup> The reactions themselves require 15-20 min incubation. This time cannot be eliminated; however, if the fluidics is operated in a steady stream then after an initial lag time samples would be produced at a rate limited by the reagent addition rate. Alternatively, tubes could be prepared in parallel and reactions could be done in batch. Finally, the ESI-MS rate was 0.5 to 1 Hz here and faster rates may be possible with a faster scanning MS.

## Conclusion

A label-free all-droplet assay system was developed in this work. Its robustness, ultralow reagent consumption, and high throughput were demonstrated by the screening of Cathepsin B inhibitors. Compared with MWP-based fluorescence assay systems, this approach eliminates the need of labeling and reduces the sample requirement over 1000-fold. These results suggest the potential for screening reactions for optimization, chemical probe discovery, and drug discovery, especially when reagent or protein target are expensive or difficult to obtain. Further development is required for routine high-



throughput screening. One limitation of the system is the built-up of carry-over in a multi-step reaction. Modifications of the tee such as changing the dimension of the channels will be explored in order to reduce the carry-over. In pursuit of higher throughput, parallel droplet generation, parallel droplet-based reactions and faster mass spectrometer may be incorporated.

## **CHAPTER 3**

# **DROPLET-ELECTROSPRAY IONIZATION-MASS SPECTROMETRY FOR LABEL FREE HIGH THROUGHPUT SCREENING FOR ENZYME INHIBITORS**

### **Introduction**

High throughput screening (HTS) is important in drug discovery, chemical biology, and chemistry. Current technology relies mostly on performing reactions in multi-well plates (MWP) with robotic manipulation of fluids followed by interrogation using optical plate-readers.<sup>1,2</sup> Mass spectrometry (MS) is a potentially powerful technique for HTS because it is fast, has high resolution, and can detect chemicals without labels.<sup>7,102</sup> This latter advantage is important because it eliminates false signals based on a label or indicator reaction and avoids the time, expense, and expertise needed to modify target compounds for optical assay. Use of MS in screening<sup>3,116-118</sup> has often relied on the multiplexing capability to analyze mixtures of compounds; however, this use is limited because most chemical libraries are formatted as arrays of individual compounds and

most screening is performed by testing one compound on one reaction at a time. MS is not commonly used for such screening because traditional sample introduction methods are too slow; although advances have been made with high flow rate separation and multiplexed autosamplers.<sup>19,24</sup> As we describe here, a way to overcome this limitation is use of segmented flow sample introduction to enable label-free HTS by electrospray ionization (ESI)-MS.

Segmented flow and other formats wherein aqueous sample droplets are compartmentalized within an oil carrier fluid have seen a resurgence of interest due to advances in microfluidic manipulation tools.<sup>26,30,119-122</sup> Although most droplet experiments rely on optical detection, ESI-MS can also be used to analyze droplets.<sup>38-40,82,123-125</sup> Droplet sample introduction for MS allows fast analysis and greatly reduced sample consumption suggesting potential for HTS. So far experiments have focused on methods of interfacing droplets to MS on small scale demonstrations under conditions not compatible with HTS. A potential approach to HTS by droplet MS is to complete entire screening reactions at the droplet level yielding both label-free detection and miniaturization.<sup>82</sup> However, a substantial infrastructure investment in MWP-based technology suggests that it is also of interest to combine such tools with MS, i.e. to develop a “MS plate reader”. Herein we describe coupling MWP-based fluid manipulation with segmented flow ESI-MS to rapidly screen a compound library.

The system is applied to cathepsin B,<sup>43</sup> a cysteine protease implicated in tumorigenesis, arthritis, and parasite infection.<sup>47,51,126,127</sup> Both *in vivo* and *in vitro* studies have demonstrated that certain cathepsin B inhibitors reduce tumor cell motility and

invasiveness.<sup>50,128</sup> Because of these links, considerable effort has been made to identify cathepsin B inhibitors. Successful inhibitors include epoxysuccinyl, aziridinyl, biguanide, and  $\beta$ -lactam derivatives.<sup>129,130</sup>

Our approach to plate reading by MS is a two-step process of reformatting MWP samples into droplets and then infusion into an ESI-MS (**Figure 3-1**). We first examined the rate of ESI-MS analysis possible by this approach. For ESI, samples in a fluorinated ethylene propylene (FEP) tube are pumped into a metal-coated fused silica capillary that acts as the ESI needle (**Figure 3-1B**).<sup>123</sup> The inner surface of the capillary is fluorinated so that it is wetted by the perfluorodecalin (PFD) carrier fluid. ESI voltage is applied continuously but electrospray stops and starts with each aqueous plug that exits the channel. The off-axis MS inlet prevents PFD, which is nebulized but does not form charged droplets, from entering the MS inlet (**Figure 3-1B**); thus a separation of oil and sample occurs in the gas phase.

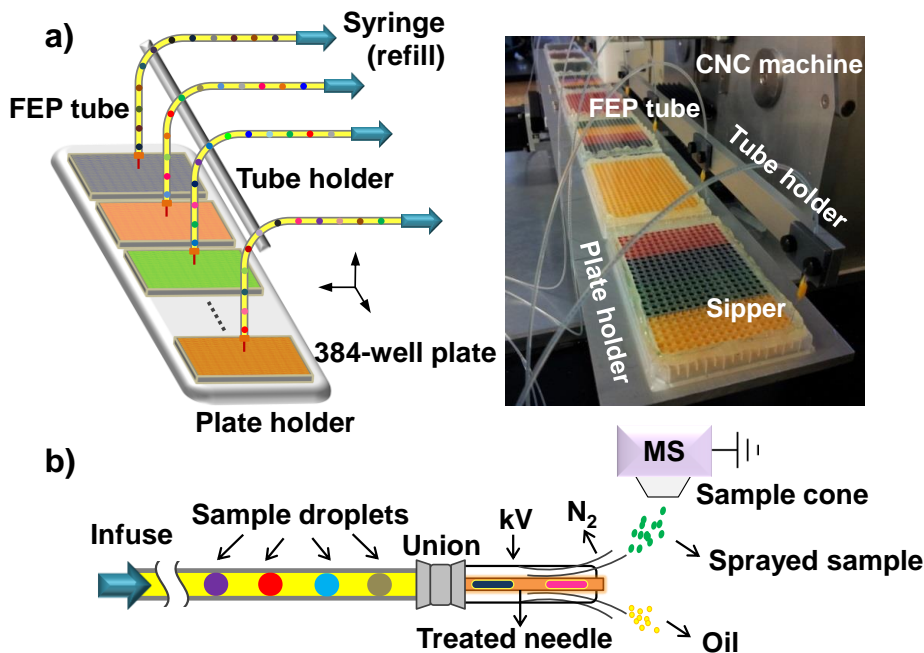


**Figure 3-1** A) Left: Scheme of parallel oil-segmented droplet generation from MWPs. FEP tubes are programmed to dwell in sample or oil for predetermined time, and then move to another well. The syringe pump operates in refill mode at a constant flow rate. Right: Picture of parallel droplets generation with different color food dye as samples. B) Diagram of ESI-MS analysis by direct infusion of segmented flow. Droplets are pumped into the ESI source through a treated ESI needle. ESI voltage is applied on the needle. In the gas phase, charged sample droplets (green) enter the MS and nebulized oil (yellow) does not.

## Experimental Section

**Chemicals and Materials.** Unless otherwise specified, all solvents were purchased from Honeywell Burdick & Jackson (Muskegon, MI) and were certified ACS grade or better. Reagents were purchased from Sigma Aldrich (St. Louis, MO). Peptides used for cathepsin B assay were synthesized by Pierce Biotechnology, Inc. (Rockford, IL). Compounds for cathepsin B screening were from Prestwick Chemical Library®

(Prestwick Chemical, Washington, DC), provided by the Center of Chemical Genomics of University of Michigan.

**Parallel Droplet Generation.** Oil-segmented droplets of 50 nL each were created in parallel from eight 384-well plates into eight 0.01 inch i.d.  $\times$  1/16 inch o.d. fluorinated ethylene propylene (FEP) tubes (IDEX Health and Science, Oak Harbor, WA). A 2 cm 100  $\mu$ m i.d.  $\times$  238  $\mu$ m o.d. fused-silica capillary, sealed with Sticky Wax (KerrLab, Orange, CA), was inserted into the inlet of each FEP tube to act as a “sipper”. Capillaries were fluorinated by pumping 1:100 (v/v) trichloro(1H,1H,2H,2H-perfluorooctyl) silane in anhydrous hexadecane through them. Samples in 384-well plates (Nunc™ 384-Well ShallowWell plates, Thermo Scientific) were covered with perfluorodecalin (PFD, 95% purity, Acros Organics, NJ). The edges of plates were built-up to 5 mm height with epoxy to hold PFD over the wells (**Figure 3-1A**).

For droplet formation, the 384-well plates and the inlets of the FEP tubes were mounted onto a computer numerical control (CNC) machine (Cameron Micro Drill Press, Sonora, CA) so that a sipper was above the first well on each plate. The other end of FEP tubes were connected to 500  $\mu$ L Hamilton syringes (Fisher Scientific, Pittsburgh, PA), which were mounted on a multi-channel syringe pump (Fusion 400, Chemyx Inc. Stafford, TX). The syringes and FEP tubes were pre-filled with PFD. As the syringes were aspirating at 4  $\mu$ L/min, the G-code programmed CNC machine controlled the movement of tubes and plates so that the sipper could alternatively dwell in sample for 1 s and in oil for 0.25 s, as well as move from sample to sample for 0.5 s. Droplets with 50

nL volume separated by equal size of oil were produced with these parameters (**Figure 3-2**).

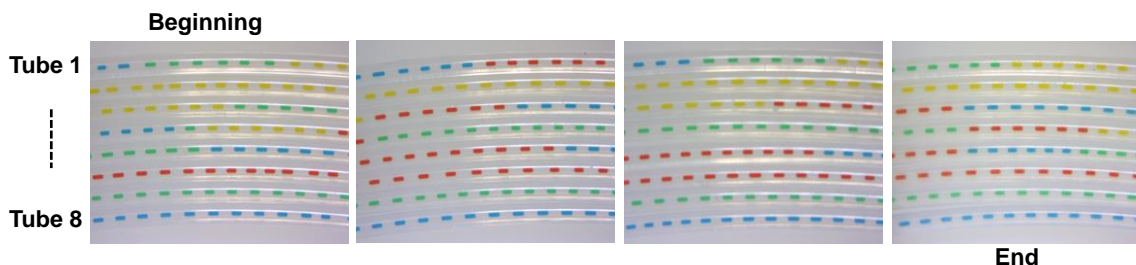


**Figure 3-2** Droplets of food dye solution generated in 8 FEP tubes at 4.5 Hz. The RSD of droplets within each tube is <5% and across tubes <10%. Photos show close-up view of 8 tubes at different lengths along the tube.

**Mass Spectrometry Analysis.** A Micromass Quattro Ultima triple quadrupole MS (Waters Corporation, Milford, MA) was used for analysis. The original stainless steel ESI needle was replaced by a piece of fused silica capillary (18 cm in length, 100  $\mu\text{m}$  i.d.  $\times$  238  $\mu\text{m}$  o.d.) coated on the outside with gold and with the inner surface fluorinated as described above for sipper capillaries. The FEP tube containing sample droplets was connected to the treated ESI needle with a 1/16 inch bore VICI Cheminert union (Valco Instruments Co. Inc. Houston, TX).

For analysis, a syringe pump drove sample droplets through the needle into the source. ESI voltage was +2.5 to 3.0 kV, the source was heated to 100  $^{\circ}\text{C}$ , the cone gas was set at 50 L/h, the desolvation gas was 200 L/h, and the nebulizing gas was adjusted to the best flow based on the infusing rate of droplets. The ESI mode and the MS method

were dependent upon molecules to be analyzed. Extracted ion currents (XICs) of target molecules were obtained by MassLynx (Version 4.1, Waters Inc.). Sample droplets are detected as bursts of current in the XICs because the oil, being not conductive or charged, does not generate ESI-MS signal.

**Cathepsin B Assay Development.** The assay was developed from a previous report.<sup>82</sup> The non-fluorogenic peptide GFGFVGG was used as substrate for cathepsin (Figure 3-3A). Reactions were performed in 20 mM ammonium formate and 200  $\mu$ M 1,3-dithioerythritol (DTE) buffer. The buffer is MS compatible which allows direct infusion analysis (Figure 3-3B). Reactions were stopped with equal volume of the quenchant consisting of ice-cold 50% methanol, 50% water and 0.3% formic acid (v/v). The quenchant also contained 20  $\mu$ M of stable isotope labeled product (FVG\*G, +3 Da) as internal standard. Calibration curves for detection of product peptide (FVGG), measured as a ratio to the internal standard, were linear from 0 to 500  $\mu$ M in this solvent as shown in Figure 3-3C. The rate of product formation was linear for 60 min when using 50 nM cathepsin B and 80  $\mu$ M substrate (Figure 3-3D). Michaelis-Menten analysis yielded a  $K_m$  of 90.6  $\mu$ M (Figure 3-3E). Based on the kinetic studies, each screening reaction contained a final concentration of 80  $\mu$ M substrate and 50 nM cathepsin B, and was incubated for 25 min.



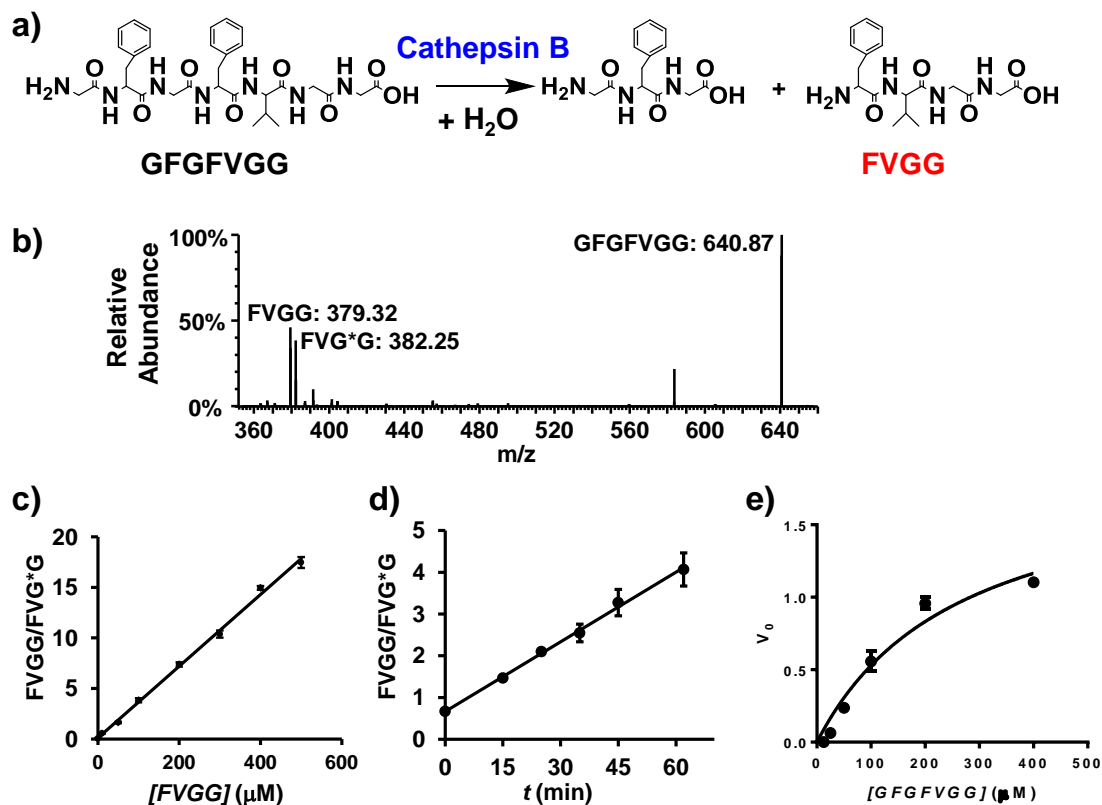


**Figure 3-3.** A) Assay reaction is cleavage of heptapeptide substrate GFGFVGG by cathepsin B; B) Full scan mass spectrum of direct infusion of the reaction mixture; C) Linear calibration of FVGG from 0 to 500  $\mu\text{M}$ ; D) Reaction progression in 60 min with 100  $\mu\text{M}$  GFGFVGG and 50 nM cathepsin B; E) Michaelis-Menten data of the reaction ( $K_m > 200 \mu\text{M}$ ).

Assay conditions were validated with a 24-compound pilot screen including 4 known inhibitors: E-64, leupeptin, antipain and chymostatin at 25  $\mu\text{M}$  each. Dose response curves of those 4 inhibitors were also obtained under the same conditions (Figure 3-4).

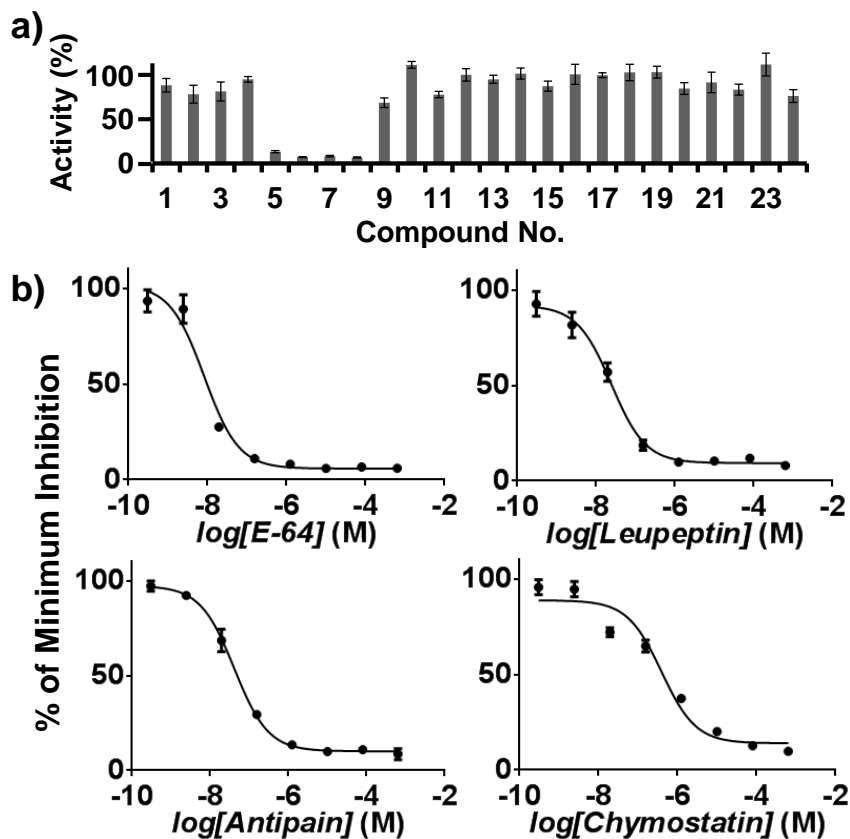


**Figure 3-4.** Data from validation of assay conditions. A) 20 test compounds (No. 5-24) and 4 negative controls (No. 1-4) were used. Compound 5, 6, 7, 8 are known cathepsin B inhibitors: chymostatin, antipain, leupeptin and E-64, respectively. The rest are non-inhibitors. B) Dose response curves of the 4 known inhibitors. Fitted  $IC_{50}$  values are  $8.3 \pm 0.5$  nM for E-64,  $24 \pm 8$  nM for leupeptin,  $41 \pm 6$  nM for antipain and  $0.40 \pm 0.04$   $\mu$ M ( $n = 3$ ) for chymostatin, which generally agree with the published values: E-64 = 55 nM, leupeptin = 21.5 nM,<sup>130</sup> antipain = 0.48  $\mu$ M and chymostatin = 1.8  $\mu$ M.<sup>131</sup>

**High Throughput Cathepsin B Inhibitor Screening.** To screen the Prestwick Library, 8  $\mu$ L of 100  $\mu$ M of GFGFVGG was deposited into each well of four 384-well standard assay plates (Greiner Bio-one, Monroe, NC) by Multidrop Combi (Thermo Scientific, Waltham, MA). 50 nL of 5 mM test compounds from the Prestwick Library

(1280 chemicals) was then added with a Caliper Life Sciences Sciclone ALH 3000 Workstation (PerkinElmer, Waltham, MA). 2  $\mu\text{L}$  of 0.25  $\mu\text{M}$  cathepsin B was deposited into the mixture afterwards. The final concentrations were 80  $\mu\text{M}$  GFGFVGG, 50 nM cathepsin B, and 25  $\mu\text{M}$  test compound. 0.5% DMSO was present in each reaction. After incubation at 37  $^{\circ}\text{C}$  for 25 min, reactions were quenched with 10  $\mu\text{L}$  of ice-cold quenchant. In total 1408 reactions, including 64 negative controls (DMSO) and 64 positive controls (25  $\mu\text{M}$  E-64) were performed. Assay plates were then spun to remove air bubbles. All mixtures were finally transferred into 384-well readout plates with elevated edges (see above) by Biomek Fx<sup>P</sup> Laboratory Automation Workstation (Beckman Coulter, Brea, CA). Samples were reformatted to droplets as described above. Each sample was collected as 3 droplets in sequence. Four FEP tubes of 1 m length were used for each plate. Droplet and oil gap had equal volume of 75 nL. The analysis was performed using ESI-MS in multiple reaction monitoring with m/z transition 379.5 $\rightarrow$ 247.1 for FVGG and 382.5 $\rightarrow$ 247.1 for FVG\*G. The collision energy was set as 18 eV, dwell time was 0.01 s and inter-channel delay was 0.01 s for both transitions. The ESI voltage was +2.7 kV. Droplets in FEP tubes were pumped into the sample cone at 15  $\mu\text{L}/\text{min}$ . Droplet traces were acquired by MassLynx and processed with Origin 8.5.

**Hits Validation.** Inhibitor hits were tested by dose dependent experiments, which were performed under the same condition as the screening. Each reaction contained a test compound from 0.1  $\mu\text{M}$  to 100  $\mu\text{M}$  (unless shown otherwise on the data plots). Peak height ratio of the product FVGG and the isotopic standard FVG\*G were used for analysis. The data were normalized to a control reaction which contained no inhibitor.

Such normalization accounted for variation in reaction yield seen from day to day, possibly due to enzyme variation during storage. IC<sub>50</sub> values were obtained from dose response curves, which were fitted by GraphPad Prism 6.01.

**Fluorescent Assays.** Six of the inhibitor hits were re-tested by fluorescent assays. 20 μM of fluorogenic substrate Z-Arg-Arg-7-amido-4-methylcoumarin hydrochloride (ZRR-AMC, Sigma Aldrich), 50 nM cathepsin B and 0.1 μM to 100 μM (or wider range) test compound were used. Reaction conditions were the same as MS-based dose dependent experiments. The results were readout by Packard Fusion Microplate Reader (PerkinElmer) with excitation wavelength at 348 nm and emission wavelength at 440 nm. The comparison with MS assay is shown in **Figure 3-11**.

## **Results and Discussion**

Mass spectra obtained for segmented samples are comparable to direct infusion. We do not detect signals that can be attributed to PFD at any time during infusion of samples (**Figure 3-5**), which suggests effective separation and no detrimental effects of oil on the MS performance.

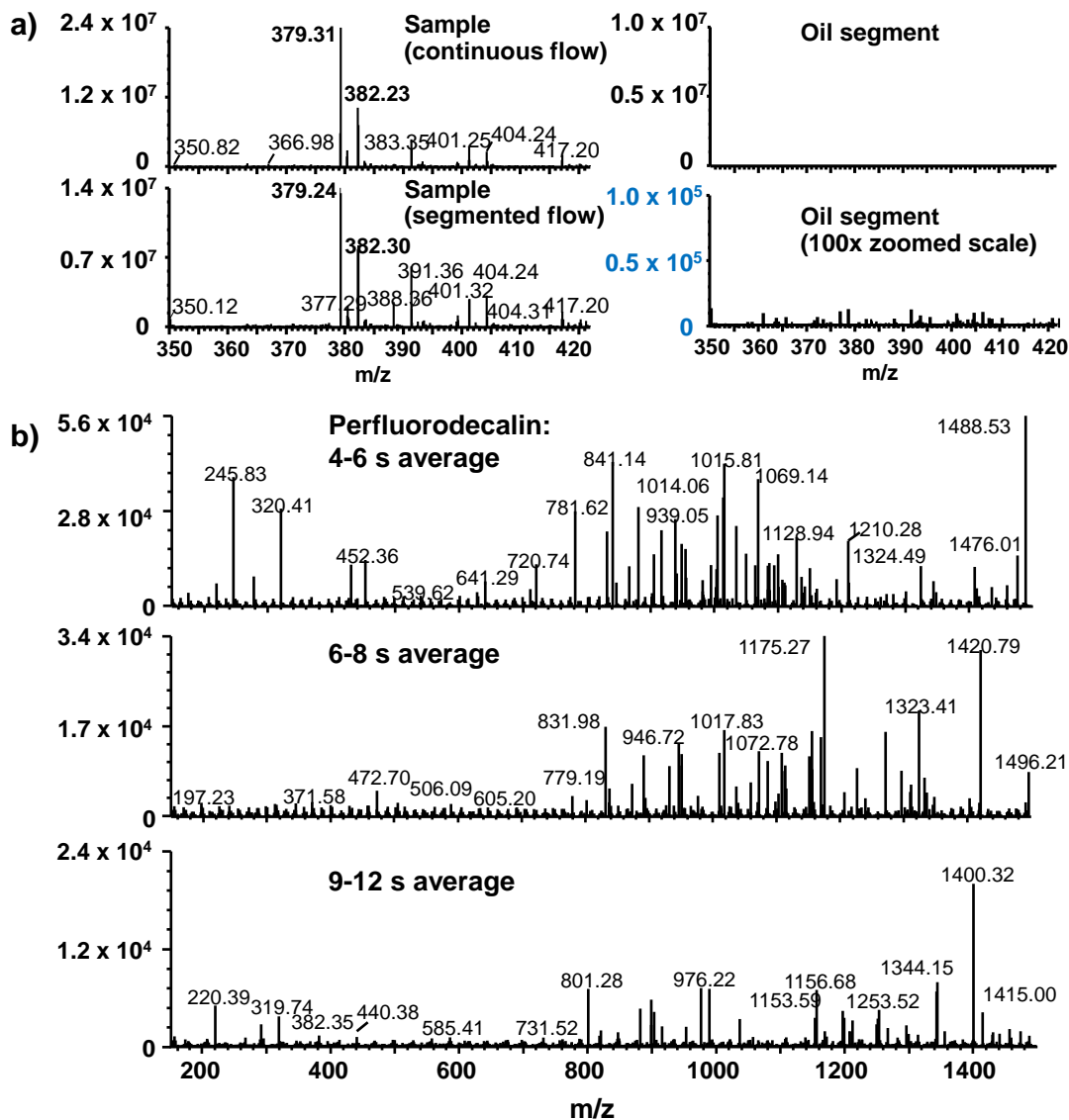


**Figure 3-5** Demonstration that oil does not affect the analysis of target molecules: A) left: averaged mass spectra of direct infusing FVGG (m/z 379) and FVG\*G (m/z 382) in continuous flow (top) and in segmented flow (bottom); right: oil segments in 10<sup>7</sup> y-axis scale (top) and same oil segments in 10<sup>5</sup> y-axis scale (bottom); B) averaged mass spectra of perfluorodecalin at different periods of time. The signal intensity of the oil is low. The absence of consistent peaks indicates that the oil is not ionized in the source and does not interfere with the analysis of any other compound.

The rate of mass spectra acquisition sets the ultimate limit for analysis rate. The highest scan rate of the MS used for this work is 62 scans/s for single ion monitoring and 27 scans/s for two ions. For quantitative analysis, it was desirable to obtain 6-8 scans per droplet which means that the analysis rate can be up to 5 Hz (i.e., 5 samples/s) for measuring a single ion and 2 Hz for two ions (assuming a 1:1 ratio of sample:oil). For 50 nL droplets, the MS-limited rate of 5 Hz could be achieved with an infusion flow rate of 30  $\mu\text{L}/\text{min}$ . This rate produced stable traces and reproducible detection of a select ion showing that the ESI can stop and start at such rates (**Figure 3-6**). We could reliably infuse up to 500 droplets at a time, the largest read length tested.

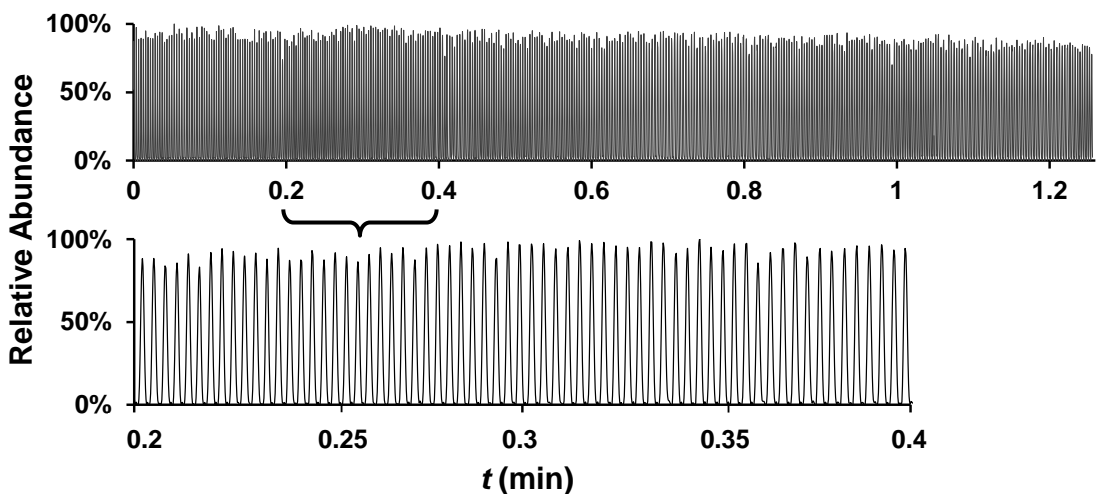


**Figure 3-6** Top: Traces of 384 droplets containing 5  $\mu\text{M}$  adenosine (solvent: 20% methanol, 0.1% formic acid) analyzed in 1.3 min (5 Hz). Droplets are 50 nL each and the infusion rate is 30  $\mu\text{L}/\text{min}$ . Bottom: the zoom-in view of 0.2-0.4 min. The RSD of droplet signal is  $\sim 5\%$ . Droplets are segmented by oil plugs which are not charged thus do not yield signal. MS method: single reaction monitoring (SRM),  $m/z$  268 $\rightarrow$ 136. Each droplet-oil pair consists of 10 to 12 data points.

Analysis rate is also affected by the amount of carry-over that can be tolerated because we found a link between carry-over in the mass spectrometry signals and analysis rate. For example, for 5  $\mu\text{M}$  adenosine followed by a blank droplet we detected no carry-over at 1 sample/s; but 10% at 2 samples/s and 20-30% at 4 samples/s (**Figure 3-7**). We observed no cross-contamination between droplets within the storage tubes, presumably due to low partition coefficients into the carrier fluid and wetting of the FEP surface by PFD. Therefore, the carry-over may be due to cross-droplet contamination occurring during transfer from FEP to ESI needle, within the needle, or in the gas phase. With the present system, carry-over can be reduced by decreasing the analysis rate or by introducing replicate samples. In the latter case, contamination becomes negligible in subsequent droplets so that averaging the signal from 3 droplets gives good quantification. Use of triplicate samples also provides redundancy for cases where a noise spike affects a measurement.

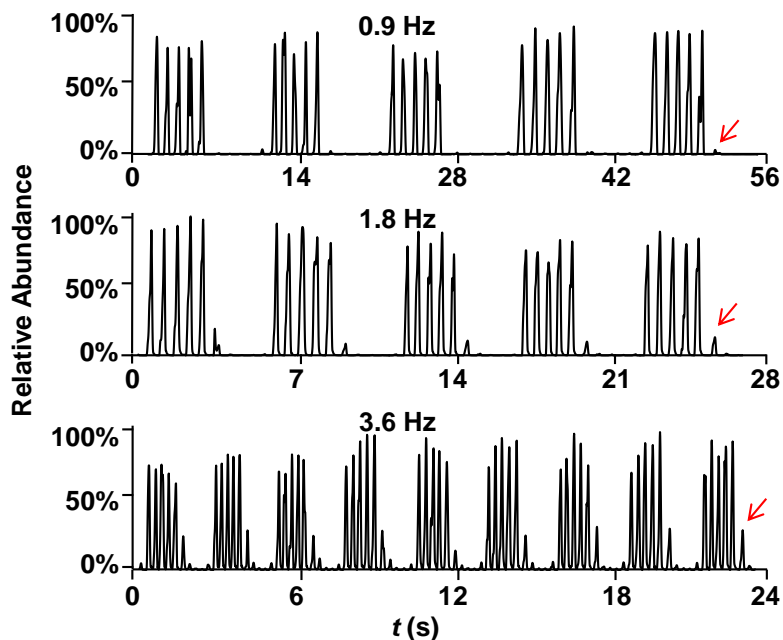


**Figure 3-7** Carry-over evaluation at different analysis rate. 5  $\mu\text{M}$  adenosine and solvent (20% methanol, 0.1% formic acid) alternating droplets (5 each) were infused into the ESI source for analysis. At 0.9 Hz, the carry-over is almost zero; at 1.8 Hz, it increases to 10%; at 3.6 Hz, it becomes as high as 20~30%. Red arrows indicate blank droplet that contains signal due to carry-over.

It is necessary to have rapid reformatting from MWP to droplets for overall high throughput. Previous reports demonstrated up to 0.15 droplets/s for forming segmented arrays from MWP which would be rate limiting in this case;<sup>132</sup> therefore, we explored increasing the rate of this step. Reformatting followed the general procedure previously described for PCR in droplets.<sup>133</sup> In this method, samples in a MWP are covered with a continuous layer of oil. The tip of a FEP tube, connected at the opposite end to a syringe operated in withdraw mode, is moved from well-to-well to generate samples separated by oil segments. Fast movement and high aspiration rate contribute to high droplet



generation rate. Using an aspiration rate of 4  $\mu\text{L}/\text{min}$  allowed at least 400 droplets of 50 nL to be formed inside a 90 cm long tube at a rate of 0.58 Hz and a droplet size relative standard deviation (RSD)  $<5\%$  (**Figure 3-2**). Higher aspiration rate tended to produce progressively smaller droplets as the tube was filled, likely due to increased leaking as the flow resistance increased with more droplets. To prevent droplet generation from being rate limiting, tubes can be operated in parallel. For example, we operated 8 tubes simultaneously to give an overall sample generation rate of 4.5 Hz with an RSD of droplet size across tubes  $<10\%$  (**Figure 3-2**).

We used this system to screen the Prestwick Chemical Library, consisting of 1,280 FDA-approved drugs, against cathepsin B. The assay used the heptapeptide GFGFVGG, a sequence representing the proteolytic preference of cathepsin B, as substrate.<sup>111</sup> Although we have previously demonstrated an MS assay for cathepsin B,<sup>82</sup> we modified reaction conditions for screening to use substrate concentration (80  $\mu\text{M}$ ) below the  $K_m$  and an incubation time that ensured linear reaction velocity. During the screen, the product peptide (FVGG) and a stable isotope-labeled form of this peptide (FVG\*G), added after the reaction was complete, were detected. Although adding detection of isotope-labeled standard required a slower MS scan rate, it was necessary to correct ion suppression and signal drift. The screen used standard MWP fluid manipulation for creating the reaction mixtures in 384-well plates and therefore can be incorporated into existing MWP screening systems.

Performing the assay, including reagent dispensing, incubation, and transferring to detection plates, took 1 h. The 1,408 reaction mixtures (1,280 test compounds and 128

controls) were reformatted into 4,224 droplets of  $70 \pm 7$  nL. Droplets were generated at 0.5 Hz/tube and MS analysis was conducted continuously at 1.6 Hz (**Figure 3-8**). The analysis of all sample droplets took ~45 min. Carry-over was lower than 15% from droplet to droplet during the screen, which did not affect the analysis of triplicate samples (**Figure 3-9**). The assay was robust as the Z-factors of all plates were above 0.72.

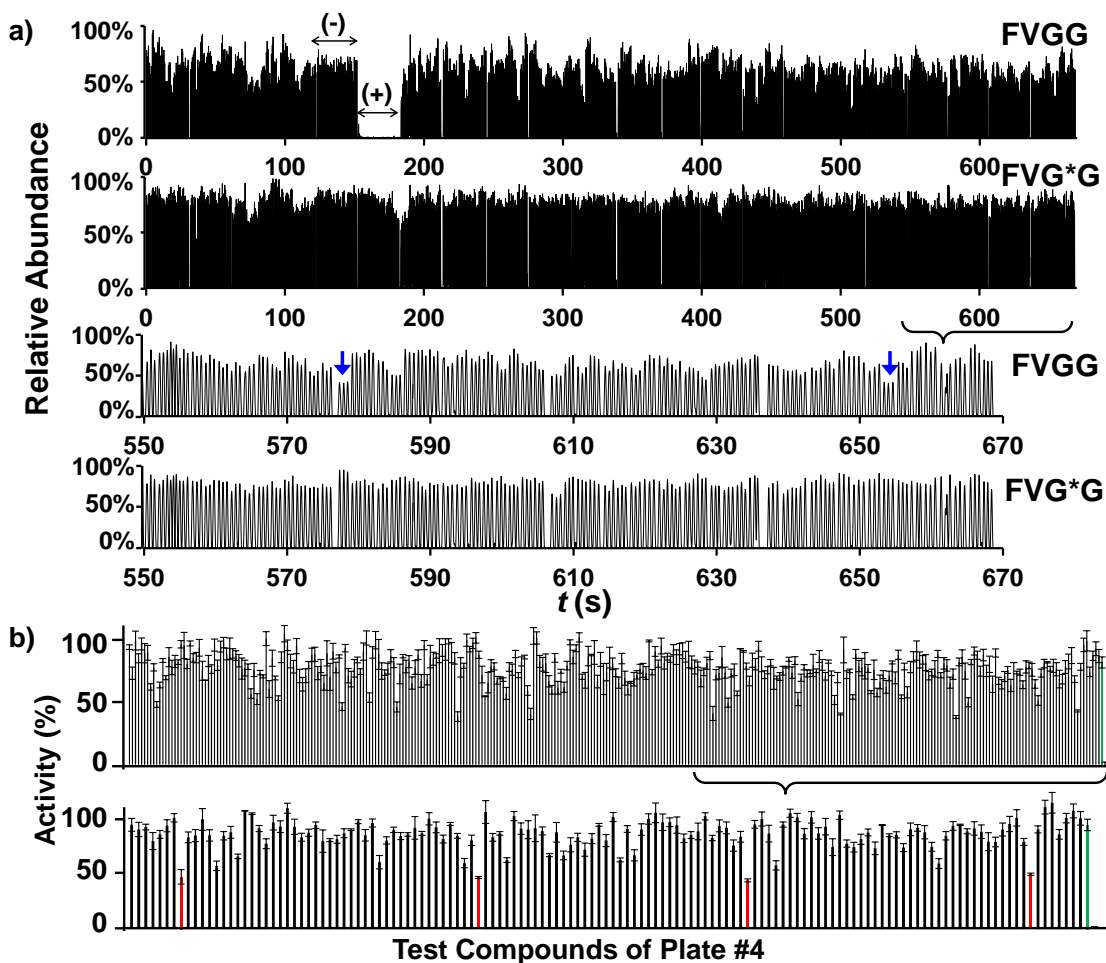


**Figure 3-8** A) Top: droplet traces of partial cathepsin B inhibitor screening (Plate #4, 320 test compounds, 16 negative controls (-), and 16 positive controls (+)). Each reaction is analyzed in triplicate. The analysis rate is 1.6 Hz (1056 droplets detected in 670 s. Bottom: The enlarged view of 550-670 s. Inhibitors (blue arrows) are identified by the

low intensity ratio of FVGG/FVG\*G. B) Top: the analysis result of Plate #4. Each bar is the averaged FVGG/FVG\*G of an assay. The negative control is normalized to 100% activity. Bottom: the last 135 reactions and controls (green). Inhibitors (red) are identified by the low % of activity (n = 3).

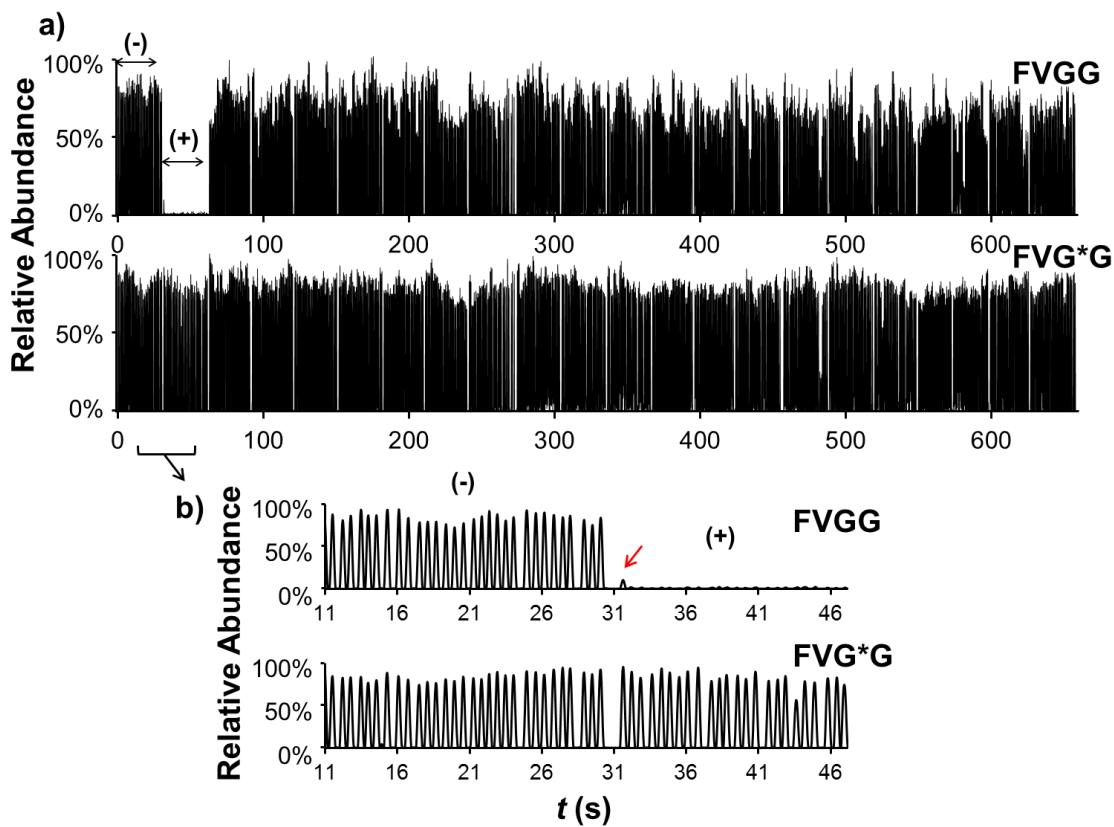


**Figure 3-9.** A) Sample droplet traces for portion of cathepsin B inhibitor screening (Plate #3, 320 test drugs, 16 negative controls (-), and 16 positive controls (+)). The analysis rate is 1.6 droplets/s; B) Zoom-in view shows the transition from negative control to positive control. The carry-over (red arrow) is only 12.5% for the first positive control. For the first 3 positive controls, the carry-over only affects the signal by 4.8%.

Among 1,280 test compounds, 9 reduced the reaction yield more than 50% and 15 inhibited the reaction ~40%. Interestingly, all hits were confirmed by dose response

assays (**Figure 3-10**), showing a low false positive rate (See **Appendix B** for goodness of fit of the sigmoidal model, and **Appendix C** for the structures of all hits).

Of the 24 chemicals that reduced the reaction yield 40% or more, 4 were known cathepsin or cysteine proteases inhibitors (chlorhexidine, luteolin, ethacrynic acid, and disulfiram). Another 6 hits (triclabendazole, hexachlorophene, anthralin, raloxifene, triclosan, and diacerein) have not been reported as cathepsin inhibitors, but are used to treat diseases in which cathepsins play a role. For example, triclabendazole is used to treat liver flukes which secrete cathepsins.<sup>134,135</sup>

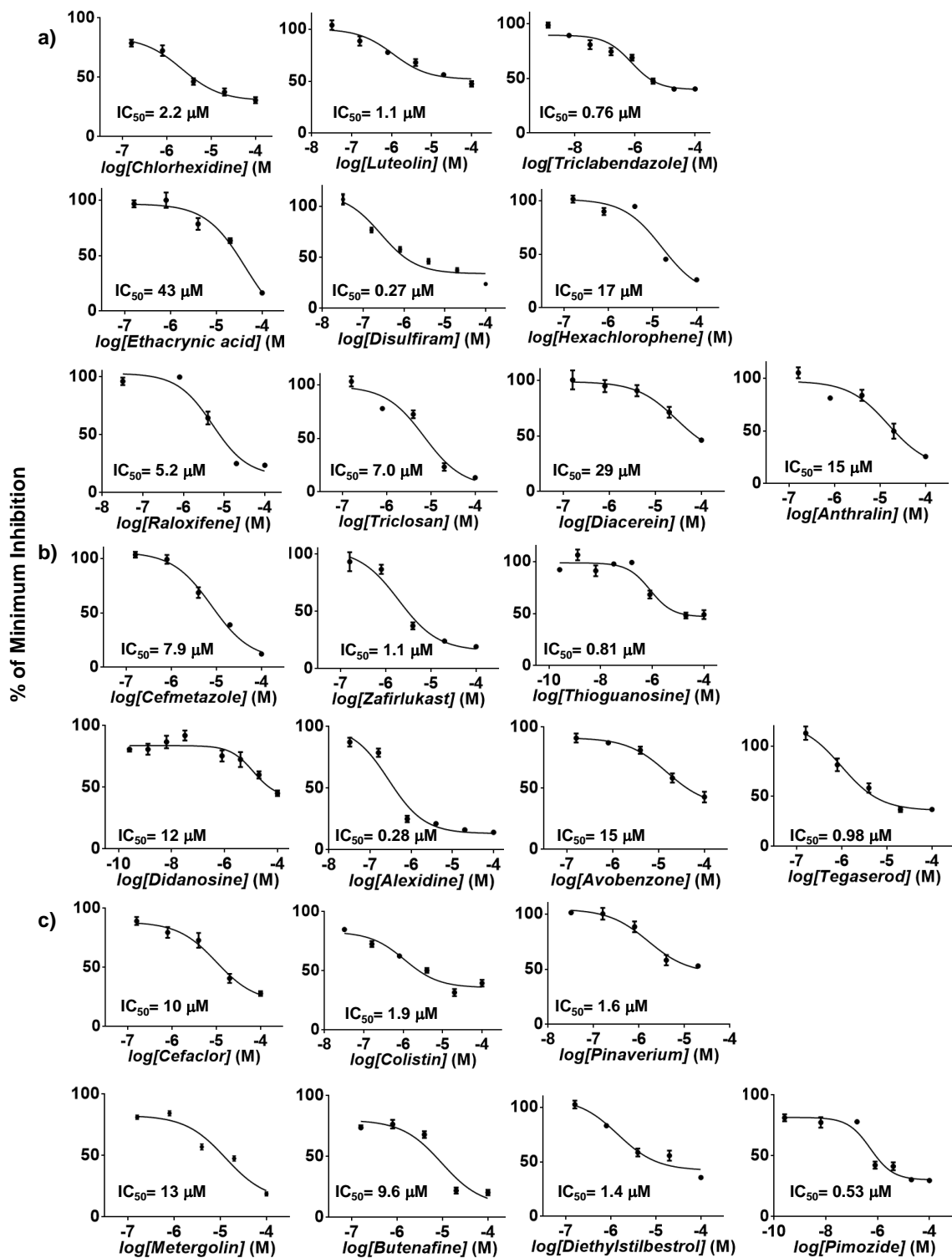


**Figure 3-10.** Dose response curves of the identified inhibitors. A) inhibitor hits that found to be related to cathepsins (chlorexid<sup>136</sup>, luteolin,<sup>137</sup> triclabendazole,<sup>134,135</sup>

ethacrynic acid,<sup>138</sup> disulfiram,<sup>139</sup> hexachlorophene (also strong inhibitor),<sup>140,141</sup> anthralin,<sup>142</sup> raloxifene,<sup>143</sup> triclosan,<sup>144-146</sup> and diacerein (strong inhibitor)<sup>147,148</sup>); B) drug molecules that reduced the yield by more than 50% in the primary screen but had no prior link to cathepsins (cefmetazole, zafirlukast, thioguanosine, didanosine, alexidine, avobenzone, and tegaserod); and C) those reduced the yield by ~40% in the primary screen but had no previous link to cathepsins (cefaclor, colistin, pinaverium, metergolin, diethylstilbestrol, butenafine and pimozide). Error bars are for 3 replicates.

The cathepsin inhibitory effect of the other 14 hits has yet to be studied, which suggests potential new therapeutic use for these compounds. Among them, 3 contain known ‘warheads’ of small molecule cathepsin B inhibitors (cefmetazole and cefaclor are  $\beta$ -lactams and alexidine contains a biguanide<sup>130</sup>). The remaining 11 hits do not contain structures established as cathepsin B inhibitors, suggesting an opportunity to develop modulators based on novel moieties.

To further validate the results, we performed fluorescent assays on several of these hits to test results in an orthogonal assay (**Figure 3-11**). The tested compounds all yielded dose response curves in both assays with similar IC<sub>50</sub> values. Variation may be attributed at least in part to use of different substrates for the assays.

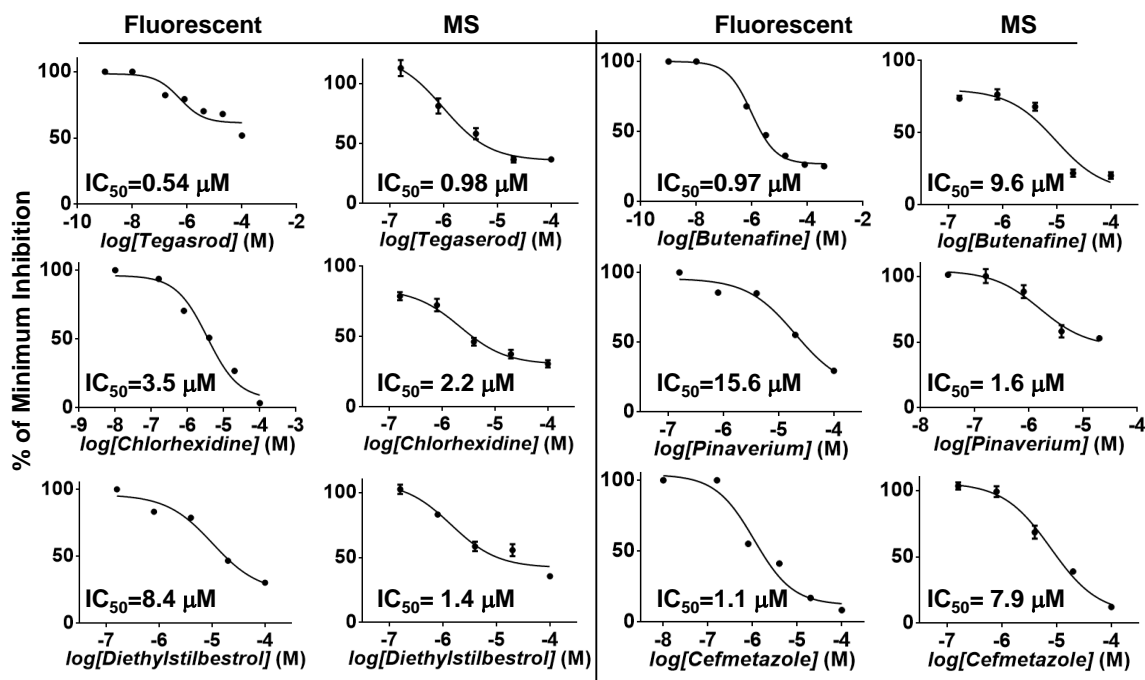


**Figure 3-11.** Comparison of dose response curves of 6 hits from fluorescent assay with MS assay. Fitted  $IC_{50}$  values generally agree with each other.

In principle, this system can achieve high throughput for a large number of samples. For example, 3,072 droplets can be created from eight 384-well plates within 12 min and analyzed in 26 min. Switching tubes from aspiration to MS manually required 4 min for 8 tubes. By overlapping droplet generation of the new batch with the analysis of the previous one, 147,456 droplets could be analyzed in 24 h suggesting the potential for ultra-high throughput MS analysis (**Figure 3-12**). The switching of tubes could be automated for faster analysis. Improving the read length could also reduce the number of times that this step is required further improving throughput. Another improvement may be integrating high throughput sample preparation prior to the reformatting. Utilizing

parallel desalting multi-well plates could extend the applicability of the system to the assays that strictly require non-volatile buffers or additives.

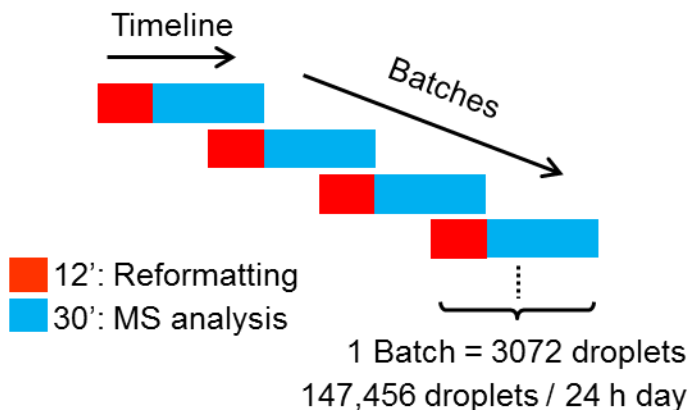


**Figure 3-12** Timing diagram for batch mode operation using mass spectrometry plate reader. Reformatting samples from MWP into 3,072 droplets takes 12 min (4.5 Hz); MS analysis takes 30 min (2 Hz, plus the tubing switching time). By overlapping the reformatting and analysis of continuous batches, 147,456 droplets could be analyzed in a day.

## Conclusion

These results demonstrate that droplet ESI-MS has the robustness and throughput to be used for HTS applications. The system provided reliable results for over 4,000 samples in a HTS workflow. The low false positives and identification of novel compounds support the idea that high-throughput, droplet-based ESI-MS can be a powerful tool for label-free screening. Although the current droplet system has higher throughput than systems which use solid-phase extraction or LC,<sup>149,150</sup> it is restricted to assays that can be performed in ESI-MS compatible buffers. Although many targets will



likely be compatible with such buffers, this limitation does suggest that future work should be directed towards methods of rapid sample clean-up, e.g. parallel solid phase micro-extraction<sup>151</sup> or in-plate solid-phase extraction<sup>152,153</sup> so that so the high throughput capability could be used with a wider range of assays. Another important advantage relative to current MS-based methods is that this approach uses miniscule fractions of a sample and therefore could be compatible with lower volume, higher-density well plates for reduction of reagent consumption. Overall, these results suggest that the droplet based method adds to or complements existing MS screening systems.

## **CHAPTER 4**

# **DEVELOPMENT OF LABEL-FREE SIRTUIN 1 ASSAY FOR HIGH THROUGHPUT MODULATOR SCREENING USING SEGMENTED FLOW-ELECTROSPRAY IONIZATION MASS SPECTROMETRY**

### **Introduction**

High throughput screening (HTS) is a technology that can rapidly identify biological active compounds against a panel of targets through millions of assays. Though HTS is dominated by optical detection methods, especially fluorescence plate readers, label-free analyses have gained increasing attention in recent years.<sup>1,2</sup> Performing assays without incorporating artificial labels are beneficial in several ways: minimal manipulation on the reaction components, less assay artifacts such as auto-fluorescence from test compounds, relatively simplified assay development, and lower reagent cost for large-scale screenings.<sup>6,7</sup>

One of the most powerful label-free analyzers is mass spectrometry (MS). The capability of identifying analytes solely based on mass to charge ratio, and features of

high sensitivity, rapid scanning and multiplexing make MS a promising detector for high throughput screening (HTS).<sup>7,24,102,116</sup> The potential high analysis rate of MS is often compromised by slow sample introduction approaches or the requirement of sample preparation. It inspired us to seek for alternatives. Droplet microfluidics is an attractive platform for HTS because it can reliably manipulate nanoliter scale samples and conduct miniaturized reactions with high speed, precision and automation.<sup>26</sup> Previous works have shown that oil-segmented droplets can be directly infused into electrospray ionization (ESI) source for rapid analysis of discrete samples with minimal carry-over.<sup>40,82,123</sup> Screenings for enzyme modulators have been carried out using droplets-ESI-MS system.<sup>41,82,83</sup>

Sirtuins are a class of conserved NAD<sup>+</sup>-dependent deacetylases. There are seven mammalian homologues identified: SIRT1 to SIRT7. The activities of sirtuins influence DNA repair, gene silencing, cellular stress resistance, tumorigenesis, energy metabolism and longevity. The relation between sirtuins and aging-related diseases has attracted most attention.<sup>56</sup> Mammalian SIRT1 is evolutionarily closest to the founding member of sirtuin family, yeast Sir2. It is localized in nucleus, but can be shuttled to the cytoplasm in need, dependent on the tissue.<sup>154</sup> The function of SIRT1 encompasses a wide spectrum. It improves genomic stability by deacetylating various factors related to DNA repair; protects cells against stress by regulating the heat shock response; interacts with p53 to modulate the threshold for cell death in response to stress; deacetylates PGC-1 $\alpha$  which is a transcriptional coactivator regulating hepatic gluconeogenesis and fatty acid oxidation; elevates the secretion of insulin under stimulation of glucose; affects vascular biology

through influence several factors; and counteracts inflammation in age-related diseases by negatively regulates NF- $\kappa$ B.<sup>154-156</sup> Due to the increasing evidence that SIRT1 may mitigate metabolic dysfunctions, researchers have never ceased the effort in searching for its activators. Several SIRT1 activators have been discovered by a fluorogenic assay. In vivo studies confirmed their beneficial effects in metabolism. However, due to the involvement of the fluorescent label, whether they directly impact SIRT1 remains disputable.<sup>60</sup>

In this work, we seek to develop a label-free SIRT1 assay which can be analyzed by droplet-ESI-MS system without sample preparation. SIRT1 was first dialyzed into an ESI-compatible formate buffer prior to the screening. Reactions were then conducted in the formate buffer, instead of the commonly used Tris buffer. Afterwards, samples in a multi-well plate were reformatted into oil-segmented nanoliter droplets and finally infused into ESI-MS for analysis (**Figure 4-1**). The assay was tested by a pilot screen involving 80 test compounds with known properties. Inhibitor hits were validated by dose response experiments. The system is applicable to any scale SIRT1 modulator screening and is possible to be generalized to other enzymes.

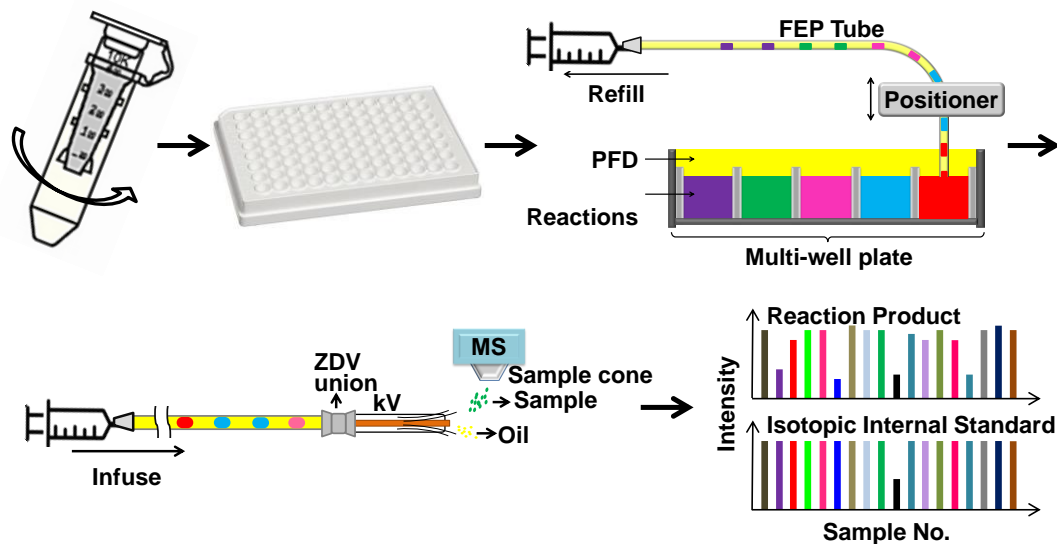


**Figure 4-1** Diagram of SIRT1 assay: SIRT1 was dialyzed from Tris buffer into formate buffer using a centrifugal dialysis unit; then the deacetylation reactions were conducted in formate buffer in a multi-well plate; reaction mixtures were afterwards reformatted into oil-segmented droplets in a piece of FEP (fluorinated ethylene propylene) tube; finally, droplets were infused into an orthogonal ESI source through a modified ESI needle. The FEP tube and the needle were connected by a ZDV (zero dead volume) union. The signal intensity of the reaction product and its isotopic internal standard are monitored. Oil segment did not generate any ESI signal thus showed as spacing between sample droplets.

## Experimental Section

**Chemicals and Materials.** Unless otherwise specified, all solvents were purchased from Honeywell Burdick & Jackson (Muskegon, MI) and were certified ACS grade or better. Reagents were purchased from Sigma Aldrich (St. Louis, MO). Human recombinant SIRT1 and Epigenetic Screening Library were purchased from Cayman Chemical (Ann Arbor, MI). Histone H3K9(Ac) and H3K9 were purchased from AnaSpec

(Fremont, CA). Isotope labeled H3K9 was synthesized by the Marsh lab, University of Michigan.

**MS-based SIRT1 Assay.** The original buffer of SIRT1 (50 mM Tris-HCl and 140 mM total inorganic salts, pH 8.0) was exchanged into an ESI-MS-compatible buffer (200 mM ammonium formate, 200  $\mu$ M dithiothreitol (DTT) and 200  $\mu$ M NAD<sup>+</sup>, pH was adjusted to 8.0 by ammonium hydroxide) using Amicon Ultra-0.5 mL (EMD Millipore, Billerica, MA) with 50 kD cutoff. Each 50  $\mu$ L SIRT1 (1 mg/mL) was dialyzed against 500  $\mu$ L formate buffer twice. The collected SIRT1 was diluted by the new buffer to the designated concentration. The procedure was conducted at 4°C.

An unlabeled 21-mer peptide H3K9(Ac) (ARTKQTARK(Ac)STGGKAPRKQLA) was selected to be the substrate. The deacetylation product is H3K9 (ARTKQTARKSTGGKAPRKQLA) (**Figure 4-2**). Reactions were performed in the formate buffer and terminated with equal volume of quenching reagents consisting of 50% methanol, 50% water, 0.2% formic acid (v/v) and 10  $\mu$ M isotope-labeled H3K9 (H3K9\*, +12 Da).

The linearity of the reaction was assessed by a series of assays incubated for 0, 15, 30, 60, 90, 120 min. Each assay contained final concentration of 0.5  $\mu$ M SIRT1 and 20  $\mu$ M H3K9(Ac). The Michaelis–Menten kinetics were measured by varying H3K9(Ac) concentration from 0 to 160  $\mu$ M and quenching the reaction at different times from 0 to 120 min. The  $K_m$  value was fit by Michaelis-Menten model with GraphPad Prism 6.01.

The detection of product H3K9 was calibrated by measuring the intensity ratio of H3K9 over H3K9\*. The curve was linear from 0 to 25  $\mu\text{M}$  H3K9 (**Figure 4-4**).

**Epigenetic Library Screening.** The screening was performed in part of a 384-well plate (Greiner Bio-one, Monroe, NC), in  $8 \times 13$  format. Screening conditions were determined by the assay development. 50  $\mu\text{L}$  SIRT1 at 11  $\mu\text{M}$  was buffer exchanged and then diluted to 650  $\mu\text{L}$  by the formate buffer. Column 1, 6 and 13 were added with 1  $\mu\text{L}$  10% DMSO as negative control. Column 2-5 and 7-12 were added with 1  $\mu\text{L}$  test compound at 200  $\mu\text{M}$  in 10% DMSO from the Epigenetic Screening Library. 6  $\mu\text{L}$  of new SIRT1 solution was then added to each well by Matrix Electronic Multichannel Pipette (Thermo Scientific, Waltham, MA). Afterwards, 3  $\mu\text{L}$  of 67  $\mu\text{M}$  H3K9(Ac) was deposited into each well. The final concentrations were 20  $\mu\text{M}$  test compounds, 0.5  $\mu\text{M}$  SIRT1, and 20  $\mu\text{M}$  H3K9(Ac). Each reaction contained 1% DMSO. Reactions were incubated at 37°C for 1.5 hours and then quenched with 10  $\mu\text{L}$  ice-cold quenching reagent.

**Droplet-MS Analysis.** Reaction mixtures were first transferred into a custom 384-well readout plate,<sup>83</sup> and then reformatted from the readout plates into oil-segmented droplets which were stored in a piece of fluorinated ethylene propylene (FEP) tube. The oil phase was perfluorodecalin (PFD). The procedure has been previously described.<sup>83</sup> Each reaction was collected as 3 droplets of 100 nL each. The oil gap was the same size with the droplet.

The MS analysis was performed by Micromass Quattro Ultima triple quadrupole MS (Waters Corporation, Milford, MA) in full scan mode (m/z 550-785). The scan time was set as 0.05 s. The ESI voltage was +3.0 kV. Droplets were pumped into the source through a custom ESI needle at 10  $\mu\text{L}/\text{min}$ .<sup>123</sup> Droplet traces were acquired by MassLynx 4.0. The intensity of  $[\text{M}+3\text{H}]^{3+}$  (m/z 752.6) and  $[\text{M}+4\text{H}]^{4+}$  (m/z 564.6) ions of the product H3K9 and isotopic standard H3K9\* (m/z 756.3 and 567.4) were measured for quantifying the reaction yield (**Figure 4-2**). Data was analyzed by Origin 8.5.

**Dose dependent experiment.** Compounds that reduced the reaction yield by more than 50% were selected as strong inhibitor hits. A series of reactions containing a concentration range of the hits (as indicated in **Figure 4-6**) were performed. Each reaction contained final concentration of 0.5  $\mu\text{M}$  SIRT1 and 20  $\mu\text{M}$  H3K9(Ac). After incubation at 37°C for 1 hour, reactions were stopped by ice-cold quenching reagents which had 20  $\mu\text{M}$  H3K9\* in it. The dose response curves were fitted using GraphPad Prism 6.01.

## Results and Discussion

**MS analysis.** H3K9 and H3K9\* are multiply charged in the full scan mass spectrum (**Figure 4-2**). Charge states from  $[\text{M}+7\text{H}]^{7+}$  to  $[\text{M}+3\text{H}]^{3+}$  are observable on the spectrum. However, scanning a wide mass range reduces the analysis rate. We found that the  $[\text{M}+4\text{H}]^{4+}$  and the  $[\text{M}+3\text{H}]^{3+}$  peaks dominate the mass spectrum and the sum of their



intensity can be linearly calibrated with peptide concentration. Therefore we narrowed down the scan range to  $m/z$  550-785. The scan time was set as 0.05 s to ensure adequate ion abundance.

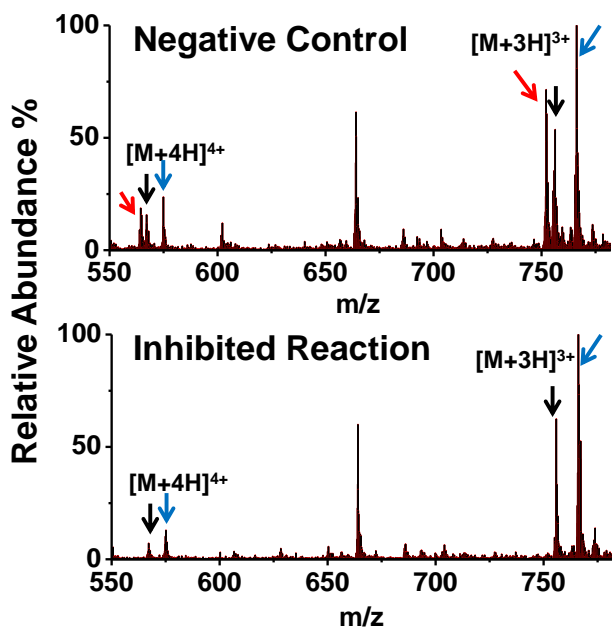
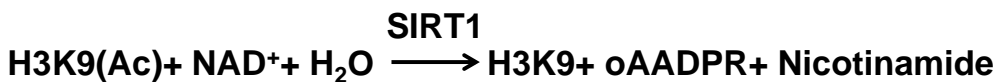


**Figure 4-2.** Deacetylation of H3K9(Ac) by SIRT1. The reaction is shown on the top. The lower mass spectra show a reaction without any modulator (negative control) and a reaction with an inhibitor. Triply charged and quadruply charged H3K9 (red arrows), H3K9\* (black arrows) and H3K9(Ac) (blue arrows) are monitored. Intensity ratio of H3K9/ H3K9\* is calculated for quantification.

**Buffer Exchange for SIRT1.** Many components in buffers for enzymatic reactions may affect the ESI process. Millimolar level non-volatile salts, such as NaCl and  $\text{K}_2\text{HPO}_4$  severely suppress the signal of other compounds. Some other components,

such as Tris or glycerol compete for the charge on the surface of the ESI droplets with the target analytes, especially when these components are very concentrated. In order to make the SIRT1 reaction directly analyzable by ESI-MS, we have developed a reaction buffer containing volatile salt ammonium formate and a small molecule reducing agent DTT which would not affect the ESI process of any other compounds.

A spin dialysis unit was chosen for buffer exchange due to its high speed and efficiency. The dialysis was performed at 4°C to prevent heating of the protein during centrifugation. We found that one spinning unit can dialyze 50 µL of SIRT1 (~50 µg) with best desalting effect and recovery. For complete removal of salts and other interferences, 1000 µL of formate buffer was used, 500 µL each time. We explored several combinations of centrifugal force and centrifuging time and found that using 8000 g and 4 min/spin, SIRT1 could be completely desalted, and its deacetylation activity was maintained to the largest extent.

**Ammonium Buffer for SIRT1 Assay.** We compared the deacetylation activity of SIRT1 before and after buffer exchange. The reaction yield was nearly 100% after 4 hour incubation in the original Tris buffer and about 90% in the formate buffer (See chromatograms in **Figure 4-3**). It proves that the desalting process does not adversely affect the activity of the enzyme, and the reaction runs efficiently in the formate buffer. We believe that Tris is not essential to this protein for both the structure and catalytic ability. Other enzymes which are not strict on the buffer might also react under such condition, which allows direct ESI-MS analysis.

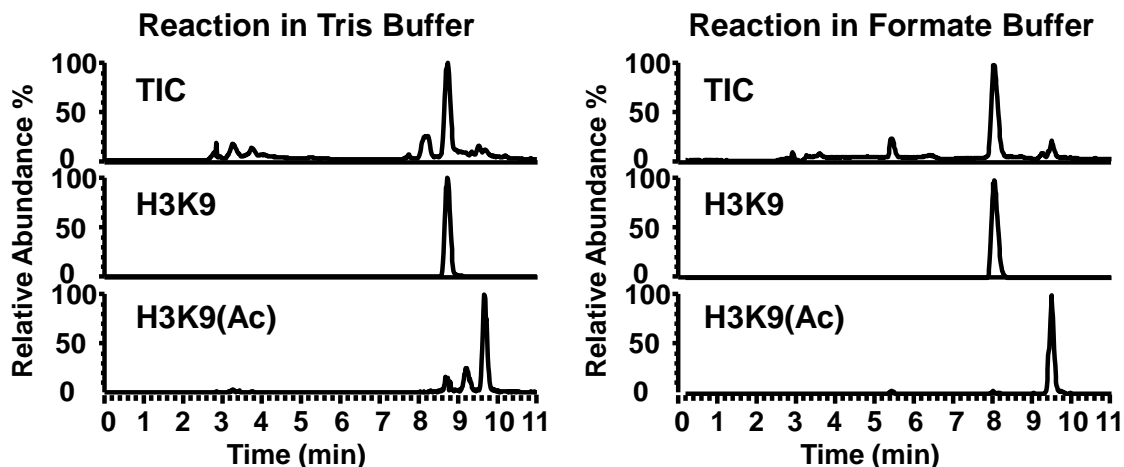


**Figure 4-3.** Left: reaction conducted in the Tris buffer. Observed from TIC (total ion current), nearly 100% yield was achieved. Right: reaction conducted in the formate buffer. A little substrate was not converted. But the yield was still high enough which indicates good enzyme activity. (Column: made-in-house 8 cm fused- silica capillary column (75  $\mu\text{m}$  i.d./360  $\mu\text{m}$  o.d.) packed with 5  $\mu\text{m}$  C18 particle.<sup>157</sup> Mobile phase A: 0.15% formic acid aqueous solution. Mobile phase B: methanol. Linear gradient: initial, 0% B; 10 min, 50% B; 15 min, 50% B; 18 min, 95% B; 20 min, 100% B).

**Assay Condition Optimization.** We chose a known SIRT1 substrate: H3K9(Ac) (Ac-Histone H3 lysine 9) as the assay substrate. Because it is not labeled, it avoids any possible interference, and it can only be analyzed by MS. To better mimic deacetylation of histone H3 protein by SIRT1, we chose a peptide consisting of 21 amino acids. Smaller peptides might not interact with the SIRT1 catalytic site in the similar way with the whole protein, while larger peptides will challenge the analysis rate, sensitivity and quantification of MS.

It is necessary to study the kinetics of an enzyme before screening for modulators. Competitive or reversible modulators are of most interest because they are usually less

toxic than irreversible ones. Performing the assay under its initial velocity conditions increases the sensitivity to the desired modulators. The concentration of the substrate needs to be under or equal its  $K_m$  value so that it will not saturate the catalytic site of the protein. The reaction time should be limited to when the product is still accumulating linearly. By that time the substrate has not been largely converted into product and the reverse reaction does not significantly affect the turnover rate.<sup>1</sup> Searching for activators require more critical conditions. It is crucial to keep the substrate concentration low so that the reaction rate can be elevated by activators.

We studied SIRT1 kinetics by conducting a set of assays starting with different substrate concentrations and were quenched at a range of times. We found that the  $K_m$  value of H3K9(Ac) is 22  $\mu\text{M}$  (published  $K_m$  is  $\sim 40 \mu\text{M}$ <sup>71</sup>). For 0.5  $\mu\text{M}$  SIRT1, reaction yield grows linearly for up to 2 hours when H3K9(Ac) is 20  $\mu\text{M}$  (**Figure 4-4A, B**). Therefore, we decided to use 20  $\mu\text{M}$  H3K9(Ac) and 1.5 h incubation for the screening.

Linear response for the target analyte is crucial. In the SIRT1 assay, we monitored H3K9 and its isotopic internal standard. The intensity ratio of H3K9 over H3K9\* increases linearly with H3K9 concentration up to 25  $\mu\text{M}$  ( $R^2 > 0.99$ ) (**Figure 4-4C**).

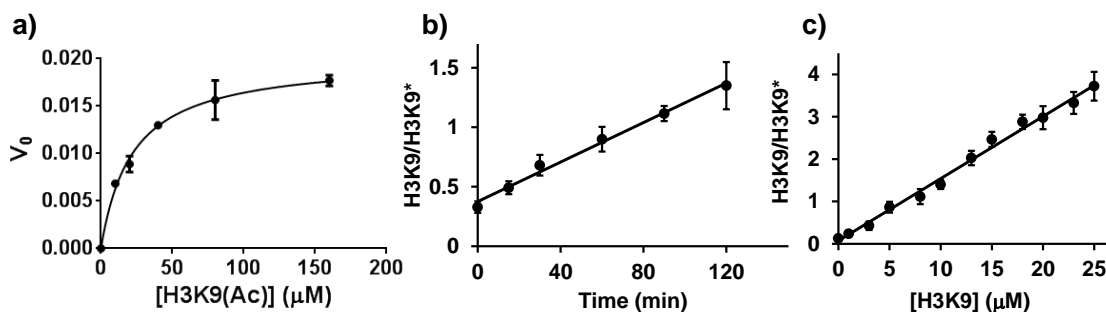


**Figure 4-4.** A) Michaelis-Menten model of H3K9(Ac) with 0.5  $\mu\text{M}$  SIRT1. The fitted  $K_m$  value is 22  $\mu\text{M}$ . B) Linear reaction within 2 h. C) Linear calibration curve of 0 to 25  $\mu\text{M}$  H3K9. Intensity ratio of H3K9 to H3K9\* was measured ( $n = 3$ ).

**Screening.** The assay conditions were tested by a pilot screening against the Epigenetic Screening Library, which is made up of 80 epigenetic modulators, including known SIRT1 inhibitors. Another 24 reactions only containing 1% DMSO were performed as the negative control. The controls were placed at the beginning, in the middle, and at the end of the screening. To avoid precipitation or aggregation effect, test compounds are typically in 10-30  $\mu\text{M}$  range. Also, low concentration can rule out weak modulators. For our screening, each test compound was 20  $\mu\text{M}$ . The concentration of H3K9(Ac) and the incubation time were determined based on the enzyme kinetic studies. Matrix multichannel pipette was utilized for rapid and reproducible reagents dispensing to make the start time of all reactions was as close as possible. The similar intensity ratio of H3K9 over H3K9\* of all negative controls demonstrates the simultaneous reaction initiation (**Figure 4-5A**). Therefore, the yield in test reactions can be compared with the negative control.

After transferring reactions from the assay plate into custom readout plate which was described before,<sup>83</sup> 104 reactions were made into triplicate droplets (312 droplets in total) at 0.5 Hz. Replicates are necessary because it provides backup data when signal spikes or occasional fluctuation affecting the detection. Besides, if the carryover affects the measurement, the first droplet of each sample set may not be analyzed.

Droplets were detected by MS in a full scan mode, yielding stable signals (**Figure 4-5A**). The detection of all 312 droplets took ~5 min (0.8 Hz). The results are straightforward as a low H3K9/H3K9\* suggests a potential inhibitor (**Figure 4-6B, C**). The assay was reliable as the Z-factor was 0.7. The isotopic internal standard is useful for correcting the impact of certain test compounds on the ESI process of the product peptide.

In this 80-compound screening, we set the inhibitor criteria as reducing the yield by more than 50%. This standard might miss some weak SIRT1 inhibitors, but we aimed at identifying strong inhibitors. 4 compounds met the criteria: suramin, EX-527, C646 and anacardic acid. Suramin and EX-527 are known SIRT1 inhibitors.<sup>158-160</sup> Anacardic acid has recently been found to have potential to inhibit sirtuins.<sup>161,162</sup> Inhibition by C646 has not been reported yet. Their inhibitory potency was evaluated by dose response experiments (**Figure 4-6**). The fitted IC<sub>50</sub> of EX-527 and suramin agree with the published values (EX-527: 100 nM;<sup>159</sup> suramin: 300 nM<sup>158</sup>). Other known SIRT1 inhibitors which were not identified in this screening might because their inhibition potency is relatively low. For example, the IC<sub>50</sub> of nicotinamide is > 50 μM,<sup>163</sup> sirtinol is 131 μM,<sup>164</sup> and Tenovin-6 inhibits 40% of SIRT1 activity at 20 μM.<sup>165</sup> Those compounds showed 22%, 30% and 30% inhibition at 20 μM in my screening, respectively.

The activator criterion is elevating the yield by more than 50%. In this screening, no activator was identified (**Figure 4-5C**). The Epigenetic Library includes resveratrol and piceatannol, both of which are allegedly SIRT1 activator (being reported to increase the turnover rate by at least 3 times<sup>59,71</sup>). However, the result of our MS assay as well as

other label-free assays<sup>68,69</sup> do not confirm such activation effect. The real mechanism of these activators calls for further study.

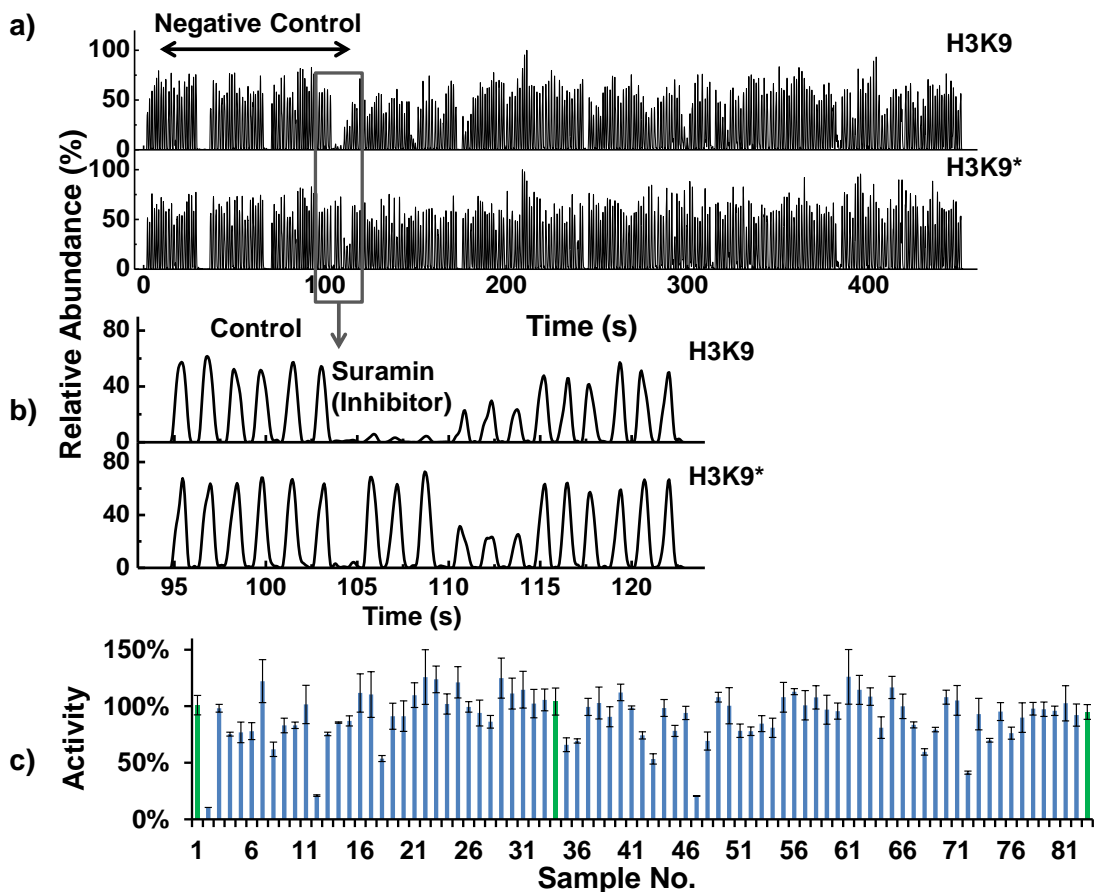


**Figure 4-5.** Epigenetic library screening: A) Raw droplet traces of the screening. The upper trace is the reaction product H3K9, the lower one is the isotope-labeled internal standard H3K9\*. The first 3 sets are negative controls at the beginning, in the middle, and at the end of the assay plate, respectively. B) Enlarged view of the control, reaction containing suramin, and some other test reactions droplets. C) The final analysis of the screening. Each bar is the averaged H3K9/H3K9\* of an assay. The negative control (green) is normalized to 100% enzyme activity. 4 reactions showed that the enzyme activity was lowered by more than 50% (n = 3).

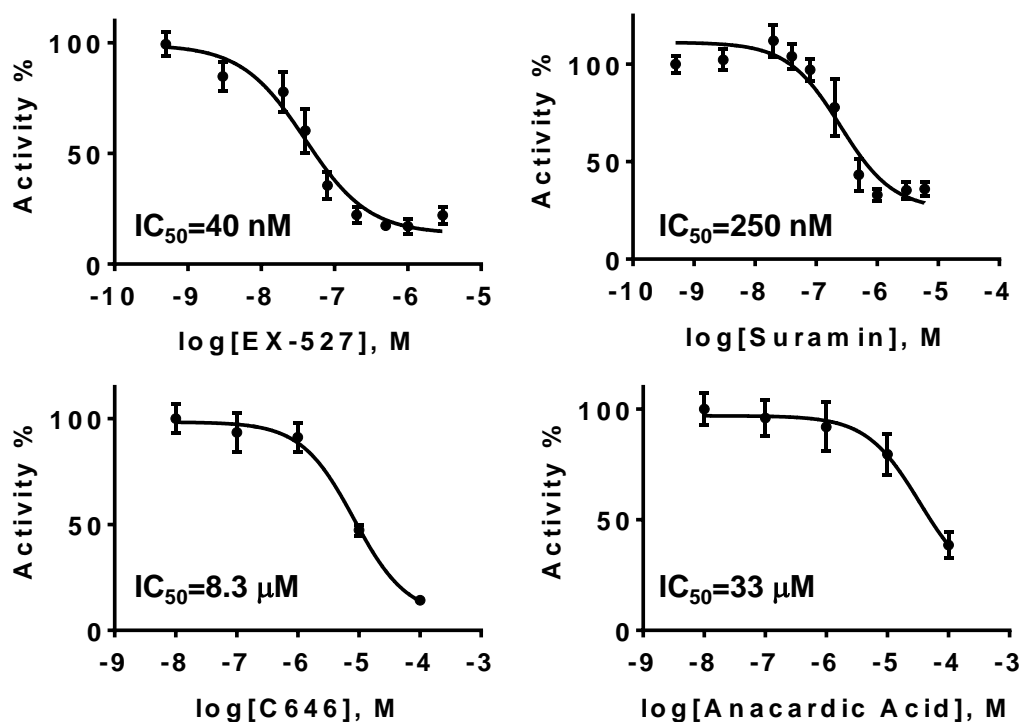


**Figure 4-7.** Dose response curves of 4 inhibitor hits. The negative control of each experiments were normalized to 100% activity (n = 2).

## Conclusion

We have developed a label-free SIRT1 assay which can be applied to droplet-ESI-MS high throughput screening system. The screen against Epigenetic Screening Library involving 80 test compounds demonstrated the high throughput (0.8 Hz) and high reliability (Z-factor = 0.7) of the assay. The approach can be logically generalized to any enzyme that maintains good activity in the described MS-compatible condition. The wide applicability of ESI-MS makes possible the detection of a variety of reaction products. This method can be complementary to but faster and more economical than the solid



phase extraction (SPE)-ESI-MS screening method<sup>19</sup>. Future directions include applying the label-free SIRT1 assay to large scale SIRT1 modulator screening in search of molecules that directly interact with SIRT1. Other MS-compatible conditions can be explored to further improve the universality of this concept.

## **CHAPTER 5**

### **DEVELOPMENT OF MASS SPECTROMETRY-BASED ASSAYS FOR HIGH THROUGHPUT SIRTUIN 6 MODULATOR SCREENING**

#### **Introduction**

Sirtuin 6 (SIRT6) is one of the 7 mammalian human sirtuins, which are a group of highly conserved NAD<sup>+</sup>-dependent deacetylases. SIRT6 is predominantly localized inside the nucleus and associated with the chromatin. SIRT6 mainly acts as adenosine diphosphate (ADP) ribosylase, histone deacetylase and deacylase. SIRT6-knockout mice suffer from increased genomic damage and instability, progeroid syndrome, hypoglycemia, and early death. A study showed that transgenic mice overexpressing SIRT6 have had lifespan enhanced by 15%. Though the effect was only observed in male mice, it suggests that SIRT6 might be central in controlling aging.<sup>75</sup> SIRT6 protects telomeres on chromatin through deacetylating histone H3 lysine 9.<sup>56</sup> SIRT6 removes ADP-ribose from PARP-1 that leads to DNA repair. Besides, SIRT6 regulates the transcription of hundreds of genes thus participates in many metabolic pathways.<sup>154</sup>

Because of the beneficial effect of SIRT6 overexpression, molecules that activate SIRT6 are especially interested in treating aging-related metabolic diseases. To date, only a few SIRT6 modulators have been reported.<sup>79,81,166</sup> Motivated by the success of our cathepsin B inhibitor screening, we plan to make our contribution to the search for SIRT6 modulators by using the mass spectrometry plate reader.

In this work, we developed 2 SIRT6 MS assays which are readily to be used in a large-scale screening. In the first assay, we strive to conduct the reaction in the SIRT6-preferred environment. Deacetylation of H3K9(Ac) by SIRT6 was performed in the traditional Tris buffer. Reactions were diluted by 20 folds before reformatting into droplets. A test screening against 25 test compounds proved the high reliability of this method. We also evaluated the data quality of single detection compared with triplicated detection (making one droplet per reaction versus making three). Without replicates, the analysis rate was reduced from up to 2 Hz to 0.7 Hz to avoid carryover and high spikes which tend to occur in rapid analysis. But unlike triplicate detection, the actual throughput (samples/s) is not 1/3 of the droplet analysis rate (droplets/s). Therefore, single detection leads to slightly higher throughput than triplicate detection. Besides, less droplets are required to be generated for the whole screening.

The second assay was developed with another substrate: decanoylated histone H3 lysine 9 (H3K9(decanoyl)). SIRT6 has been shown to be very efficient in deacylation. Long chain fatty acylated proteins are potentially endogenous SIRT6 substrates.<sup>78</sup> Modulators discovered from this assay may have completely different physiological functions with the deacetylation assay.

## Experimental Section

**Chemicals and Materials.** Unless otherwise specified, all solvents were purchased from Honeywell Burdick & Jackson (Muskegon, MI) and were certified ACS grade or better. Human recombinant SIRT6 was purchased from Cayman Chemical (Ann Arbor, MI). Histone H3K9(Ac) and H3K9 were purchased from AnaSpec (Fremont, CA). Isotope labeled H3K9 was synthesized by the Marsh lab, University of Michigan. Histone H3K9(decanoyl) was synthesized by Pierce Biotechnology Inc. (Rockford, IL).

**Deacetylation of H3K9(Ac) by SIRT6.** 3  $\mu\text{M}$  of human recombinant SIRT6 (1 mg/mL in 50 mM Tris-HCl, 140 mM total inorganic salts, and 10% glycerol) and 60  $\mu\text{M}$  of H3K9(Ac) (NH<sub>2</sub>-ARTKQTARK(Ac)STGGKAPRKQLA-OH) were mixed into NAD<sup>+</sup>-Tris buffer (500  $\mu\text{M}$  NAD<sup>+</sup>, 50 mM Tris-HCl and 200  $\mu\text{M}$  DTT, pH was adjusted to 7.5 by ammonium hydroxide). 100  $\mu\text{M}$  oleic acid or different concentrations of DMSO was added as needed. After incubation at 37°C for 4.5 hours, the reactions were quenched by 19-time volume of ice-cold quenchant (30% MeOH, 70% H<sub>2</sub>O, 0.1% formic acid (v/v)), and 0.5  $\mu\text{M}$  isotope-labeled internal standard H3K9\* (+12 Da)).

**Mass Spectrometry Analysis.** The quenched and diluted reaction mixture was infused into a triple quadrupole mass spectrometer (Micromass Quattro Ultima, Waters Corporation, Milford, MA). The MS parameters were set as follows: capillary voltage 2.5 kV, cone voltage 40 V, cone gas 50 L/h, desolvation gas 200 L/h, and nebulizing gas

adjusted for most abundant ion currents. The scan mode was MS1 full scan, with mass range 360 to 480.  $[M+6H]^{6+}$  and  $[M+5H]^{5+}$  peaks of product H3K9 (m/z 376.98 and 452.13), internal standard H3K9\* (m/z 378.65 and 454.24) and substrate H3K9(Ac) (m/z 383.97 and 460.53) were monitored. The data was acquired by MassLynx (Version 4.1, Waters Inc.).

**Calibration of H3K9.** A series of H3K9 solutions at different concentrations were mixed with single concentration H3K9\* solution and different concentration H3K9(Ac) solutions. The buffer was 20-fold diluted  $NAD^+$ -Tris buffer. The final concentration was: H3K9 0, 0.1, 0.3, 0.5, 0.7 and 1  $\mu M$ ; H3K9\* 0.5  $\mu M$ ; and H3K9(Ac) 3, 2.9, 2.7, 2.5, 2.3 and 2  $\mu M$ . The mixed solutions were directly pumped into the MS. The signal intensity ratio of H3K9 over H3K9\* of each solution was plot against the concentration of H3K9 using Origin 8.5.

**SIRT6 Kinetic Studies with H3K9(Ac) as Substrate.** 2.5  $\mu M$  SIRT6 was added into different concentrations of H3K9(Ac) (0 to 150  $\mu M$ ). The buffer was the same  $NAD^+$ -Tris buffer described above. Reactions were quenched at 0, 1, 2, 3, 4, 5 hours. The analysis was performed by uPLC-MS (uPLC: Waters NanoAcquity). The mass spectrometer was Agilent 1640 series triple quadrupole MS (Agilent: Santa Clara, CA). Mobile phase A contained 0.15% formic acid, 150 mM ammonium formate. Mobile phase B was 100% acetonitrile. The linear gradient was: initial, 0% B; 2.01 min, 30% B; 4 min, 50% B; 4:01 min: 95% B; 8.5 min: 100% B. The amount of product yielded in each reaction was calculated based on the peak area of the product and the substrate. The

Michaelis-Menten model was fitted by GraphPad Prism 6.01. The reaction progress was monitored in the course of 24 hours, with initial 60  $\mu\text{M}$  substrate and 2.5  $\mu\text{M}$  SIRT6.

**Test Screen for Modulators for SIRT6 Deacetylation Activity.** A test screening involving 25 compounds was performed using 60  $\mu\text{M}$  H3K9(Ac) and 2.5  $\mu\text{M}$  SIRT6. The test compounds were selected from the Epigenetic Screen Library (Cayman Chemical, Ann Arbor, MI). The procedure was: 1) 30  $\mu\text{L}$  of 11  $\mu\text{M}$  SIRT6 was diluted into 70  $\mu\text{L}$   $\text{NAD}^+$ -Tris buffer to make Mix A; 1.8  $\mu\text{L}$  of 11  $\mu\text{M}$  SIRT6 was diluted into 4.2  $\mu\text{L}$  Tris buffer (no  $\text{NAD}^+$ ) to make Mix B. 2) 0.5  $\mu\text{L}$  of 2 mM test compound (in 10% DMSO) was pipetted into a polypropylene 384-well plate (Costar<sup>®</sup>, Corning Inc. Tewksbury, MA), occupying well #1-24. 3) 0.5  $\mu\text{L}$  10% DMSO was added into well # 25-27. 4) 0.5  $\mu\text{L}$  of 800  $\mu\text{M}$  oleic acid (in 10% DMSO) was added into well #28- 30. 5) 1  $\mu\text{L}$  of 240  $\mu\text{M}$  H3K9(Ac) was added into well #1-32. 6) 3  $\mu\text{L}$  of Mix A was pipetted into well #1-30; 3  $\mu\text{L}$  of Mix B was pipetted into well #31-32. The final concentration of each assay component was: H3K9(Ac) 60  $\mu\text{M}$ , SIRT6 2.5  $\mu\text{M}$ , test compounds 25  $\mu\text{M}$  and DMSO 1.25% (v/v). 7) Sealed and incubated the plate for 4.5 hours. 8) Quenched all reactions using 76  $\mu\text{L}$  of ice-cold quenchant which contained 30% MeOH, 0.1% formic acid and 0.5  $\mu\text{M}$  H3K9\*. 9) Reformatted quenched reaction mixtures into 3 droplets/reaction or 1 droplet/reaction droplet array. 10) Infused the droplet array into ESI-MS. The detection parameters were the same with above described.

The analysis was based on the intensity ratio of H3K9 to H3K9\* in each droplet. The activator and inhibitor criteria were set as  $AVE_{(\text{negative control})} \pm 3 \times SD_{(\text{negative control})}$ . Data was processed using Origin 8.5.

**Deacetylation of H3K9(decanoyl) by SIRT6.** A 10-mer histone H3K9 lysine (decanoyl) (KQTARK(decanoyl)STGG) was used as substrate. SIRT6 was first buffer exchanged into formate-DTE buffer using a 10 kD cut-off centrifugal dialysis unit Amicon Ultra-0.5 mL (EMD Millipore, Billerica, MA). The procedure and the formate buffer were the same with SIRT1 dialysis described in Chapter 4. 20  $\mu\text{M}$  H3K9(decanoyl) was mixed with 1  $\mu\text{M}$  desalted SIRT6 and then incubated at 37°C for 1 hour. The reaction was quenched by equal volume ice-cold quenchant which contained isotope labeled 10-mer internal standard H3K9(10-mer)\*. The reaction mixture was pumped into LCQ quadrupole ion trap MS (Thermo Fisher Scientific, Waltham, MA) for analysis. The full scan mass range was set as 490-610. Micro-scan was set to be 1. The intensity ratio of H3K9(10-mer) to H3K9(10-mer)\* was calculated for analysis.

**SIRT6 Kinetic Studies with H3K9(decanoyl) as Substrate.** A series of H3K9(decanoyl) solutions were mixed with desalted SIRT6. The final concentration of the substrate was 0, 5, 10, 20, 40, 80 and 160  $\mu\text{M}$ . SIRT6 was 1  $\mu\text{M}$ . The reactions were incubated in the formate buffer at 37°C for 0.5, 1, 2, 4, 6, and 8 h. The ice-cold quenchant contained 50% MeOH, 50% H<sub>2</sub>O, 0.15% formic acid and 5  $\mu\text{M}$  isotope-labeled standard H3K9(10-mer)\* (+8 Da). The analysis was performed by an LCQ MS in full scan. The  $[M+2H]^{2+}$  peaks for H3K9(10-mer): m/z 517.6, H3K9(10-mer)\*: m/z 522.1 and

H3K9(decanoyl): m/z 594.7 were monitored. The intensity ratio of H3K9(10-mer) over H3K9(10-mer)\* was quantified for modeling the Michaelis-Menten curve.

## Results and Discussion

**Substrate Selection for SIRT6 Screening.** To date, SIRT6 has been proved to deacetylate histone H3K9 and histone H3K56,<sup>74,167</sup> as well as remove the long-chain fatty acyl group from the lysine on sequence-independent proteins.<sup>78</sup> To select proper substrates for SIRT6 modulator screening, We investigated the hydrolysis efficiency of SIRT6 towards the 3 types of substrates. We chose a 21-mer H3K9(Ac), a 20-mer H3K56(Ac) and a 10-mer H3K9(decanoyl) peptides as surrogate substrates. In accordance with observation of others, SIRT6 is highly efficient in de-decanoylation. For deacetylation, my experiments consistently showed better yield for H3K9(Ac) than H3K56(Ac) reactions. Because deacetylation and deacylation might lead to completely different biological functions of SIRT6, corresponding modulators could be different. Therefore, we will develop assays with both H3K9(Ac) and H3K9(decanoyl).

**SIRT6 Kinetics with H3K9(Ac) as Substrate.** The SIRT6 deacetylation reaction is shown in **Figure 5-1**. For a screening, the substrate concentration should be under its  $K_m$  value. The reported  $K_m$  of H3K9(Ac) peptide is as high as 810  $\mu\text{M}$ .<sup>78</sup> I studied SIRT6 kinetics with H3K9(Ac) concentration ranging from 0 to 150  $\mu\text{M}$ . As expected, the fitted Michaelis-Menten model showed that within this range, the initial velocity increased linearly (**Figure 5-2A**). A long-term-incubation experiment showed a very slow catalysis:



the reaction yield increased linearly for up to 8 hours before leveling off (**Figure 5-2B**).

Based on those results, I chose 60  $\mu\text{M}$  H3K9(Ac) and 4.5 h incubation for the screening.

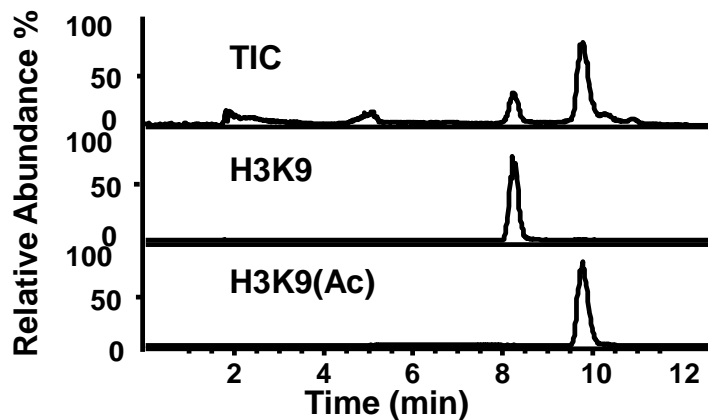


**Figure 5-1.** Deacetylation of H3K9(Ac) by SIRT6. LC-MS chromatogram showed a 24 h incubated reaction (3  $\mu\text{M}$  SIRT6, 60  $\mu\text{M}$  H3K9(Ac) and 500  $\mu\text{M}$   $\text{NAD}^+$ ). The yield was only ~20%.

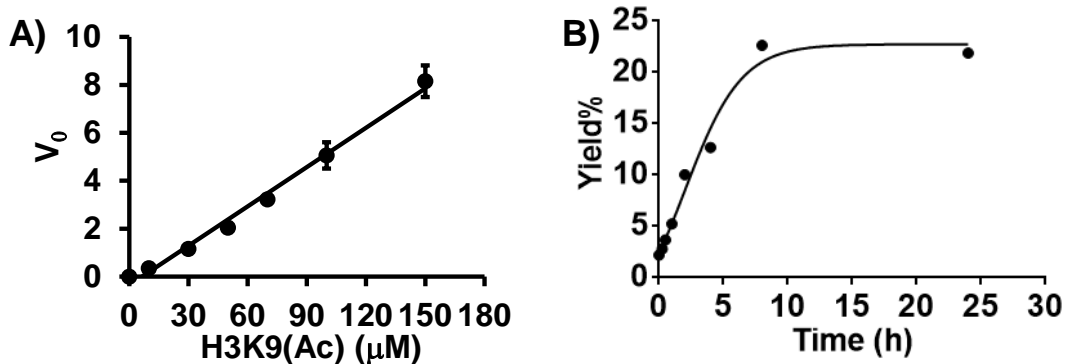


**Figure 5-2.** A) The linear part of Michaelis-Menten model. The velocity linearly increased for at least 0-150  $\mu\text{M}$  H3K9(Ac), thus the  $K_m$  should be higher than 75  $\mu\text{M}$ . B) Reaction progress of SIRT6 deacetylating H3K9(Ac).

**MS-compatible Deacetylation Assay.** Similar to modifying the SIRT1 assay, I tried to buffer exchange SIRT6 and then conducted the reaction in the formate buffer. But unfortunately, SIRT6 is barely active in ammonium formate, as nearly no product peaks were detected by either LC-MS or direct infusion MS. Among all pH 7.5 buffers I have tried, including ammonium formate, ammonium acetate, ammonium bicarbonate, phosphate, HEPES and Tris, I found that SIRT6 deacetylates most efficiently in Tris buffer. High concentration Tris in the sample severely suppresses the signal of all analytes, which makes direct infusion impossible. Cleaning up all reactions before analysis is one choice to avoid ion suppression, but considering the high cost of SPE plates and low throughput, it is desirable to minimize the sample preparation. Another choice is diluting the reaction for direct MS analysis.<sup>123</sup> After trying a range of folds for dilution, we found that 20-fold diluted reaction yields relatively abundant peaks of H3K9 and H3K9\*. The unidentified interfering peaks near  $[M+6H]^{6+}$  peaks were from the buffer which contains Tris, inorganic salts and glycerol (**Figure 5-3**). Though interfering peaks exist, the quantification of H3K9 is not affected (see the calibration curve of H3K9 in **Figure 5-4**). Therefore, we plan to use this method for future screenings.

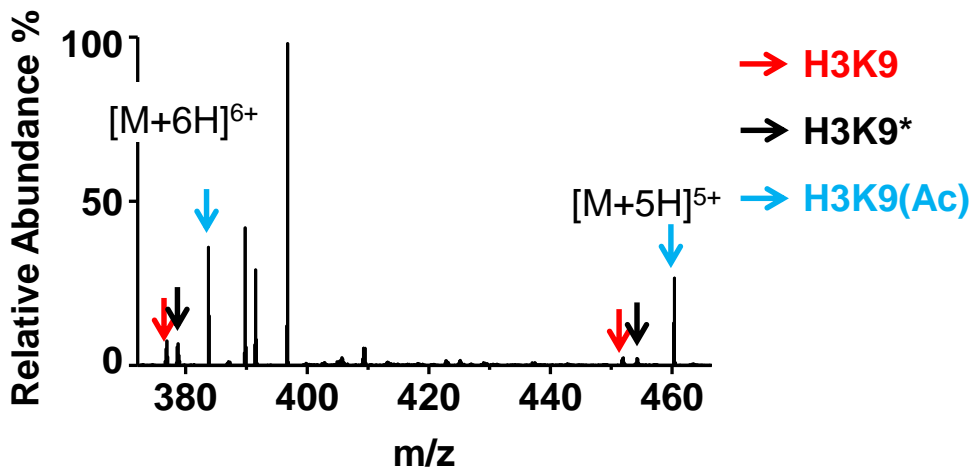


**Figure 5-3.** Direct MS analysis of 20-fold diluted reaction mixture (4.5 h incubation). Despite of the presence of noises, peaks of H3K9, H3K9\*, and H3K9(Ac) can be detected.

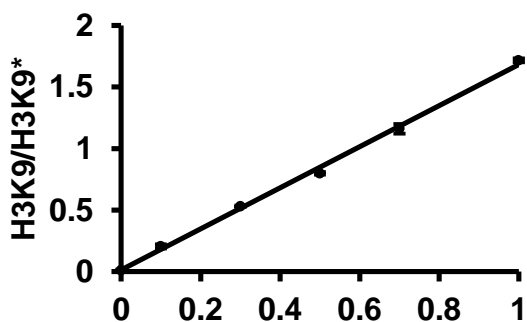


**Figure 5-4.** Linear calibration of reaction product H3K9. 0, 0.1, 0.3, 0.5, 0.7 and 1  $\mu\text{M}$  of H3K9 was calibrated against 0.5  $\mu\text{M}$  isotopic internal standard H3K9\*. Each solution also contained 3, 2.9, 2.7, 2.5, 2.3 and 2  $\mu\text{M}$  H3K9(Ac) and 20-fold-diluted  $\text{NAD}^+$ -Tris buffer ( $n = 3$ ). The  $R^2$  of linearity is 0.998.

**SIRT6 Activation by Fatty Acids.** Up to now, fatty acids are the only group of activators being discovered for SIRT6. 300  $\mu\text{M}$  of oleic acid was proved to increase the

SIRT6 deacetylation rate by 6 fold.<sup>79</sup> However, in high throughput screening, the concentration of test compound is empirically kept under 30  $\mu\text{M}$ , otherwise low solubility, aggregation and co-precipitation issues might occur. For direct MS analysis, high concentration test compounds affect the ionization efficiency of other analytes, thus we tried to lower the concentration of fatty acid to reach a balanced point that abundant peptide peaks can be observed and good activation can be achieved. We tried 25, 50, and 100  $\mu\text{M}$  and found that 100  $\mu\text{M}$  oleic acid can activate the reaction by about 2 folds, which generally agreed with the published dose response experiment.<sup>79</sup> The mass spectrum was noisier than the negative control, but the activation effect was observed as the product/substrate ratio was higher (**Figure 5-5**).

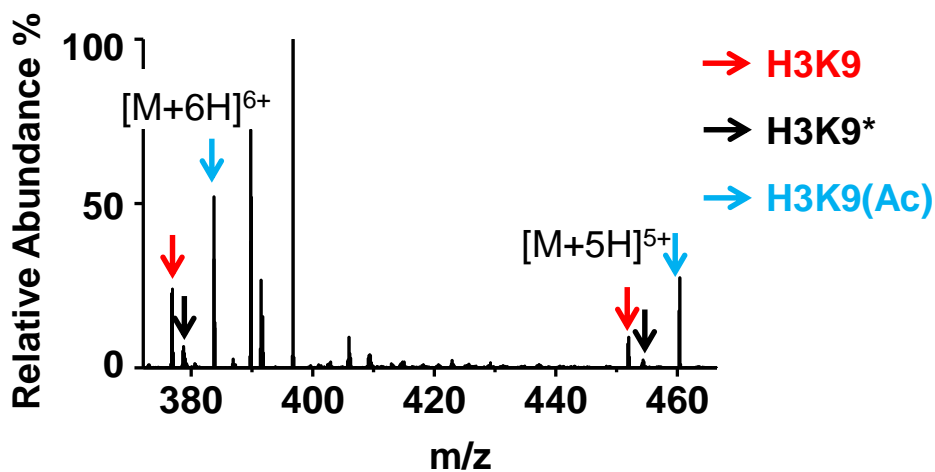


**Figure 5-5.** Direct MS analysis of 100  $\mu\text{M}$  oleic acid activated SIRT6 reaction (4.5 h incubation). Compared with the negative control (see **Figure 5-3**), the yield was twice high.

**Impact of DMSO** Nearly all chemical libraries are dissolved in DMSO. The tolerance of DMSO of an assay should be evaluated before a screening. For library compound depositing, Caliper Life Sciences Sciclone ALH 3000 Workstation (PerkinElmer, Waltham, MA) can reliably handle as low as 50 nL solution. Given the concentration of the compound stock solution, mostly 2, 5, or 10 mM, at least 1% DMSO will be present in a 5  $\mu$ L reaction. We conducted SIRT6 deacetylation reactions with 1%, 5%, 10% DMSO and 100  $\mu$ M oleic acid (the oleic acid reaction contained 1% DMSO). We found that 1% DMSO does not affect the activation effect of the oleic acid. 5% and 10% DMSO reduce SIRT6 activity, as well as lower the intensity of peptides (**Figure 5-6**). Thus, the final concentration of DMSO should be around 1%. Based on this study, 2 mM library should be used for  $\sim$ 5  $\mu$ L reactions.

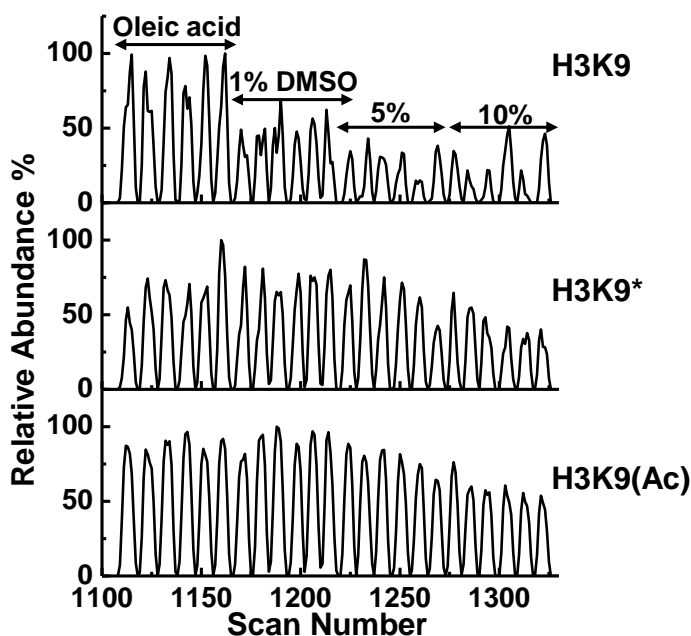


**Figure 5-6.** Droplet trace of DMSO evaluation assay (3 droplets/reaction, reactions were duplicated). The top trace is product H3K9, the middle is internal standard H3K9\*, and the bottom is substrate H3K9(Ac). 100  $\mu$ M oleic acid reactions show higher yield than 1% DMSO, which means the reactions were activated. 5% and 10% DMSO reactions show low yield and low peptide intensity.

**Test Screen for Modulators for SIRT6 Deacetylation Activity.** 25 compounds were screened in this small screening. One of the compound EX-527 was reported to inhibit ~60% SIRT6 activity at 200  $\mu$ M.<sup>81</sup> Reactions without NAD<sup>+</sup> served as the inhibitor control (-), reactions with 100  $\mu$ M oleic acid were the activator control (+), and reactions with 1% DMSO were the negative control (0). Both triplicate detection and single detection were performed in the same MS run. The droplet traces showed (**Figure 5-7**) that the reaction yield in the activator controls was about twice of the negative control. The inhibitor controls showed no H3K9 produced. EX-527 reactions (**red arrows in Figure 5-7**) had slightly lower yield than the negative control. We observed almost no difference between triplicate and single detection regarding low carryover, strong activation effect of oleic acid and weak inhibition effect of EX-527. The analysis rate of this screening was 0.7 droplets/s. Z-factor of both triplicate and single detection was 0.6.

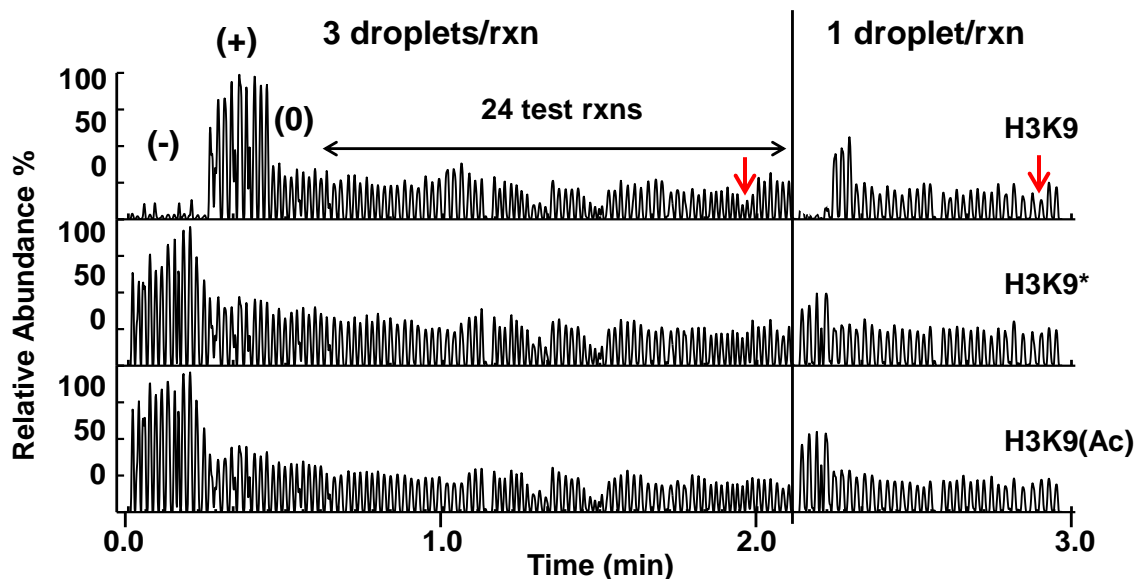


**Figure 5-7.** Droplet traces of 25-compound test screening. Top to bottom: product H3K9, internal standard H3K9\*, and substrate H3K9(Ac). Left: triplicate detection in which each reaction was made into 3 droplets. Right: single detection for 1 droplet/reaction. (-): inhibitor controls in which no  $\text{NAD}^+$  were in the buffer. (+): activator controls in which 100  $\mu\text{M}$  oleic acid was in the reactions. (0): negative controls in which 1% DMSO was in the reactions. Red arrows: reactions with 25  $\mu\text{M}$  EX-527.

Analyzing the data using intensity ratio of H3K9/H3K9\* proved that at 0.7 Hz, the screen result of single detection was very similar to the triplicate detection (**Figure 5-8**). The small error bars in the triplicate detection indicate good reliability. For this screen, the hit selection standard is  $\text{AVE}_{(\text{negative control})} \pm 3 \times \text{SD}_{(\text{negative control})}$  (The red line is for the activator, and the black line is for the inhibitor). This criterion is less strict than the 50% cutoff. Given that only a few SIRT6 modulators have been found, a more tolerant standard may pick more hits, which might be developed into strong modulators by further modification. In the triplicate detection, only C11 reaction (EX-527) just met the inhibitor standard. In the single detection, though no inhibitors could be identified, C11 reaction

had the lowest H3K9/H3K9\*. Therefore, we concluded that the 2 detection methods generally agreed with each other. Single detection can be used for large scale screening.

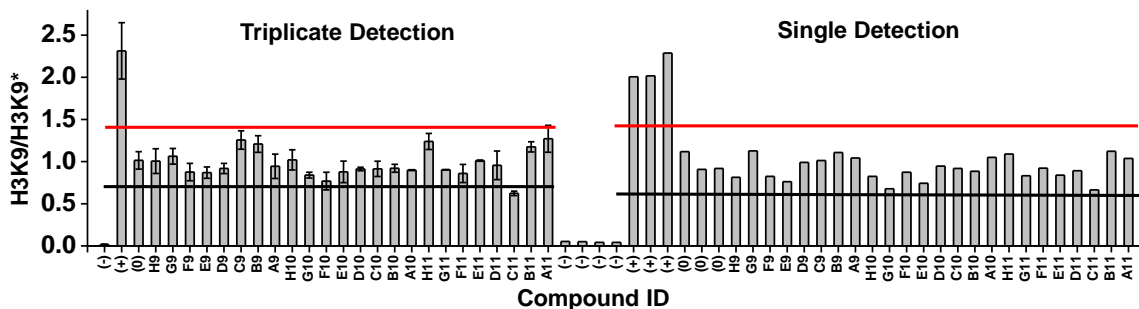


**Figure 5-8.** The analysis of the screening. The y-axis is the intensity ratio of H3K9 over H3K9\*. The x-axis is compounds ID. The red line is the activator criteria, and the black line is the inhibitor criteria. C11 is EX-527 reaction. Triplicate detection means each reaction was made into 3 droplets. Single detection means each reaction was made into 1 droplet.

**Efficient Deacylation by SIRT6.** SIRT6's capability in removing the long fatty acyl chain of peptides was reported in 2013.<sup>78</sup> Regardless of the peptide sequence, such deacylation efficiency is hundreds of times greater than deacetylation. For example, the  $K_m$  value of the substrate decreased from about 800  $\mu\text{M}$  for H3K9(Ac) to 3  $\mu\text{M}$  for H3K9(myristoyl).<sup>78</sup> It suggests the possible involvement of SIRT6 of a totally different set of post-translational modification. We selected a 10-residue decanoylated H3K9 as a surrogate fatty acylated protein substrate. Because of the high activity, it is possible to perform the reaction in the formate buffer. **Figure 5-9** shows the direct MS analysis of a 1 h incubated reaction (in the ammonium formate-DTE buffer). Nearly 70% substrate was converted. A Tris buffer reaction was performed for comparison. The yield was almost 100%.



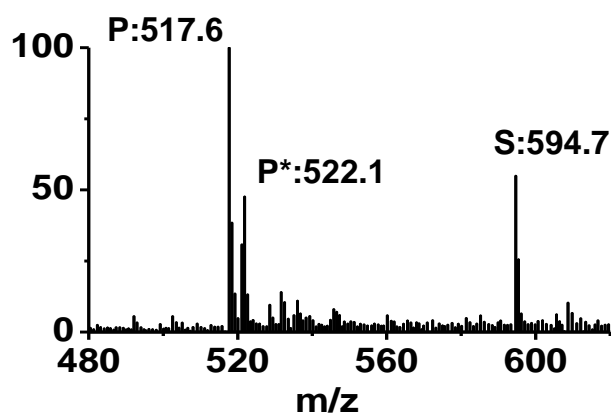


**Figure 5-9.** Direct infusion the MS-compatible SIRT6 deacylation assay using formate buffer. P: product H3K9(10-mer), P\*: isotope-labeled internal standard H3K9(10-mer)\*, S: substrate H3K9(decanyl).

We also studied the SIRT6 kinetics for de-decanoylation. The fitted  $K_m$  value is 27  $\mu\text{M}$  (**Figure 5-10A**). It is higher than other fatty acylated peptides possibly because the formate buffer compromised the activity of SIRT6. Fast hydrolysis was observed by the shorter linear range of the reaction progress: the maximum yield was achieved in 2 h (**Figure 5-10B**).

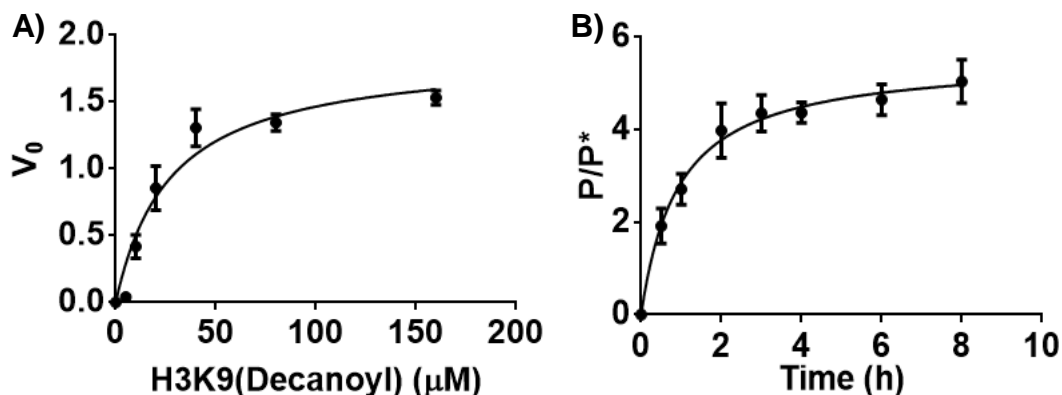


**Figure 5-10.** SIRT6 kinetics with 10-mer H3K9(decanoyl) as the substrate. A) Michaelis-Menten model. The fitted  $K_m$  of H3K9(decanoyl) is 27  $\mu\text{M}$ . B) Reaction progress of SIRT6 de-decanoylation. Reaction rate decreased after 2 h.

### Conclusion

In this work, we have developed 2 mass spectrometry-based SIRT6 assays using 2 different substrates: H3K9(Ac) and H3K9(decanoyl). Dependent on the hydrolysis efficiency of SIRT6, either traditional condition (Tris buffer) or MS-compatible condition (formate buffer) was used. Both assays showed adequate yield for large-scale screenings. The enzyme kinetic studies suggested appropriate substrate concentration and incubation time. Due to the low turnover rate of deacetylation, the substrate H3K9(Ac) is especially suitable for activator screening. On the other hand, H3K9(decanoyl) is good for inhibitor search. The conditions of the H3K9(Ac) assay were validated by a 25-compound test screening. Because H3K9(Ac) is a known endogenous substrate for SIRT6, any modulators identified in the screening using the deacetylation assay will be physiologically relevant. The H3K9(decanoyl) assay is also interesting because as our

knowledge of SIRT6 building up, it is highly possible that long-chain fatty acylated histones naturally exist and sirtuin-relevant. Those substrates are especially suitable for finding SIRT6 inhibitors, which are likely to be utilized to treat cancers exacerbated by SIRT6.

## CHAPTER 6

### FUTURE DIRECTIONS

#### Carryover Reduction of Reagent Addition Chip

The performance of the all-droplet system (Chapter 1) largely depends on the reagent addition chip. High carryover was observed in the original design (PDMS tee), thus one sacrificial droplet was necessary for each sample set. To address this issue, we proposed an alternative design in which the droplet channel was all Teflon. The later reduced the carryover by two thirds.

There have been several studies on reducing cross-contamination in reagent addition. A desired chip design consists of a wide hydrophobic droplet channel and a narrow hydrophilic reagent channel. Besides, the linear flow rate of the reagent should be higher than the droplets flow.<sup>115</sup> A multi-channel chip was later reported to perform reagent addition in low carryover (almost zero) and high addition ratio (up to 1:1).<sup>32</sup> (**Figure 6-1**) However, we found that those designs are good for surfactant-containing biphasic system. Even though many ESI-MS-compatible surfactants have been developed,

including acid-labile surfactants and nonionic surfactants, we have noticed that the present of surfactant can lower the voltage threshold for spraying the oil in ESI. This phenomenon elevates the baseline noise in droplet analysis. Therefore, the use of surfactant should be cautious and minimized. As mentioned in Chapter 2, an expansion at droplet outlet was constructed for better synchronizing the reagent and droplet flow. The trade-off of this expansion is higher carryover.

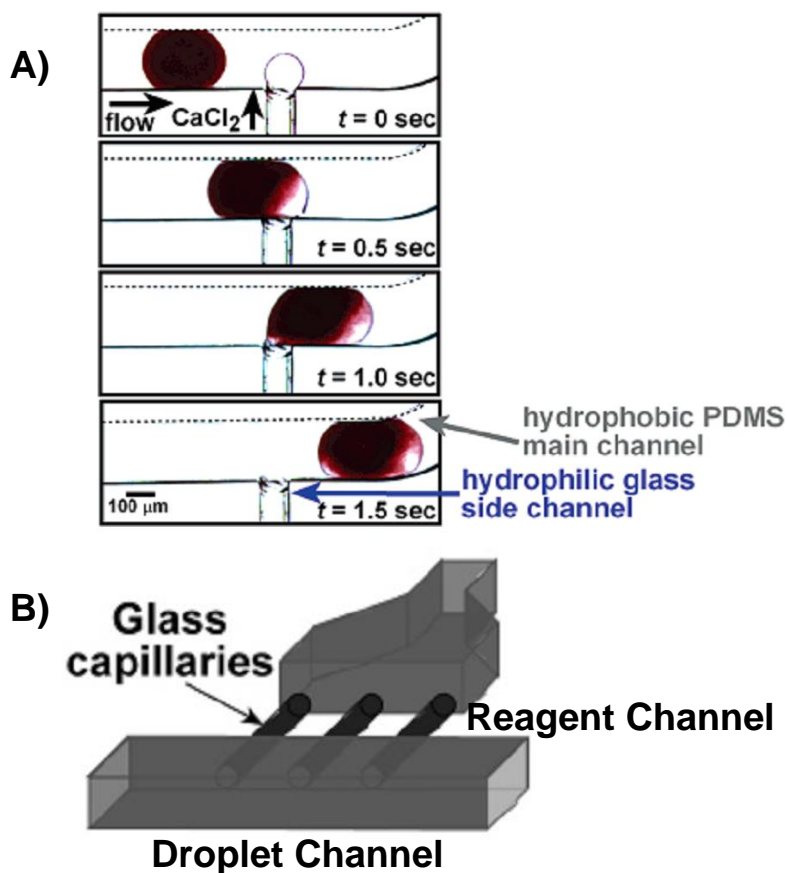


**Figure 6-1.** A) Single-channel reagent addition device that reported to have low carryover;<sup>115</sup> B) Multi-channel reagent addition chip.<sup>32</sup> Reproduced with permission from ACS Publications.

To reduce the carryover, chip geometry, properties of channels' inner surface, and connections between channels. Potential solutions are: 1) Teflon is very resistant to carryover. So it could be beneficial to build a whole Teflon droplet channel with a wider outlet; 2) connections between channels should be minimized. Our first design was built by inserting 2 pieces of capillaries and 1 piece of Teflon tubing into a PDMS mold. The small gaps at the junction contributed to the carryover. For that, one-piece mold will be a better design; 3) the competition between convection and diffusion has been used to explain the carryover in reagent addition.<sup>32</sup> Convection injects the reagent into the droplet, while carryover is caused by the reagent diffusing out of the droplet. Increasing the linear flow rate of the reagent can improve convection and reduce the effective diffusion, and thus reduce carryover. This can be achieved by narrowing the reagent channel.

### **Large-scale All-droplet Enzyme Modulator Screening**

The miniaturizing feature of the all-droplet system will be especially beneficial for screenings which involve a large number of assays. Because the cost of reagent always limits the scale, conducting all reactions inside droplets can be considerable economical. SIRT6 is an expensive and low activity enzyme. It works at micromolar level, which is nearly 100-fold higher than the normal concentration of an enzyme in a screening. The traditional MWP-based screening usually requires at least 5  $\mu\text{L}$  for each reaction. Such low volume not only heavily demands the precision and the speed of the liquid handling equipment, but also exacerbates the evaporation. Considering the

milliliter level dead volume of most automatic liquid dispenser, the expense for SIRT6 is forbidden. Besides, transferring reagents and samples by MWP-based HTS equipment costs a large amount of pipette tips. In contrast, a built-in-house all-droplet system requires only nanoliters of reaction volume, does not have evaporation issue, has no dead volume and needs no transfer. **Table 6-1** compares the reagent consumption and cost for an MWP-based SIRT6 modulator screening and an all-droplet-system-based screen.

**Table 6-1.** Comparison between MWP-based SIRT6 modulator screening and all-droplet-system-based screening. (SIRT6 is 3  $\mu\text{M}$ /reaction, ~\$270/nanomole; H3K9(Ac) is 50  $\mu\text{M}$ /reaction, ~\$0.5/nanomole; H3K9\* is 0.5  $\mu\text{M}$ /diluted reaction, ~\$1.5/nanomole).

	<b>MWP-based screen</b>	<b>All-droplet screen</b>
<b>Number of reactions</b>	10000	10000
<b>Reaction Volume</b>	4 $\mu\text{L}$	10 nL
<b>Dead volume of dispenser</b>	3 mL	0
<b>SIRT6 (4 <math>\mu\text{M}</math> stock) consumption</b>	33 mL	75 $\mu\text{L}$
<b>H3K9(Ac) (200 <math>\mu\text{M}</math> stock) consumption</b>	13 mL	25 $\mu\text{L}$
<b>H3K9* (200 <math>\mu\text{M}</math> stock) consumption</b>	2 mL	5 $\mu\text{L}$
<b>Total cost of SIRT6</b>	\$36000	\$81
<b>Total cost of H3K9(Ac)</b>	\$1300	\$2.5
<b>Total cost of H3K9*</b>	\$600	\$1.5
<b>Cost of pipette tips</b>	\$2000	0
<b>Total cost</b>	\$40000	\$85

Currently, we are exploring miniaturizing SIRT6 modulator screening by implementing a microfabricated multi-step reaction addition device. A temporary design is a multi-channel reagent addition PDMS chip. The droplet channel will be fluorinated

polymer-coated PDMS. The screening will be explored either by a fluorescent assay (with a fluorescent label far away from the acetylated lysine) or a MS assay.

To save the compounds from the libraries, a droplet splitter<sup>31</sup> can be hyphenated to the droplet flow. Samples can be aspirated from MWP into large plugs and then split into two daughter plugs with designated splitting ratio. One of the daughter plugs can be introduced into the all-droplet system for enzymatic assay. The other plug can go through a different assay which yields complementary results, or be stored as droplet library for future use.

### **Automation of Mass Spectrometry Plate Reader**

To realize large-scale high throughput screening by the MS plate reader, automation of the system will be explored. In sample-droplet reformatting step, tube alignment should be precisely controlled by a computer. Because the perfluorinated oil on top of the plate is very thin, it is necessary to ensure all sippers start from the right height. For infusing sample droplets into ESI-MS, sample tubes (FEP) are now switched by hand, and the interface between the sample tube and the ESI housing requires screwing in a union head. A smoother interface can reduce the force applied on the sample tube, which lowers the possibility to crash the droplets inside and also facilitates automatic manipulator for tube switching. With all steps fully automated, the MS plate reader has a potential to analyzed nearly 150,000 samples in 24 hours.



## Sample Cleanup

Droplet-ESI-MS systems can be improved by adding a step of sample preparation prior to either droplet generation or MS analysis. Removing the salts and high concentration buffer components can improve the quality of mass spectra, increase the signal to noise ratio of the target analytes, lower the demand on high reagent concentration, and prolong the lifetime of the instrument.

One way to clean up the sample is utilizing high throughput solid phase extraction (SPE) plates before droplet generation. There are 96 and 384-well SPE plates commercially available. The extraction phase is usually reverse phase material, either hydrophobic filters or common separation media (**Figure 6-2A, B**). Coated-magnetic beads have also been proved efficacious (**Figure 6-2C**).<sup>168</sup>

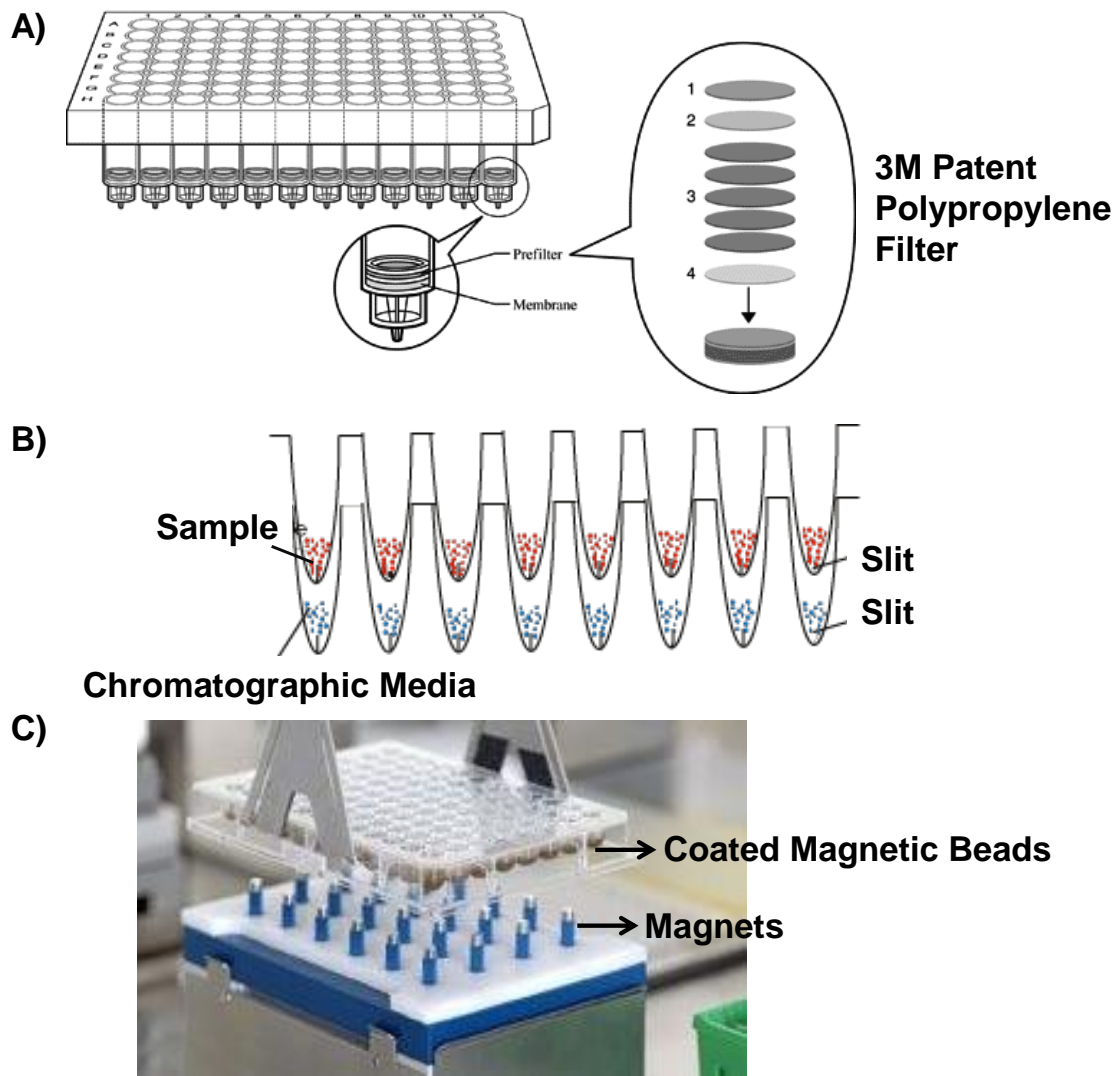


**Figure 6-2.** Solid phase extraction plates. A) Filter-based SPE plate (3M Empore™: each well of the plate contains a standard density Empore™ polypropylene membrane for efficient sample extraction). B) Particle-based SPE plate (Glysci Slit Plate™: separation media is filter-less chromatographic particles. A 1-2  $\mu\text{m}$  slit at the bottom of each well in Slit Plate permits liquid to pass through). C) Magnetic beads-based SPE (Xiril AG Magnetic Plate-X: separation particles are coated on magnetic beads residing in each well. Separation is realized by attracting beads to the corner of each well of the assay plate by the magnets array inserted under the assay plate).

We have tried parallel sample preparation using multiple C18 spin columns. The whole process was finished in 3 min (1 min spin for binding, 1 min for washing and 1 min for eluting). High quality mass spectra were obtained. Product peaks from a low-yield reactions were observed, which would be very difficult for direct infusion of the untreated reaction mixture (**Figure 6-3**)

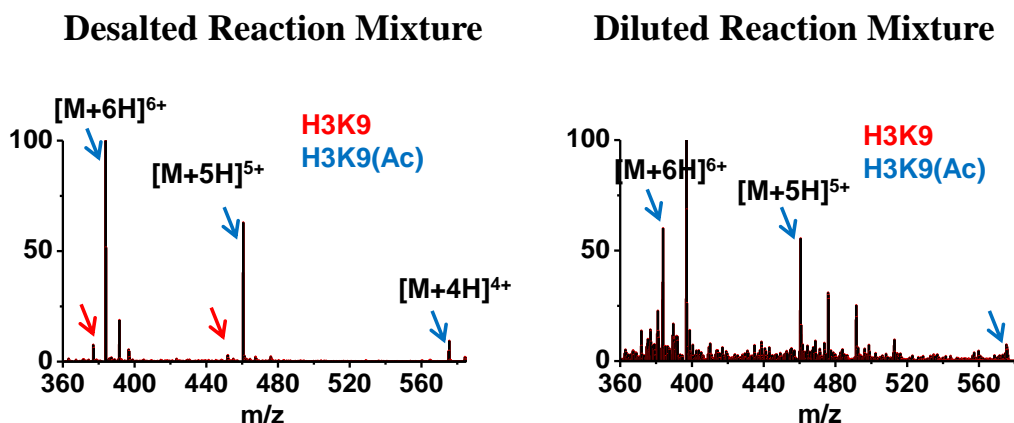


**Figure 6-3.** Comparison of mass spectra of the desalted reaction (left, desalted by C-18 spin column, undiluted) and the intact reaction mixture (right, diluted by 20 folds in order to observe peptides). The noise level of treated reaction is significantly lower. Despite the low yield, product peaks are observed in the desalted reaction mass spectrum.

Another sample cleaning method is to engineering an extraction bed inside the needle. Our group has explored the possibility of packing a short C18 chromatographic bed into the rear end of a nanospray tip. The target analyte partitions into the stationary phase when a sample plug passes through the bed. The water droplet coming later washes off the soluble impurities. Then an eluting droplet containing organic solvent elutes the

analyte out of the bed and transfers it into ESI-MS. Different samples can be separated by another water droplet as a ‘wash’ to prevent cross-contamination (**Figure 6-4**).<sup>169</sup>

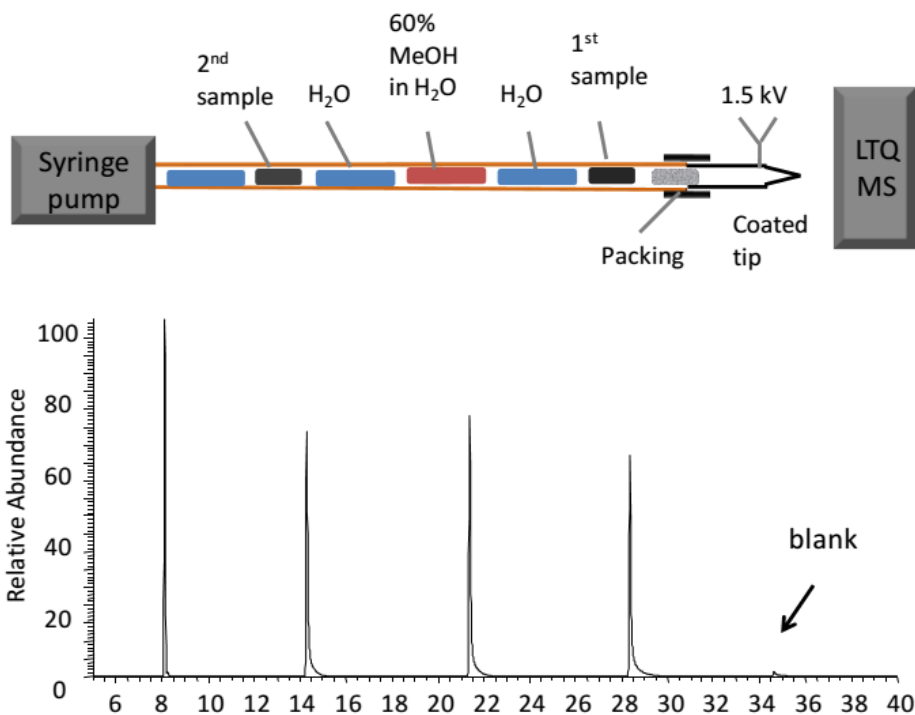


**Figure 6-4.** Top: scheme of droplet-based SPE. Bottom: total ion current of sequentially injected 4 samples.<sup>169</sup> Reproduced with permission from Qiang Li and University of Michigan.

### Tracking a Screening

Because the data output in segmented-flow-based screening is a series of droplet trace, tracking a screen requires translating the sequence of droplets back to the position on the MWPs. If any miscounting occurs, wrong hits will be picked. This problem can be solved by taking advantage of the multiplexing ability of MS: detecting multiple

compounds simultaneously. For HTS, a rapid MS scan covering certain range of  $m/z$  can not only monitor the target analytes, but also identify compounds which have an effect on the enzyme (see examples in Chapter 2). It saves time for back tracking the assay based on the order. Though for a triple quadrupole MS, full scan is generally slower than MRM, the lower speed can be overcome by using a fast spectrometer, such as time-of-flight (TOF) MS. A standard TOF-MS can scan 1000 Da in 10-20 ms. Based on our experience, 10-12 data points per droplet-oil pair ensure reproducible droplet trace. 20 ms/spectrum enables at least 4 Hz analysis.

### **Custom Data Analysis Program**

Facing the vast dataset produced by a screening, data analysis can be rate limiting. A customized droplet-ESI-MS screening analysis software should be able to:

- 1) Smooth out the droplet peaks. Signal fluctuation is a common phenomenon in ESI-MS. Peak picking software such as Origin 8.5 will mistakenly identify one droplet peak as multiple if droplets are not appropriately smoothed. Signal spikes are expected when ESI is turned on and off at high frequency. A proper program to remove the artificial spikes would facilitate the peak identification. Besides, the smoothing needs to preserve the real peak height of each droplet, otherwise quantification will be compromised.

2) Reliably pick high throughput droplet peaks from extract ion current. Any shoulder peak or occasionally high noise between sample droplets should be ignored. Any split-top droplet peak which is not completely smoothed out should be identified as one peak. In a large-scale screening, tens of thousands of droplet peaks will be collected. The order of the droplet corresponds to the sample position on MWPs. It is crucial to ensure a correct order.

3) Automatically calculate the intensity (peak height) ratio of the target analyte over its internal standard and identify promising hits based on built-in criteria. Common criteria include percent of inhibition/activation, z-score, strictly standardized mean difference (SSMD) and t-statistic.<sup>170,171</sup> Percent of inhibition/activation is most straightforward, but it doesn't take data variability into account. Z-score method assumes standard normal distribution. Z-score equals mean  $\pm k$  SD (standard deviation), where  $k$  is usually set as 2 or 3. SSMD is defined as the ratio of mean to standard deviation of the test sample and the negative control. The t-statistic is suitable for screens with replicates, in which the p-value is dependent on both the effect and the sample size. The software should be programmed with all established statistical methods at researcher's convenience. After hits selection, the software should be able to design replicated assays or dose dependent experiments.

## APPENDICES

### APPENDIX A

#### Sequence of test compounds in Cathepsin B Assay

1. In-well Cathepsin B inhibitor screening using ZRR-AMC as substrate

The sequence of 23 test compounds and a non-inhibitor control is E-64, leupeptin, antipain, control, methionine, arginine, tyrosine, histamine, thyronine, proline, lysine, valine, asparagine, tryptophan, isoleucine, leucine, phenylalanine, cysteine, aspartic acid, GABA, serine, glycine, acetylcholine, adenosine.

2. In-well screening using Ac-GFGFVGG-NH<sub>2</sub> as substrate

The sequence of 11 test compounds and a non-inhibitor control is E-64, leupeptin, antipain, control, methionine, arginine, tyrosine, thyronine, proline, lysine, phenylalanine, asparagine, GABA.

3. All-droplet screening using ZRR-AMC as substrate with PDMS tees

The sequence of 24 test compounds and the non-inhibitor control is control, antipain, cysteine, phenylalanine, leucine, lysine, proline, asparagine, E-64, valine, adenosine, acetylcholine, glycine, serine, GABA, aspartic acid, leupeptin, isoleucine, tryptophan, thyronine, histamine, tyrosine, arginine, methionine, p-nitrophenol.

4. All-droplet screening using Ac-GFGFVGG-NH<sub>2</sub> as substrate with Teflon tees

One control and three test compounds are in 9 replicates, and two inhibitors are in 8 replicates. The sequence is: control, E-64, tyrosine, thyronine, leupeptin, and proline.

## APPENDIX B

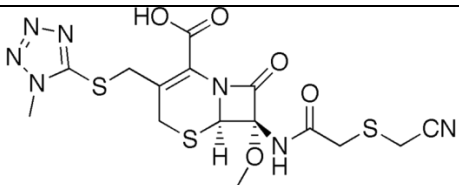
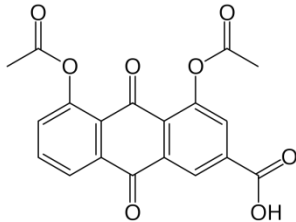
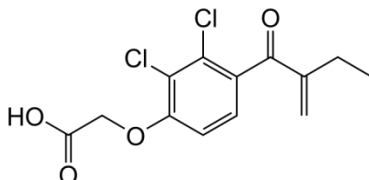
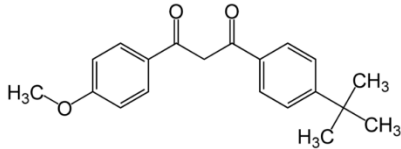
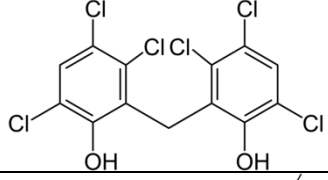
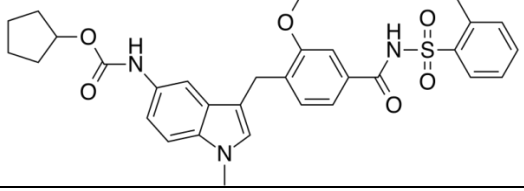
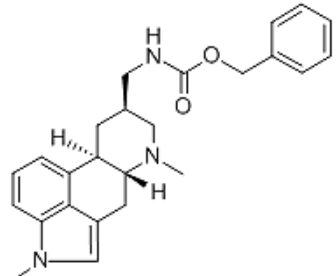
### Goodness of Fit of Inhibitor Hits in Cathepsin B Inhibitor Screening

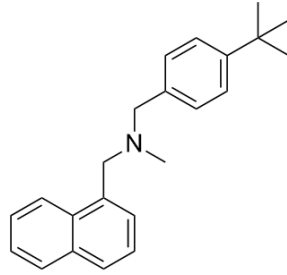
Hits	R <sup>2</sup>
cefmetazole	0.9875
diacerein	0.9471
ethacrynic acid	0.9630
avobenzon	0.9757
hexachlorophene	0.9473
zafirlukast	0.9594
metergolin	0.9350
butenafine	0.9205
triclosan	0.9478
diethylstilbestrol	0.9357
anthralin	0.9333
thioguanosine	0.9248
pimozide	0.9315
didanosine	0.9196
luteolin	0.9266
alexidine	0.9518
colistin	0.9391
disulfiram	0.9429
triclabendazole	0.9356
raloxifene	0.9587
pinaverium	0.9557
chlorhexidine	0.9688
tegaserod	0.9711
cefaclor	0.9648



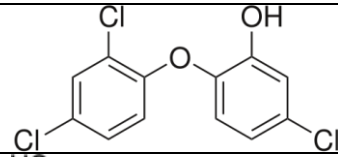
## APPENDIX C

### Structures of Inhibitor Hits in Cathepsin B Inhibitor Screening

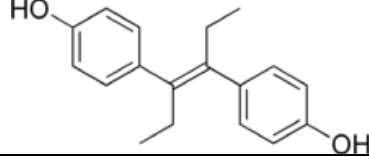
Hits	Structure
cefmetazole	
diacerein	
ethacrynic acid	
avobenzone	
hexachlorophene	
zafirlukast	
metergolin	



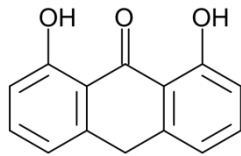
butenafine



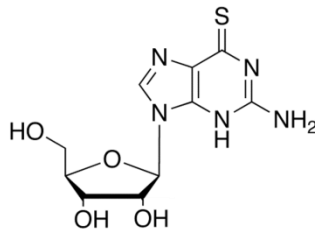
triclosan



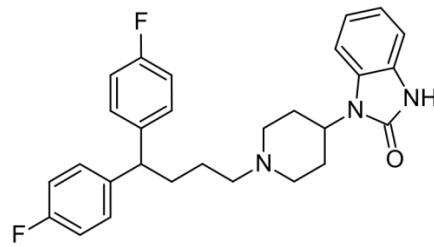
diethylstilbestrol



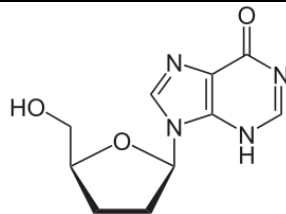
anthralin



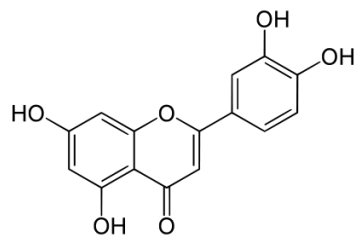
thioguanosine



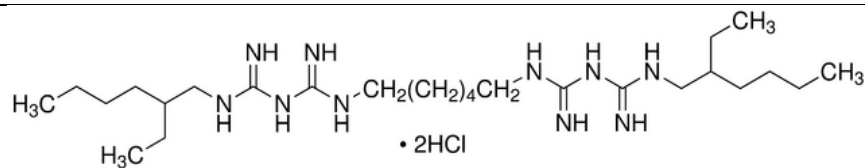
pimozide



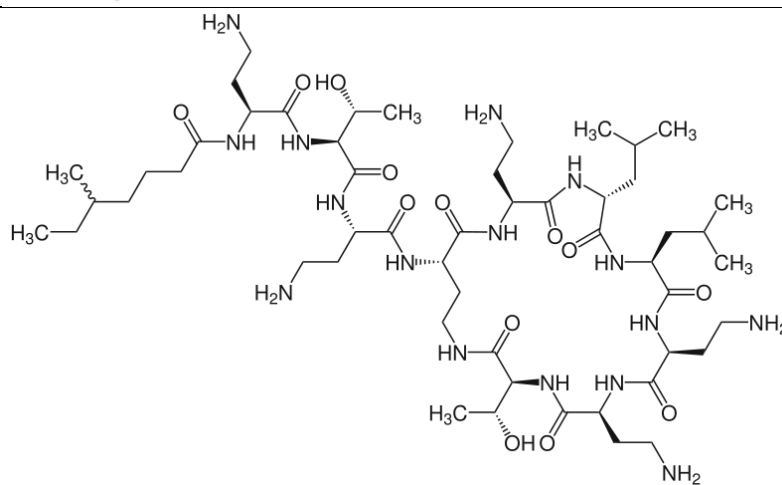
didanosine



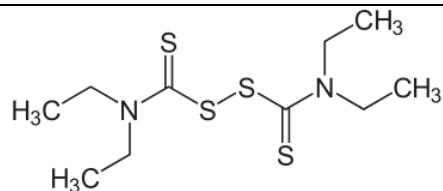
luteolin



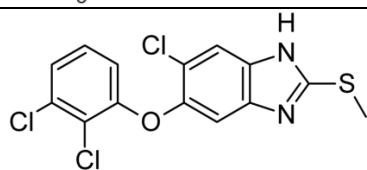
alexidine



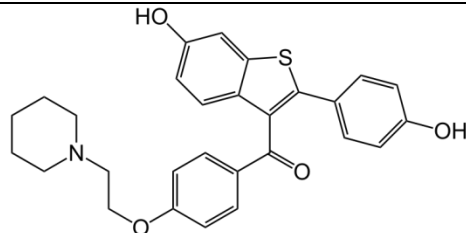
colistin



disulfiram

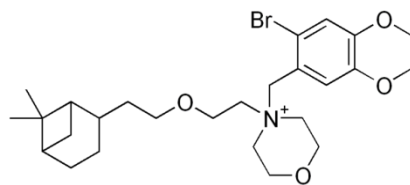


triclabendazole

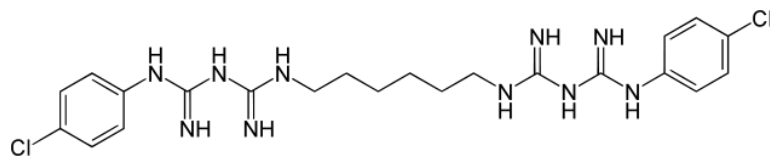


raloxifene

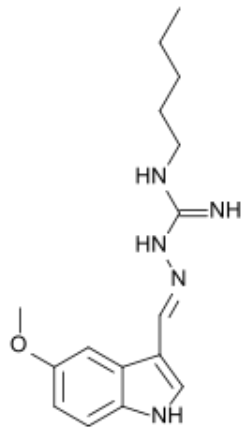
pinaverium



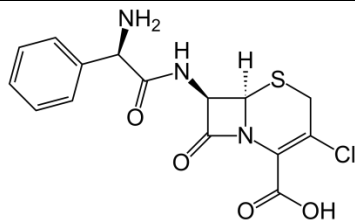
chlorhexidine



tegaserod



cefaclor



## REFERENCES

- (1) Inglese, J.; Johnson, R. L.; Simeonov, A.; Xia, M.; Zheng, W.; Austin, C. P.; Auld, D. *S. Nat. Chem. Biol.* **2007**, *3*, 466-479.
- (2) Gomez-Hens, A.; Aguilar-Caballos, M. P. *TrAC, Trends Anal. Chem.* **2007**, *26*, 171-182.
- (3) de Boer, A. R.; Lingeman, H.; Niessen, W. M. A.; Irth, H. *TrAC, Trends Anal. Chem.* **2007**, *26*, 867-883.
- (4) Kassel, D. B. *Chem. Rev.* **2001**, *101*, 255-267.
- (5) von Ahsen, O.; Bomer, U. *Chembiochem* **2005**, *6*, 481-490.
- (6) Shiau, A. K.; Massari, M. E.; Ozbal, C. C. *Comb. Chem. High Throughput Screen* **2008**, *11*, 231-237.
- (7) Cunningham, B. T.; Laing, L. G. *Expert Opin. Drug Dis.* **2008**, *3*, 891-901.
- (8) Hsieh, F.; Keshishian, H.; Muir, C. J. *Biomol. Screening* **1998**, *3*, 189-198.
- (9) Konermann, L.; Ahadi, E.; Rodriguez, A. D.; Vahidi, S. *Anal. Chem.* **2013**, *85*, 2-9.
- (10) Wu, X.; Oleschuk, R. D.; Cann, N. M. *Analyst* **2012**, *137*, 4150-4161.
- (11) Annesley, T. M. *Clin. Chem.* **2003**, *49*, 1041-1044.
- (12) Jessome, L. L.; Volmer, D. A. *Lc Gc North America* **2006**, *24*, 498-+.
- (13) Furey, A.; Moriarty, M.; Bane, V.; Kinsella, B.; Lehane, M. *Talanta* **2013**, *115*, 104-122.
- (14) Ackermann, B. L.; Berna, M. J.; Eckstein, J. A.; Ott, L. W.; Chaudhary, A. K. *Annu. Rev. Anal. Chem.* **2008**, *1*, 357-396.
- (15) Maurer, H. H.; Peters, F. T. *Ther. Drug Monit.* **2005**, *27*, 686-688.
- (16) Roddy, T. P.; Horvath, C. R.; Stout, S. J.; Kenney, K. L.; Ho, P. I.; Zhang, J. H.; Vickers, C.; Kaushik, V.; Hubbard, B.; Wang, Y. K. *Anal. Chem.* **2007**, *79*, 8207-8213.
- (17) Annis, D. A.; Nazef, N.; Chuang, C.-C.; Scott, M. P.; Nash, H. M. *J. Am. Chem. Soc.* **2004**, *126*, 15495-15503.

- (18) Comess, K. M.; Schurdak, M. E.; Voorbach, M. J.; Coen, M.; Trumbull, J. D.; Yang, H.; Gao, L.; Tang, H.; Cheng, X.; Lerner, C. G.; Mccall, J. O.; Burns, D. J.; Beutel, B. A. *J. Biomol. Screening* **2006**, *11*, 743-754.
- (19) Leveridge, M.; Buxton, R.; Argyrou, A.; Francis, P.; Leavens, B.; West, A.; Rees, M.; Hardwicke, P.; Bridges, A.; Ratcliffe, S.; Chung, C. *J. Biomol. Screening* **2014**, *19*, 278-286.
- (20) Oellig, C.; Schwack, W. *J. Chromatogr. A* **2014**, *1351*, 1-11.
- (21) Pavlic, M.; Schubert, B.; Libiseller, K.; Oberacher, H. *Forensic Sci. Int.* **2010**, *197*, 40-47.
- (22) Fuhrer, T.; Heer, D.; Begemann, B.; Zamboni, N. *Anal. Chem.* **2011**, *83*, 7074-7080.
- (23) Morand, K. L.; Burt, T. M.; Regg, B. T.; Chester, T. L. *Anal. Chem.* **2000**, *73*, 247-252.
- (24) Roddy, T. P.; Horvath, C. R.; Stout, S. J.; Kenney, K. L.; Ho, P.; Zhang, J.; Vickers, C.; Kaushik, V.; Hubbard, B.; Wang, Y. K. *Anal. Chem.* **2007**, *79*, 8207-8213.
- (25) Jonker, N.; Kool, J.; Irth, H.; Niessen, W. A. *Anal. Bioanal. Chem.* **2011**, *399*, 2669-2681.
- (26) Theberge, A. B.; Courtois, F.; Schaerli, Y.; Fischlechner, M.; Abell, C.; Hollfelder, F.; Huck, W. T. S. *Angew. Chem. Int. Ed.* **2010**, *49*, 5846-5868.
- (27) Trivedi, V.; Doshi, A.; Kurup, G. K.; Ereifej, E.; Vandevord, P. J.; Basu, A. S. *Lab Chip* **2010**, *10*, 2433-2442.
- (28) Baret, J.-C. *Lab Chip* **2012**, *12*, 422-433.
- (29) Macarron, R.; Hertzberg, R. P. *Molecular Biotechnology* **2011**, *47*, 270-285.
- (30) Agresti, J. J.; Antipov, E.; Abate, A. R.; Ahn, K.; Rowat, A. C.; Baret, J.-C.; Marquez, M.; Klibanov, A. M.; Griffiths, A. D.; Weitz, D. A. *Proc. Nat. Acad. Sci. U.S.A.* **2010**.
- (31) Nie, J.; Kennedy, R. T. *Anal. Chem.* **2010**, *82*, 7852-7856.
- (32) Li, L.; Boedicker, J. Q.; Ismagilov, R. F. *Anal. Chem.* **2007**, *79*, 2756-2761.
- (33) Niu, X.; Gielen, F.; Edel, J. B.; deMello, A. J. *Nature Chemistry* **2011**, *3*, 437-442.
- (34) Hatakeyama, T.; Chen, D. L.; Ismagilov, R. F. *J. Am. Chem. Soc.* **2006**, *128*, 2518-2519.
- (35) Cho, S.; Kang, D. K.; Sim, S.; Geier, F.; Kim, J. Y.; Niu, X. Z.; Edel, J. B.; Chang, S. I.; Wootton, R. C. R.; Elvira, K. S.; deMello, A. J. *Anal. Chem.* **2013**, *85*, 8866-8872.
- (36) Zheng, B.; Roach, L. S.; Ismagilov, R. F. *J. Am. Chem. Soc.* **2003**, *125*, 11170-11171.
- (37) Miller, O. J.; El Harrak, A.; Mangeat, T.; Baret, J. C.; Frenz, L.; El Debs, B.; Mayot, E.; Samuels, M. L.; Rooney, E. K.; Dieu, P.; Galvan, M.; Link, D. R.; Griffiths, A. D. *Proc. Nat. Acad. Sci. U.S.A.* **2012**, *109*, 378-383.

- (38) Kelly, R. T.; Page, J. S.; Marginean, I.; Tang, K.; Smith, R. D. *Angew. Chem. Int. Ed.* **2009**, *48*, 6832-6835.
- (39) Fidalgo, L. M.; Whyte, G.; Ruotolo, B. T.; Benesch, J. L. P.; Stengel, F.; Abell, C.; Robinson, C. V.; Huck, W. T. S. *Angew. Chem. Int. Ed.* **2009**, *48*, 3665-3668.
- (40) Pei, J.; Li, Q.; Lee, M. S.; Valaskovic, G. A.; Kennedy, R. T. *Anal. Chem.* **2009**, *81*, 6558-6561.
- (41) Pei, J.; Li, Q.; Kennedy, R. T. *J. Am. Soc. Mass. Spectrom.* **2010**, *21*, 1107-1113.
- (42) Li, Q.; Pei, J.; Song, P.; Kennedy, R. T. *Anal. Chem.* **2010**, *82*, 5260-5267.
- (43) Mohamed, M. M.; Sloane, B. F. *Nat. Rev. Cancer* **2006**, *6*, 764-775.
- (44) Mort, J. S.; Buttle, D. J. *Int. J. Biochem. Cell Biol.* **1997**, *29*, 715-720.
- (45) Tomoo, K. *Curr. Top. Med. Chem.* **2010**, *10*, 696-707.
- (46) Sloane, B. F.; Yan, S.; Podgorski, I.; Linebaugh, B. E.; Cher, M. L.; Mai, J.; Cavallo-Medved, D.; Sameni, M.; Doseescu, J.; Moin, K. *Sem. Cancer Biol.* **2005**, *15*, 149-157.
- (47) Gondi, C. S.; Rao, J. S. *Expert Opin. Ther. Tar.* **2013**, *17*, 281-291.
- (48) Vasiljeva, O.; Reinheckel, T.; Peters, C.; Turk, D.; Turk, V.; Turk, B. *Curr. Pharm. Des.* **2007**, *13*, 387-403.
- (49) Bell-McGuinn, K. M.; Garfall, A. L.; Bogoyo, M.; Hanahan, D.; Joyce, J. A. *Cancer Res.* **2007**, *67*, 7378-7385.
- (50) Withana, N. P.; Blum, G.; Sameni, M.; Slaney, C.; Anbalagan, A.; Olive, M. B.; Bidwell, B. N.; Edgington, L.; Wang, L.; Moin, K.; Sloane, B. F.; Anderson, R. L.; Bogoyo, M. S.; Parker, B. S. *Cancer Res.* **2012**, *72*, 1199-1209.
- (51) Smooker, P. M.; Jayaraj, R.; Pike, R. N.; Spithill, T. W. *Trends Parasitol.* **2010**, *26*, 506-514.
- (52) Požgan, U.; Caglič, D.; Rozman, B.; Nagase, H.; Turk, V.; Turk, B. In *Biol. Chem.* , 2010, p 571.
- (53) Sun, B.; Zhou, Y.; Halabisky, B.; Lo, I.; Cho, S.-H.; Mueller-Steiner, S.; Devidze, N.; Wang, X.; Grubb, A.; Gan, L. *Neuron* **2008**, *60*, 247-257.
- (54) Sundelöf, J.; Sundström, J.; Hansson, O.; Eriksdotter-Jönhagen, M.; Giedraitis, V.; Larsson, A.; Degerman-Gunnarsson, M.; Ingelsson, M.; Minthon, L.; Blennow, K.; Kilander, L.; Basun, H.; Lannfelt, L. *J. Alzheimers Dis.* **2010**, *22*, 1223-1230.
- (55) Hook, V.; Funkelstein, L.; Wegrzyn, J.; Bark, S.; Kindy, M.; Hook, G. *Biochimica et Biophysica Acta (BBA) - Proteins and Proteomics* **2012**, *1824*, 89-104.
- (56) Hall, J. A.; Dominy, J. E.; Lee, Y.; Puigserver, P. *J. Clin. Invest.* **2013**, *123*, 973-979.
- (57) Chang, H.; Guarente, L. *Trends Endocrin Met* **2014**, *25*, 138-145.

- (58) Satoh, A.; Brace, Cynthia S.; Rensing, N.; Cliften, P.; Wozniak, David F.; Herzog, Erik D.; Yamada, Kelvin A.; Imai, S. *Cell Metab.* **2013**, *18*, 416-430.
- (59) Howitz, K. T.; Bitterman, K. J.; Cohen, H. Y.; Lamming, D. W.; Lavu, S.; Wood, J. G.; Zipkin, R. E.; Chung, P.; Kisielewski, A.; Zhang, L. L.; Scherer, B.; Sinclair, D. A. *Nature* **2003**, *425*, 191-196.
- (60) Hubbard, B. P.; Sinclair, D. A. *Trends Pharmacol. Sci.* **2014**, *35*, 146-154.
- (61) Milne, J. C.; Lambert, P. D.; Schenk, S.; Carney, D. P.; Smith, J. J.; Gagne, D. J.; Jin, L.; Boss, O.; Perni, R. B.; Vu, C. B.; Bemis, J. E.; Xie, R.; Disch, J. S.; Ng, P. Y.; Nunes, J. J.; Lynch, A. V.; Yang, H. Y.; Galonek, H.; Israelian, K.; Choy, W.; Iffland, A.; Lavu, S.; Medvedik, O.; Sinclair, D. A.; Olefsky, J. M.; Jirousek, M. R.; Elliott, P. J.; Westphal, C. H. *Nature* **2007**, *450*, 712-716.
- (62) Lagouge, M.; Argmann, C.; Gerhart-Hines, Z.; Meziane, H.; Lerin, C.; Daussin, F.; Messadeq, N.; Milne, J.; Lambert, P.; Elliott, P.; Geny, B.; Laakso, M.; Puigserver, P.; Auwerx, J. *Cell* **2006**, *127*, 1109-1122.
- (63) Feige, J. N.; Lagouge, M.; Canto, C.; Strehle, A.; Houten, S. M.; Milne, J. C.; Lambert, P. D.; Matak, C.; Elliott, P. J.; Auwerx, J. *Cell Metab.* **2008**, *8*, 347-358.
- (64) Mitchell, S. J.; Martin-Montalvo, A.; Mercken, E. M.; Palacios, H. H.; Ward, T. M.; Abulwerdi, G.; Minor, R. K.; Vlasuk, G. P.; Ellis, J. L.; Sinclair, D. A.; Dawson, J.; Allison, D. B.; Zhang, Y. Q.; Becker, K. G.; Bernier, M.; de Cabo, R. *Cell Rep.* **2014**, *6*, 836-843.
- (65) Yi, Y. W.; Kang, H. J.; Kim, H. J.; Kong, Y. L.; Brown, M. L.; Bae, I. *Oncotarget* **2013**, *4*, 984-994.
- (66) Yamazaki, Y.; Usui, I.; Kanatani, Y.; Matsuya, Y.; Tsuneyama, K.; Fujisaka, S.; Bukhari, A.; Suzuki, H.; Senda, S.; Imanishi, S.; Hirata, K.; Ishiki, M.; Hayashi, R.; Urakaze, M.; Nemoto, H.; Kobayashi, M.; Tobe, K. *Am. J. Physiol.-Endocrinol. Metab.* **2009**, *297*, E1179-E1186.
- (67) Kaeberlein, M.; McDonagh, T.; Heltweg, B.; Hixon, J.; Westman, E. A.; Caldwell, S. D.; Napper, A.; Curtis, R.; DiStefano, P. S.; Fields, S.; Bedalov, A.; Kennedy, B. K. *J. Biol. Chem.* **2005**, *280*, 17038-17045.
- (68) Pacholec, M.; Chrnyk, B. A.; Cunningham, D.; Flynn, D.; Griffith, D. A.; Griffor, M.; Loulakis, P.; Pabst, B.; Qiu, X.; Stockman, B.; Thanabal, V.; Varghese, A.; Ward, J.; Withka, J.; Ahn, K. *J. Biol. Chem.* **2010**.
- (69) Beher, D.; Wu, J.; Cumine, S.; Kim, K. W.; Lu, S.; Atangan, L.; Wang, M. *Chem. Bio. Drug Des.* **2009**, *74*, 619-624.
- (70) Borra, M. T.; Smith, B. C.; Denu, J. M. *J. Biol. Chem.* **2005**, *280*, 17187-17195.
- (71) Hubbard, B. P.; Gomes, A. P.; Dai, H.; Li, J.; Case, A. W.; Considine, T.; Riera, T. V.; Lee, J. E.; E, S. Y.; Lamming, D. W.; Pentelute, B. L.; Schuman, E. R.; Stevens, L. A.; Ling, A. J. Y.; Armour, S. M.; Michan, S.; Zhao, H.; Jiang, Y.; Sweitzer, S. M.; Blum,



- C. A.; Disch, J. S.; Ng, P. Y.; Howitz, K. T.; Rolo, A. P.; Hamuro, Y.; Moss, J.; Perni, R. B.; Ellis, J. L.; Vlasuk, G. P.; Sinclair, D. A. *Science* **2013**, *339*, 1216-1219.
- (72) Dai, H.; Kustigian, L.; Carney, D.; Case, A.; Considine, T.; Hubbard, B.; Perni, R.; Riera, T.; Szczepankiewicz, B.; Vlasuk, G.; Stein, R. *J. Biol. Chem.* **2010**, *285*, 32695-32703.
- (73) Michan, S.; Sinclair, D. *Biochem. J* **2007**, *404*, 1-13.
- (74) Michishita, E.; McCord, R. A.; Berber, E.; Kioi, M.; Padilla-Nash, H.; Damian, M.; Cheung, P.; Kusumoto, R.; Kawahara, T. L. A.; Barrett, J. C.; Chang, H. Y.; Bohr, V. A.; Ried, T.; Gozani, O.; Chua, K. F. *Nature* **2008**, *452*, 492-U416.
- (75) Kanfi, Y.; Naiman, S.; Amir, G.; Peshti, V.; Zinman, G.; Nahum, L.; Bar-Joseph, Z.; Cohen, H. Y. *Nature* **2012**, *483*, 218-221.
- (76) Gertler, A. A.; Cohen, H. Y. *Biogerontology* **2013**, *14*, 629-639.
- (77) Masri, S.; Rigor, P.; Cervantes, M.; Ceglia, N.; Sebastian, C.; Xiao, C. Y.; Roqueta-Rivera, M.; Deng, C. X.; Osborne, T. F.; Mostoslavsky, R.; Baldi, P.; Sassone-Corsi, P. *Cell* **2014**, *158*, 659-672.
- (78) Jiang, H.; Khan, S.; Wang, Y.; Charron, G.; He, B.; Sebastian, C.; Du, J.; Kim, R.; Ge, E.; Mostoslavsky, R.; Hang, H. C.; Hao, Q.; Lin, H. *Nature* **2013**, *496*, 110-113.
- (79) Feldman, J. L.; Baeza, J.; Denu, J. M. *J. Biol. Chem.* **2013**, *288*, 31350-31356.
- (80) Hu, J.; He, B.; Bhargava, S.; Lin, H. N. *Org. Biomol. Chem.* **2013**, *11*, 5213-5216.
- (81) Kokkonen, P.; Rahnasto-Rilla, M.; Mellini, P.; Jarho, E.; Lahtela-Kakkonen, M.; Kokkola, T. *Eur. J. Pharm. Sci.* **2014**, *63*, 71-76.
- (82) Sun, S.; Slaney, T. R.; Kennedy, R. T. *Anal. Chem.* **2012**, *84*, 5794-5800.
- (83) Sun, S.; Kennedy, R. T. *Anal. Chem.* **2014**, *86*, 9309-9314.
- (84) Casadevall i Solvas, X.; deMello, A. *Chem. Commun.* **2011**, *47*, 1936-1942.
- (85) Chiu, D. T.; Lorenz, R. M. *Acc. Chem. Res.* **2009**, *42*, 649-658.
- (86) Furman, W. B. *Continuous-Flow Analysis. Theory and Practice*: New York, 1976.
- (87) Abate, A. R.; Hung, T.; Mary, P.; Agresti, J. J.; Weitz, D. A. *Proc. Nat. Acad. Sci. U.S.A.* **2010**, *107*, 19163-19166.
- (88) Song, H.; Chen, D. L.; Ismagilov, R. F. *Angew. Chem.-Int. Edit.* **2006**, *45*, 7336-7356.
- (89) Adamson, D. N.; Mustafi, D.; Zhang, J. X. J.; Zheng, B.; Ismagilov, R. F. *Lab Chip* **2006**, *6*, 1178-1186.
- (90) Abate, A. R.; Agresti, J. J.; Weitz, D. A. *Appl. Phys. Lett.* **2010**, *96*.
- (91) Ahn, B.; Lee, K.; Panchapakesan, R.; Oh, K. W. *Biomicrofluidics* **2011**, *5*.
- (92) Cai, L. F.; Zhu, Y.; Du, G. S.; Fang, Q. *Anal. Chem.* **2012**, *84*, 446-452.

- (93) Pei, J.; Nie, J.; Kennedy, R. T. *Anal. Chem.* **2010**, *82*, 9261-9267.
- (94) Ahn, K.; Agresti, J.; Chong, H.; Marquez, M.; Weitz, D. A. *Appl. Phys. Lett.* **2006**, *88*.
- (95) Mazutis, L.; Baret, J. C.; Treacy, P.; Skhiri, Y.; Araghi, A. F.; Ryckelynck, M.; Taly, V.; Griffiths, A. D. *Lab Chip* **2009**, *9*, 2902-2908.
- (96) Roach, L. S.; Song, H.; Ismagilov, R. F. *Anal. Chem.* **2005**, *77*, 785-796.
- (97) Srisa-Art, M.; Dyson, E. C.; deMello, A. J.; Edel, J. B. *Anal. Chem.* **2008**, *80*, 7063-7067.
- (98) He, M.; Edgar, J. S.; Jeffries, G. D. M.; Lorenz, R. M.; Shelby, J. P.; Chiu, D. T. *Anal. Chem.* **2005**, *77*, 1539-1544.
- (99) Clausell-Tormos, J.; Lieber, D.; Baret, J. C.; El-Harrak, A.; Miller, O. J.; Frenz, L.; Blouwolf, J.; Humphry, K. J.; Koster, S.; Duan, H.; Holtze, C.; Weitz, D. A.; Griffiths, A. D.; Merten, C. A. *Chem. Biol.* **2008**, *15*, 875-875.
- (100) Shim, J. U.; Olguin, L. F.; Whyte, G.; Scott, D.; Babbie, A.; Abell, C.; Huck, W. T. S.; Hollfelder, F. *J. Am. Chem. Soc.* **2009**, *131*, 15251-15256.
- (101) Kreutz, J. E.; Shukhaev, A.; Du, W. B.; Druskin, S.; Daugulis, O.; Ismagilov, R. F. *J. Am. Chem. Soc.* **2010**, *132*, 3128-3132.
- (102) Lunn, C. A. *Future Med. Chem.* **2010**, *2*, 1703-1716.
- (103) Zhu, Y.; Fang, Q. *Anal. Chem.* **2010**, *82*, 8361-8366.
- (104) Hook, V.; Funkelstein, L.; Wegrzyn, J.; Bark, S.; Kindy, M.; Hook, G. *Biochim. Biophys. Acta, Proteins Proteomics* **2012**, *1824*, 89-104.
- (105) Sevenich, L.; Schurigt, U.; Sachse, K.; Gajda, M.; Werner, F.; Muller, S.; Vasiljeva, O.; Schwinde, A.; Klemm, N.; Deussing, J.; Peters, C.; Reinheckel, T. *Proc Natl Acad Sci U S A* **2010**, *107*, 2497-2502.
- (106) Pozgan, U.; Caglic, D.; Rozman, B.; Nagase, H.; Turk, V.; Turk, B. *Biol. Chem.* **2010**, *391*, 571-579.
- (107) Jilkova, A.; Rezacova, P.; Lepsik, M.; Horn, M.; Vachova, J.; Fanfrlik, J.; Brynda, J.; McKerrow, J. H.; Caffrey, C. R.; Mares, M. *J. Biol. Chem.* **2011**, *286*, 35770-35781.
- (108) de Boer, A. R.; Letzel, T.; van Elswijk, D. A.; Lingeman, H.; Niessen, W. M. A.; Irth, H. *Anal. Chem.* **2004**, *76*, 3155-3161.
- (109) Slaney, T. R.; Nie, J.; Hershey, N. D.; Thwar, P. K.; Linderman, J.; Burns, M. A.; Kennedy, R. T. *Anal. Chem.* **2011**, *83*, 5207-5213.
- (110) McDonald, J. C.; Whitesides, G. M. *Acc. Chem. Res.* **2002**, *35*, 491-499.
- (111) Binossek, M. L.; Nägler, D. K.; Becker-Pauly, C.; Schilling, O. *J. Proteome Res.* **2011**, *10*, 5363-5373.
- (112) Gosalia, D. N.; Salisbury, C. M.; Ellman, J. A.; Diamond, S. L. *Mol. Cell Proteomics* **2005**, *4*, 626-636.

- (113) Zhang, J. H.; Chung, T. D. Y.; Oldenburg, K. R. *J. Biomol. Screening* **1999**, *4*, 67-73.
- (114) Sivasamy, J.; Chim, Y. C.; Wong, T.-N.; Nguyen, N.-T.; Yobas, L. *Microfluid. Nanofluid.* **2009**, *8*, 409-416.
- (115) Song, H.; Li, H. W.; Munson, M. S.; Van Ha, T. G.; Ismagilov, R. F. *Anal. Chem.* **2006**, *78*, 4839-4849.
- (116) Zehender, H.; Mayr, L. M. *Curr. Opin. Chem. Biol.* **2007**, *11*, 511-517.
- (117) Zehender, H.; Le Goff, F.; Lehmann, N.; Filipuzzi, I.; Mayr, L. M. *J. Biomol. Screening* **2004**, *9*, 498-505.
- (118) Khandekar, S. S.; Feng, B.; Yi, T.; Chen, S.; Laping, N.; Bramson, N. *J. Biomol. Screening* **2005**, *10*, 447-455.
- (119) Price, A. K.; MacConnell, A. B.; Paegel, B. M. *Anal. Chem.* **2014**, *86*, 5039-5044.
- (120) Bodnarchuk, M. I.; Li, L.; Fok, A.; Nachtergaele, S.; Ismagilov, R. F.; Talapin, D. V. *J. Am. Chem. Soc.* **2011**, *133*, 8956-8960.
- (121) Sgro, A. E.; Allen, P. B.; Chiu, D. T. *Anal. Chem.* **2007**, *79*, 4845-4851.
- (122) Song, H.; Li, H.-W.; Munson, M. S.; Van Ha, T. G.; Ismagilov, R. F. *Anal. Chem.* **2006**, *78*, 4839-4849.
- (123) Song, P.; Hershey, N. D.; Mabrouk, O. S.; Slaney, T. R.; Kennedy, R. T. *Anal. Chem.* **2012**, *84*, 4659-4664.
- (124) Wang, X. L.; Zhu, Y.; Fang, Q. *Analyst* **2014**, *139*, 191-197.
- (125) Sun, X.; Tang, K.; Smith, R.; Kelly, R. *Microfluid. Nanofluid.* **2013**, *15*, 117-126.
- (126) Yan, S. Q.; Sloane, B. F. *Biol. Chem.* **2003**, *384*, 845-854.
- (127) Huryn, D. M.; Smith, A. B., III. *Curr. Top. Med. Chem.* **2009**, *9*, 1206-1216.
- (128) Palermo, C.; Joyce, J. A. *Trends Pharmacol. Sci.* **2008**, *29*, 22-28.
- (129) Otto, H. H.; Schirmeister, T. *Chem. Rev.* **1997**, *97*, 133-171.
- (130) Frlan, R.; Gobec, S. *Curr. Med. Chem.* **2006**, *13*, 2309-2327.
- (131) Kim, C.; Lee, D.; Kim, C.; Lee, K.; Lee, C.; Ahn, I. *Anal. Chem.* **2014**, *86*, 3825-3833.
- (132) Kaminski, T. S.; Jakiela, S.; Czekalska, M. A.; Postek, W.; Garstecki, P. *Lab Chip* **2012**, *12*, 3995-4002.
- (133) Chabert, M.; Dorfman, K. D.; de Cremoux, P.; Roeraade, J.; Viovy, J. L. *Anal. Chem.* **2006**, *78*, 7722-7728.
- (134) Collins, P. R.; Stack, C. M.; O'Neill, S. M.; Doyle, S.; Ryan, T.; Brennan, G. P.; Mousley, A.; Stewart, M.; Maule, A. G.; Dalton, J. P.; Donnelly, S. *J. Biol. Chem.* **2004**, *279*, 17038-17046.

- (135) Sripa, J.; Brindley, P. J.; Sripa, B.; Loukas, A.; Kaewkes, S.; Laha, T. *Parasitol. Int.* **2012**, *61*, 191-195.
- (136) Scaffa, P. M. C.; Vidal, C. M. P.; Barros, N.; Gesteira, T. F.; Carmona, A. K.; Breschi, L.; Pashley, D. H.; Tjaderhane, L.; Tersariol, I. L. S.; Nascimento, F. D.; Carrilho, M. R. *J. Dent. Res.* **2012**, *91*, 420-425.
- (137) Wen, L.; Tha, S.; Sutton, V.; Steel, K.; Rahman, F.; McConnell, M.; Chmielowski, J.; Liang, K.; Obregon, R.; LaFollette, J.; Berryman, L.; Keefer, R.; Bordowitz, M.; Ye, A.; Hunter, J.; Huang, J.-K.; McConnell, R. M. In *Molecular Cloning - Selected Applications in Medicine and Biology*, Brown, G., Ed.; InTech, 2011, pp 37-58.
- (138) Kaepler, U.; Schirmeister, T. *Med. Chem.* **2005**, *1*, 361-370.
- (139) Wang, T. *Discovery and characterization of novel inhibitors against cathepsin L and exploring their potential as anti Ebola/ SARS virus infection therapeutics*. University of Pennsylvania, ProQuest, 2012.
- (140) Liu, Y.; Huang, V.; Chao, T.; Hsiao, C.; Lin, A.; Chang, M.; Chow, L. *Biochem. Biophys. Res. Commun.* **2005**, *333*, 194-199.
- (141) Kim, Y.; Mandadapu, S. R.; Groutas, W. C.; Chang, K. *Antivir. Res.* **2013**, *97*, 161-168.
- (142) Kawada, A.; Hara, K. J.; Kominami, E.; Hiruma, M.; Noguchi, H.; Ishibashi, A. *Arch. Dermatol. Res.* **1997**, *289*, 87-93.
- (143) Khedr, N. F.; El-Ashmawy, N. E.; El-Bahrawy, H. A.; Haggag, A. A.; El-Abd, E. E. *Fund. Clin. Pharmacol.* **2013**, *27*, 526-534.
- (144) Bork, S.; Yokoyama, N.; Matsuo, T.; Claveria, F. G.; Fujisaki, K.; Igarashi, I. *Am. J. Trop. Med. Hyg.* **2003**, *68*, 334-340.
- (145) Tsuji, N.; Miyoshi, T.; Battsetseg, B.; Matsuo, T.; Xuan, X.; Fujisaki, K. *PLoS Pathog.* **2008**, *4*, e1000062.
- (146) Martins, T. M.; do Rosário, V. E.; Domingos, A. *Exp. Parasitol.* **2011**, *127*, 184-194.
- (147) Baici, A.; Lang, A. *FEBS Lett.* **1990**, *277*, 93-96.
- (148) Yaron, M.; Shirazi, I.; Yaron, I. *Osteoarthr. Cartilage.* **1999**, *7*, 272-280.
- (149) Forbes, C. D.; Toth, J. G.; Ozbal, C. C.; LaMarr, W. A.; Pendleton, J. A.; Rocks, S.; Gedrich, R. W.; Osterman, D. G.; Landro, J. A.; Lumb, K. J. *J. Biomol. Screening* **2007**, *12*, 628-634.
- (150) Highkin, M. K.; Yates, M. P.; Nemirovskiy, O. V.; Lamarr, W. A.; Munie, G. E.; Rains, J. W.; Masferrer, J. L.; Nagiec, M. M. *J. Biomol. Screening* **2011**, *16*, 272-277.
- (151) Risticevic, S.; Niri, V. H.; Vuckovic, D.; Pawliszyn, J. *Anal. Bioanal. Chem.* **2009**, *393*, 781-795.
- (152) Rule, G.; Henion, J. *J. Am. Soc. Mass. Spectrom.* **1999**, *10*, 1322-1327.

- (153) Rule, G.; Chapple, M.; Henion, J. *Anal. Chem.* **2000**, *73*, 439-443.
- (154) Morris, B. J. *Free Radical Biol. Med.* **2013**, *56*, 133-171.
- (155) Finkel, T.; Deng, C.-X.; Mostoslavsky, R. *Nature* **2009**, *460*, 587-591.
- (156) Lavu, S.; Boss, O.; Elliott, P. J.; Lambert, P. D. *Nat Rev Drug Discov* **2008**, *7*, 841-853.
- (157) Zhou, Y.; Mabrouk, O.; Kennedy, R. *J. Am. Soc. Mass. Spectrom.* **2013**, *24*, 1700-1709.
- (158) Trapp, J.; Meier, R.; Hongwiset, D.; Kassack, M. U.; Sippl, W.; Jung, M. *ChemMedChem* **2007**, *2*, 1419-1431.
- (159) Napper, A. D.; Hixon, J.; McDonagh, T.; Keavey, K.; Pons, J.-F.; Barker, J.; Yau, W. T.; Amouzegh, P.; Flegg, A.; Hamelin, E.; Thomas, R. J.; Kates, M.; Jones, S.; Navia, M. A.; Saunders, J. O.; DiStefano, P. S.; Curtis, R. *J. Med. Chem.* **2005**, *48*, 8045-8054.
- (160) Peck, B.; Chen, C.-Y.; Ho, K.-K.; Di Fruscia, P.; Myatt, S. S.; Coombes, R. C.; Fuchter, M. J.; Hsiao, C.; Lam, E. W. *Mol. Cancer Ther.* **2010**, *9*, 844-855.
- (161) Sacconay, L.; Angleviel, M.; Randazzo, G. M.; Marçal Ferreira Queiroz, M.; Ferreira Queiroz, E.; Wolfender, J. L.; Carrupt, P. A.; Nurisso, A. *PLoS Negl. Trop. Dis.* **2014**, *8*, e2689.
- (162) Ryckewaert, L.; Sacconay, L.; Carrupt, P.; Nurisso, A.; SimõesPires, C. *Toxicol. Lett.* **2014**, *229*, 374-380.
- (163) Bitterman, K. J.; Anderson, R. M.; Cohen, H. Y.; Latorre-Esteves, M.; Sinclair, D. A. *J. Biol. Chem.* **2002**, *277*, 45099-45107.
- (164) Mai, A.; Massa, S.; Lavu, S.; Pezzi, R.; Simeoni, S.; Ragno, R.; Mariotti, F. R.; Chiani, F.; Camilloni, G.; Sinclair, D. A. *J. Med. Chem.* **2005**, *48*, 7789-7795.
- (165) Lain, S.; Hollick, J. J.; Campbell, J.; Staples, O. D.; Higgins, M.; Aoubala, M.; McCarthy, A.; Appleyard, V.; Murray, K. E.; Baker, L.; Thompson, A.; Mathers, J.; Holland, S. J.; Stark, M. J. R.; Pass, G.; Woods, J.; Lane, D. P.; Westwood, N. J. *Cancer Cell*, *13*, 454-463.
- (166) Parenti, M. D.; Grozio, A.; Bauer, I.; Galeno, L.; Damonte, P.; Millo, E.; Sociali, G.; Franceschi, C.; Ballestrero, A.; Bruzzone, S.; Del Rio, A.; Nencioni, A. *J. Med. Chem.* **2014**, *57*, 4796-4804.
- (167) Michishita, E.; McCord, R. A.; Boxer, L. D.; Barber, M. F.; Hong, T.; Gozani, O.; Chua, K. F. *Cell Cycle* **2009**, *8*, 2664-2666.
- (168) Bladergroen, M. R.; Derks, R. J. E.; Nicolardi, S.; de Visser, B.; van Berloo, S.; van der Burgt, Y. E. M.; Deelder, A. M. *J. Proteomics* **2012**, *77*, 144-153.
- (169) Li, Q. *Novel approaches to high sensitivity capillary liquid chromatography-mass spectrometry and application to in vivo neuropeptide monitoring*. Dissertation, University of Michigan, 2010.

(170) Brideau, C.; Gunter, B.; Pikounis, B.; Liaw, A. *J. Biomol. Screening* **2003**, *8*, 634-647.

(171) Zhang, X. D. *J. Biomol. Screening* **2011**, *16*, 775-785.